Millimetre-wave radio-over-fibre supported multi-antenna and multi-user transmission

A Thesis Submitted to The University of Kent for the Degree of Doctor of Philosophy in Electronic Engineering

By

Usman Habib

November, 2018

ABSTRACT

In this thesis, various features of the RoF supported mmW communication for future wireless systems have been analysed including photonic generation of mmW for MIMO operation, performance analysis of mmW MIMO to achieve spatial diversity and spatial multiplexing with analog RoF fronthaul, and multi-user transmission in the 60 GHz-band using multiplexing-over-fibre transport and frequency-selective antenna.

A low cost mmW generation system for two independent MIMO signals has been presented, consisting of a single optical Phase Modulator (PM). The different aspects of experimental analysis on RoF-supported mmW MIMO in this thesis, which were not considered before, include use of specific MIMO algorithm to understand the amount of improvement in coverage and data rate for a particular MIMO technique, performance comparison with SISO at several user locations, and verification of optimum RAU physical spacing for a particular transmission distance with the theoretical results. The results show that flexible and wider RAU spacings, required to obtain optimum performance in a mmW MIMO system, can be achieved using the proposed analog RoF fronthaul. The investigation was extended to verification of a method to individual measurement of mmW channel coefficients and performing MIMO processing, which shows that mmW channels are relatively static and analysis can be extended to much longer distances and making projections for N×N MIMO.

For mmW multi-user transmission, a novel low cost, low complexity system using single RoF link and single RF chain with single transmitting antenna has been presented and characterized, which was based on large number of RF chains and multiple antenna units previously. The setup involves generation and RoF transport of a composite SCM signal, upconversion at the RAU and transmission of different frequency channels towards spatially distributed users using a frequency-selective Leaky-Wave-Antenna (LWA), to convert Frequency Division Multiplexing (FDM) in to Spatial Division Multiple Access (SDMA). Analysis on low user-signal spacing for the SCM shows the feasibility to serve a large number of users within a specific transmission bandwidth and experimental demonstration to achieve sum rate of 10Gb/s is shown by serving 20 users simultaneously. Furthermore,

investigation on SNR degradation of high bandwidth signals due to beamsteering effect of the LWA and theoretical calculations of the sum data rate for different number of users is performed, which shows that the proposed system can provide much higher sum rates with high available SNR. It was also experimentally demonstrated that improvement in coverage and spectral efficiency is obtained by operating multiple LWAs using single RF chain. Finally, an experimental demonstration of a DWDM-RoF based 60 GHz multi-user transmission using single LWA is presented to show the feasibility to extend the setup for a multiple RAU based system, serving each at distinct optical wavelength and performing direct photonic upconversion at the RAU for low cost mmW generation.

ACKNOWLEDGEMENT

I owe immense gratitude to my principal supervisor Prof. Nathan Gomes for his valuable support and guidance throughout my Ph.D. His encouragement and mentoring helped me a lot to increase my potential at work. I am also grateful to my second supervisor, Dr. Chao Wang for his valuable suggestions, and other members of my supervisory team, Prof. Jiangzhou Wang and Dr. Huiling Zhu for their insightful discussions.

During this time, I had the honour to be a member of EU-Japan collaborative project "RAPID-5G", which funded my studies. I want to thank all the members for the joint effort and technical discussions we had during the project, especially Prof. Andreas Stohr and Matthias Steeg for providing the LWA. My special gratitude goes to Prof. Hiroshi Murata for his endless support during my research work at University of Osaka, Japan and successful field trials of RAPID-5G project at Suita Football Stadium. Also, to Dr. Naruto Yonemoto for his support during experimental work at ENRI, Japan.

I would also particularly like to thank Dr. Anthony Nkansah and Dr. Philippos Assimakopoulos for sharing their immense experimental expertise and feedback, and especially Dr. Anthony Aighobahi for valuable advice and support for MIMO experiments. My gratitude goes to all staff in the School of Engineering and Digital Arts and in particular to the staff of IT and technical support department for their help with the experiments. Also, to my colleagues in the laboratory; Shabnam Noor, Guoqing Wang and Chaitanya Mididoddi for their collaboration and support with sharing the laboratory equipment. My sincere thanks goes to Prof Stuart Walker, University of Essex and Dr. Terence Quinlan for providing 60 GHz integrated devices and slot array antenna for the experimental work.

Finally, I am indebted to my parents for their support, encouragement and steadfast prayers throughout my life. I owe a huge debt of thanks to my wife for her support and understanding all along the way and little ones, Saad and Hashir for their tolerance to my inattention during difficult phases of my studies.

TABLE OF CONTENTS

LIST OF PUBLICATIONS

[1] **U. Habib**, M. Steeg, A. Stöhr and N.J. Gomes, "Single Radio-over-Fiber Link and RF Chain-based 60GHz Multi-beam Transmission", submitted to *Journal of Lightwave Technology*, November 2018.

[2] **U. Habib**, M. Steeg, A. Stöhr, N.J. Gomes, "Radio-over-Fiber-supported 60GHz Multiuser Transmission using Leaky Wave Antenna", *IEEE International Topical Meeting on Microwave Photonics (MWP)*, 2018, France.

[3] **U. Habib**, A.E. Aighobahi, T. Quinlan, S. Walker and N.J. Gomes, "Analog Radio-over-Fiber Supported Increased RAU Spacing for 60GHz Distributed MIMO employing Spatial Diversity and Multiplexing", *Journal of Lightwave Technology*, April 2018.

[4] H. Murata, Y. Otagaki, N. Yonemoto, K. Ikeda, N. Shibakagi, H. Toda, H. Mano, **U. Habib**, N.J. Gomes, "Millimeter-Wave Communication System Using Photonic-Based Remote Antennas for Configurable Network in Dense User Environment", *IEEE CAMA*, Japan, 2017.

[5] N.J. Gomes, **U. Habib**, S. Noor, A.E. Aigobahi, P. Assimakopoulos, "Support of Multi-antenna and Multi-user Systems Using Radio Over Fiber", *Asia communications and Photonics conference*, China, 2017.

[6] **U. Habib**, M. Steeg, A. Stöhr, N.J.Gomes, "Radio-over-Fiber-supported 60GHz Multiuser Transmission using Leaky Wave Antenna", *IEEE International Topical Meeting on Microwave Photonics (MWP)*, Beijing, China, 2017.

[7] **U. Habib**, A. Aighobahi, T. Quinlan, S. Walker, N. J. Gomes, "Demonstration of Radio-over-Fiber-supported 60 GHz MIMO using Separate Antenna-Pair Processing", *IEEE International Topical Meeting on Microwave Photonics (MWP)*, Beijing, China, 2017, pp.1-4.

[8] **U. Habib**, A.E. Aighobahi, M. Nair, H. Zhu, T. Quinlan, S. Walker, N.J. Gomes, "Performance Improvement for OFDM-RoF Transported 60 GHz System

using Spatial Diversity and Multiplexing", *IEEE International Conference on Communications ICC Workshop (WDN-5G)*, Paris, 2017, pp.211-216.

[9] **U. Habib**, A. Aighobahi, C. Wang, N.J. Gomes, "Radio over Fiber Transport of mm-Wave 2×2 MIMO for Spatial Diversity and Multiplexing", *IEEE International Topical Meeting on Microwave Photonics (MWP)*, 2016, Long Beach USA, pp. 39-42.

[10] N. J. Gomes, P. Assimakopoulos, M. K. Al-Hares, **U. Habib** and S. Noor, "The New Flexible Mobile Fronthaul: Digital or Analog, or Both?", *18th International Conference on Transparent Optical Networks (ICTON)*, Trento, Italy, 2016, pp. 1-4

LIST OF FIGURES

LIST OF TABLES

LIST OF ABBREVIATIONS

3G	Third generation of wireless communications
4G	Fourth generation of wireless communications
ADC	Analog to Digital Converter
ASE	Amplified Spontaneous Emission
AWG	Arbitrary Waveform generator
BB	Baseband
BER	Bits Error Rate
BPF	Bandpass filter
bps	Bit per second
BS	Base Station
CN	Condition number
COTS	Commercial off-the-shelf
CP	Cyclic prefix
CSI	Channel state information
CU	Central unit
CW	Continuous-wave
DAC	Digital-to-analogue converter
DAS	Distributed antenna system
dB	decibel
DFB	Distributed Feedback
DSB	Double Side Band
DSP	Digital signal processing
DWDM	Dense Wavelength Division Multiplexing
EDFA	Erbium-doped fibre amplifier
EVM	Error vector magnitude

FDMA	Frequency Division Multiple Access
FEC	Forward error correction
FFT	Fast Fourier Transform
Gbps	Gigabits per second
GHz	Gigahertz
I/Q	In-phase and quadrature-phase components
IEEE	Institute of Electrical and Electronics Engineers
IF	Intermediate frequency
IM-DD	Intensity modulation direct detection
ITU	International Telecommunication Union
LD	Laser diode
LMS	Least mean squares
LNA	Low Noise Amplifier
LO	Local oscillator
LOS	Light-of-sight
LPF	Low pass filter
LS	Least square
LTE	Long Term Evolution
LWA	Leaky Wave Antenna
Mbps	Megabits per second
MHz	Megahertz
MIMO	Multiple-input, multiple-output
mmW	Millimetre-wave
MMIC	Microwave Monolithic Integrated Circuit
MRC	Maximal ratio combing
multi-antenna	Multiple antenna

MUX	Multiplexer
mW	Mili-Watt
MZM	Mach-Zehnder modulator
NF	Noise Figure
NLOS	Non-light-of-sight
nm	Nano-metre
OBPF	Optical band pass filter
OBSF	Optical band stop filter
OFDM	Orthogonal Frequency Division Multiplexing
OOK	On-Off Keying
PAPR	Peak-to-average power ratio
PRBS	Pseudo Random Binary Sequence
PD	Photodiode or photodetector
PM	Phase modulator
QAM	Quadrature Amplitude Modulation
QPSK	Quadrature Phase Shift Keying
RAU	Remote Antenna Unit
RF	Radio Frequency
RIN	Relative Intensity Noise
RoF	Radio-over-fibre
Rx	Receiver
SC	Selection Combining
SCM	SubCarrier Multiplexing
SDMA	Spatial Division Multiple Access
SDR	Software defined radio
SFBC	Space-frequency block coding

SG	Signal generator
SISO	Single-input, single-output
SMF	Single-mode fibre
SNR	Signal-to-noise ratio
SSB	Single Side Band
STBC	Space-Time Block Coding
SVD	Singular value decomposition
TDM	Time Division Multiplexing
Tx	Transmitter
UE	User equipment
VSA	Vector signal analyser
WLAN	Wireless local Area Network
ZF	Zero-forcing

CHAPTER 1
INTRODUCTION

1.1. Motivation

One of the major reasons for recent spectrum congestion and the increased need for high data rates in mobile communication is the migration of fixed broadband users to mobile networks [1]. The use of modern high-bandwidth services such as High Definition TV (HDTV), Virtual Reality (VR), Interactive Gaming, Video conferencing, cloud computing, Telemedicine [2], is increasing rapidly with the development of the handheld devices which make use of modern high speed digital electronics for high quality display and fast processing of huge amount of data. CISCO forecasts that data traffic from wireless and mobile devices will account for more than 63% of the total IP traffic by 2021 and IP traffic for mobile data will increase seven times in 2021 in comparison with 2016, whereas it will be only threefold for the fixed internet [3]. The limited spectrum resources of the current mobile networks and increase in bandwidth hungry applications has led to increased interest in the use of millimetre-wave (mmW) frequencies for future wireless systems, where large bandwidth is available to support high data rates. Due to the huge potential of mmW frequencies to provide support for various future mobile applications, spectrum regulatory bodies, such as the Federal Communications Commissions (FCC), have allocated different mmW bands for commercial use [4]. IEEE has specified several standards at mmW frequencies such as the high-bandwidth “wireless personal area network” (WPAN) standard, (IEEE 802.15.3c) [5] and the WiGig IEEE. 802.11ay [6] for 60 GHz-band. The high propagation loss of mmW frequencies is a bottleneck in implementation of indoor and outdoor mmW networks. Although it makes them suitable for cellular architectures based on small cells for frequency reutilization as low power levels will cause less

interference among different cells, the essential requirement of reliable coverage for mobile users is a fundamental issue to be addressed. For this reason, a large number of Remote Antenna Units (RAUs) are anticipated in the deployment of mmW communication systems and network operators are facing the challenge to minimize the capital and operating expenses [7]. The need is for a cost-effective solution for large scale distribution of mmW RAUs, which includes low cost generation and distribution of mmW signals and low-complexity RAU design. The requirements for the access technology of mmW networks include high-capacity fronthaul, support for multiple services and protocols, and a centralized approach for multiple RAUs. Centralized-Radio Access Network (C-RAN) and distributed antenna system (DAS) [8] which are useful techniques to ensure near-uniform coverage at lower frequencies [9], can be used to improve the coverage and performance of mmW transmission. In addition, the generation of a stable and low noise mmW signal is a major factor which affects the cost and complexity of the RAU. The commonly used microwave oscillators with low phase noise can be used to generate mmW signals by frequency multiplication but the issues related to such techniques are cost and high noise of the integrated hardware compared to components available at lower frequencies [10].

RoF transport is a promising solution for seamless integration of the optical distribution network with mmW interfaces, since high quality mmW signals can be generated optically using direct photonic upconversion [11], along with the advantages of low loss transmission and ultra-high capacity of the optical fibre [12]. Development of high speed optical modulators and photodetectors have enabled several RoF transport configurations for mmW generation. The use of different multiplexing-over-fibre techniques such as Wavelength Division Multiplexing (WDM) [13] and Sub-Carrier Multiplexing (SCM) [14] in RoF based mmW systems can provide a large range of applications for multi-service and multi-user transmission. RoF technology is an ideal candidate to provide transport for mmW multi-antenna systems which provides a flexible infrastructure, as the capacity to a particular antenna or user can be switched according to the demand [15], and centralized access. Enhanced Mobile Broadband (eMBB) is one of the primary use cases defined by the 3GPP for 5G New Radio (NR) to provide high data rates and coverage to a wide area. The user scenarios that need to be covered include the

support for multiple hotspots to cover a wide area where large number of users will demand broadband access, and thus represents a high capacity network with low mobility requirement, such as in shopping malls, stadium and high streets. Fig. 1.1 shows such a scenario where a WDM based RoF fronthaul has been used to support multiple RAUs, which serve a large number of users with 5G eMBB services using mmW directional beams, along with providing the coverage for the legacy wifi or LTE transmission [16].

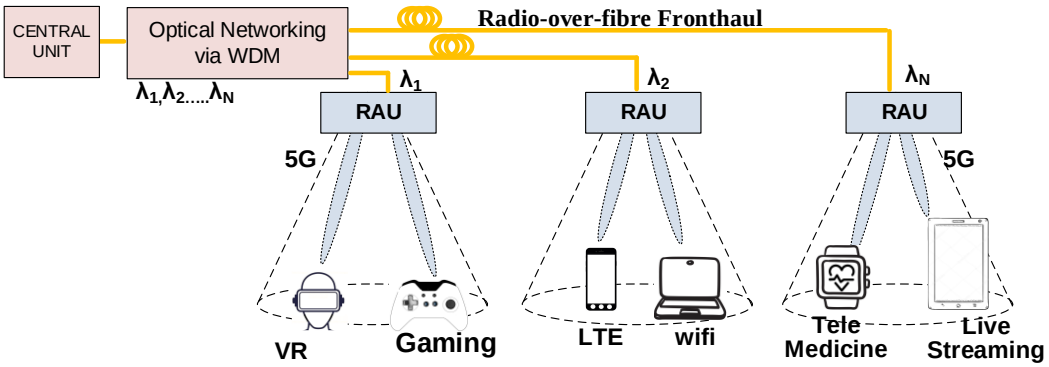

Figure. 1.1 RoF supported Heterogeneous network

Multiple-input multiple-output (MIMO) transmission makes use of spatial diversity to provide improved coverage, performance and stability of the wireless link. Higher data rates can be achieved with MIMO by multiplexing several data streams using spatial multiplexing [17]. For spatial diversity, transmitted data is encoded using Space-Time Block Coding (STBC) or Space-Frequency Block Coding (SFBC) and the improvement in performance is obtained by combined processing of the received signal. MIMO has been used previously in various mobile standards at microwave frequencies and still a key technology to be considered for mmW networks, as a solution to improve coverage and data rates. The deployment of mmW distributed MIMO systems will require RAUs to be placed at appropriate distances, to provide coverage at various user locations. RoF transport is thus a key technology for mmW MIMO transmission, by providing the centralized control and enabling wide physical spacings for RAUs. Fig. 1.2 shows a mmW distributed RAU based system where a RoF fronthaul is used to connect multiple RAUs to a Central Unit (CU), as might be expected in shopping malls, outdoor downtown areas, etc. The RAU1 depicts the user case when Gb/s service is provided to a user using a mmW link with a limited coverage region. The directional beam provides adequate coverage for the user to some extent but as the user moves, the SNR

degrades and becomes considerably low at the boundaries of the RAU1 coverage region. This results in a loss of transmission/connection from the RAU, and coordinated transmission with the adjacent RAU can be used as a solution to this problem. As shown in Fig. 1.2, two RAUs (RAU3 and RAU4) make use of spatial diversity to improve the coverage for the user over an increased area. The two RAUs transmit the same data encoded by a transmit diversity algorithm (such as STBC) to decorrelate the two signals. The coordinated multipoint transmission can also be used to increase the data rate by transmitting different data streams from two RAUs and combining them at the receiver using a spatial multiplexing algorithm (such as Minimum-Mean-Square Error or Zero Forcing).

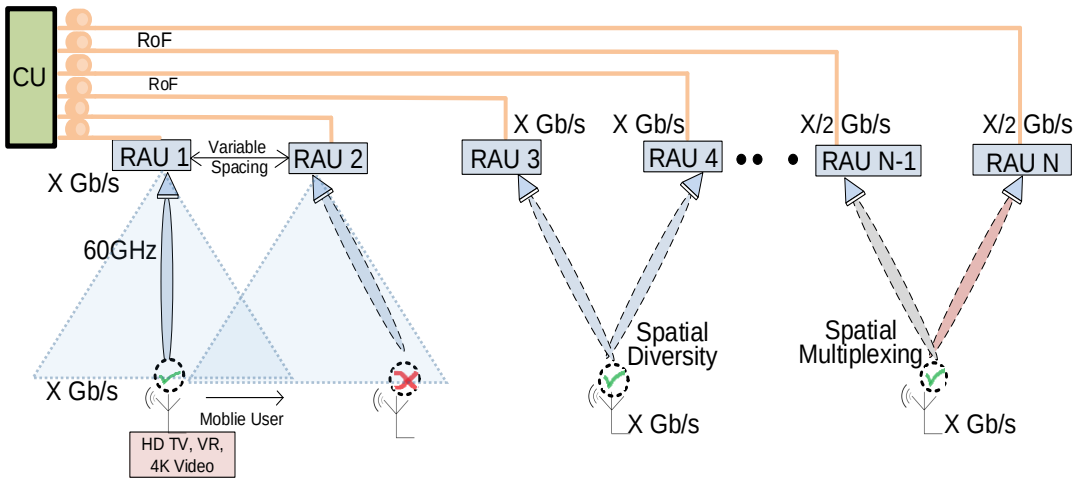

Figure 1.2 RoF supported Distributed RAU System for improvement in coverage and data rate

In addition to the challenges related to the coverage and implementation of distributed RAU system at mmW frequencies, another important design consideration for mmW future wireless systems is the support for large numbers of users from a single RAU. With the drastic increase in number of users, which is anticipated to grow at a much faster rate in future [18], dedicating a transmitting antenna to serve a single user will not be a feasible option. Large number of RF chains (with mmW components) and transmitting antennas will be required in dense user environments, to provide connectivity to each user at mmW frequency. The optimization techniques to reduce the number of required RF chains, such as Hybrid beamforming [19] and optimized beam allocation algorithm [20] can be used for state-of-the-art technologies such as Massive MIMO but still the amount of required hardware for multiple feeder chains to antenna arrays and computational complexity at the user end is a challenge for practical systems. Frequency-selective

antennas, such as Leaky-Wave-Antenna (LWA) operating in 60 GHz-band [21], which steer the beam to different angular locations according the change in carrier frequency of the input signal, can be used for multi-user transmission by using a multiple-frequency composite signal (using Frequency Division Multiplexing) and transmitting multiple beams towards spatially distributed users. The conversion of FDM to Spatial Division Multiplexing Access (SDMA) can provide a low-cost and low-complexity solution to multi-user transmission at mmW using a single RF chain and single transmitting antenna. The generation and transport of multiple user signals can be performed using a single RoF link with a multiplexing-over-fibre techniques such as Subcarrier Multiplexing (SCM) or Dense-Wavelength Division Multiplexing (DWDM).

1.2. Objectives of the research

The use of multiple antenna based techniques such as distributed Multiple-input-multiple-output (MIMO) have been targeted previously to improve the coverage and data rate at microwave frequencies, and thus can be considered for millimetre-wave (mmW) communication systems. As mmW transmission heavily depends on Line-of-sight (LOS) operation, the physical spacing between the transmitting antennas significantly affect the performance. It is still unclear how much improvement can be obtained from LOS based mmW MIMO systems *using specific MIMO algorithms* and for *several user locations* when the transmit antenna spacings or transmission distances are varied. As large number of Remote Antenna Units (RAUs) will be required at mmW frequencies for distributed MIMO operation, an analysis for *comparison of different mmW generation schemes* is required, to achieve a low cost and low complexity RAU design. Also, the issue of achieving *flexible and large spacing of the antennas* at mmW frequencies needs to be addressed, by using a fronthaul which can provide centralized access, high data rate capacity and low loss transport of MIMO signals from the Central Unit (CU) to the RAUs.

Secondly, the drastic increase in number of users and anticipated rise in the figures has caused an increased interest in Multi-user transmission techniques, which are mostly based on large numbers of RF chains and massive antenna arrays. The need

is for *a low cost and simple deign for mmW multi-user transmission* to serve a large number of spatially distributed users from a single RAU. This involves *experimental demonstration of various multiplexing-over-fibre techniques* to support the transport of multiple data signals from the CU to the RAU and transmission of user-signals at mmW using single RF chain and beamsteering characteristics of a frequency-selective antenna. Finally, the analysis on *increasing the number of users within a specific transmission bandwidth* is required and issues with frequency-selective transmission such as degradation of large bandwidth signals due to beamsteering effect, which can affect the total sum rate for large bandwidth user-signals, and low spectral efficiency and coverage needs to be considered.

1.3. Contribution of the Thesis

The unique contributions of this thesis include:

- Comparison of different RoF transport configurations and mmW generation techniques, which were only discussed individually beforehand. VPI modelling for performance analysis of RF-over-fibre systems, a sideband filtering of optical phase modulated signal based system and an MZM based system for mmW generation, along with an IF-over-fibre system have been performed through simulations, which can assist in selecting a particular scheme to design a downlink setup. For example, to understand that which setup requires less IF power, EDFA amplification or lower bandwidth for optical or RF components to meet a standard EVM requirement or receiver sensitivity.
- A unique downlink setup based on single optical Phase Modulator (PM), followed by a DWDM filter, has been presented which make use of a single laser source to generate two independent mmW separated optical two-tone signals, and generate low cost and stable mmW MIMO signals at the RAUs.
- Performance analysis of 25/60 GHz distributed MIMO *at various user locations* to understand *the amount of performance improvement* that can be achieved using *specific MIMO algorithms* for spatial diversity and spatial multiplexing, which was previously performed for single user location only

without comparison with SISO and algorithms used for mmW MIMO were unspecified. The experimental results on various RAU spacings verified that the proposed analog RoF fronthaul can provide flexible and wider spacings, in order to obtain optimum performance in mmW MIMO systems.

- An emulation of 2x2 mmW MIMO has been presented using single antenna pair and results verified that similar performance to that of mmW MIMO analysis using two antenna pairs is achieved. This shows that mmW channels are relatively static and enabled the extension of analysis to be performed at much longer distances.
- A low complexity and low cost system architecture has been proposed and experimentally demonstrated for RoF supported multi-user transmission in 60 GHz-band, for the first time, consisting of single RoF link, single RF chain and single transmitting antenna. The setup involves generation and RoF transport of a composite SCM signal, which is upconverted at the RAU and a frequency-selective antenna is used to achieve SDMA to transmit different frequency channels towards spatially distributed users.
- Analysis on SNR degradation of high bandwidth signals due to beamsteering effect of the LWA and estimation of sum data rate for different number of users, which is useful to characterize a multi-user system with mmW beamforming. It was also experimentally demonstrated that improvement in coverage and spectral efficiency is obtained by operating multiple LWAs using single RF chain.

1.4. Thesis Outline

The thesis is based on six chapters, including this one which presents the objectives, contributions and an outline of the other chapters. The detailed contents for rest of the chapters is as follows:

Chapter 2 presents the detailed background review of RoF modulation and transport techniques, with a description of different photonic techniques for mmW generation. A review is presented of LOS based mmW MIMO which achieves performance improvement through spatial diversity and spatial multiplexing. In addition, different multiplexing-over-fibre techniques and use of frequency

selective antennas to perform conversion of FDM to SDMA are discussed, for multi-user transmission at mmW frequencies.

Chapter 3 presents the simulation of different RoF transported mmW systems, based on the various RoF configuration and mmW generation techniques discussed in chapter 2, in an optical communication simulation software VPI™ for 25 GHz and 60 GHz transmission systems. Characterization of optical and RF components is performed to match the response of the components to be used in the experimental setup. Simulations are performed to analyse the performance of each technique through VPI models in terms of Error Vector Magnitude (EVM) and their feasibility is assessed for experimental work with the available components. VPI simulation models performing 25 GHz generation using sideband filtering of an optical phase modulated signal and 60 GHz generation using integrated devices are then extended to transmit and receive two independent data channels, to be used in experimental work on mmW MIMO in the next chapter.

Chapter 4 describes the experimental work on 25 GHz MIMO using DWDM-RoF setup and 60 GHz MIMO using DFB link and integrated transmitter/receiver based setup, as represented by the VPI models in Chapter 3. The improvement in coverage is achieved through spatial diversity and in data rate through spatial multiplexing, at several user locations using 2×2 MIMO operation. The effect of transmit antenna spacing is shown by analysing the EMV performance of MIMO transmission for different spacings at several wireless transmission distances. Experimental results to achieve optimum performance are compared with theoretical calculations and analogue RoF fronthaul is used to achieve the required flexible and wider antenna spacings at longer distances. An emulation of MIMO at 60 GHz is also performed, by measuring channel coefficients individually and performing MIMO processing on the captured data, and verified. Finally, the emulated MIMO is used to extend the analysis to much longer wireless transmission distances.

Chapter 5 presents a proposed low complexity and low cost multi-user mmW transmission technique which requires single RoF link, single RF chain and single transmission antenna, in order to serve multiple spatially distributed users with high data rates in the 60 GHz-band. It consists of the generation and transportation of a multi-user SCM signal from the CU using the RoF link, upconversion of the

composite signal to the 60 GHz-band at the RAU and transmission to multiple users using a single, frequency-selective Leaky Wave Antenna (LWA). The experimental implementation is performed using a DFB laser link for RoF transport and 60 GHz upconversion using an integrated transmitter, which were presented in Chapter 3. An analysis on effect of different user-signal spacings in the SCM signal and demonstration to serve large number of users is shown. Analysis on the SNR degradation of a large bandwidth signal due to the beamsteering effect of the LWA is performed and used to calculate the theoretical sum rate for different numbers of users within a specific transmission bandwidth. Improvement in spectral efficiency and coverage is shown by using two LWAs in cascade. A DWDM-RoF based setup for multi-user transmission is also presented, as another multiplexing-over-fibre technique, which was discussed in Chapter 2. Finally, the emulated MIMO technique presented in Chapter 4 is used to perform 2×2 operation using the LWA as the transmitter to show the flexibility offered by the LWA on analysis over multiple user locations, as it does not require mechanical tilting due to its beamsteering characteristics.

Chapter 6 concludes the work presented in this thesis. It also highlights suggestions for possible future work in this field.

REFERENCES

[1] S. Lee, M. Marcu and S. Lee, "An empirical analysis of fixed and mobile broadband diffusion", *Elsevier Journal of Information Economics and Policy*, Vol. 23(3-4), 2011, pp.227-233.

[2] Y. Niu, Y. Li, D. Jin, L. Su and A.V. Vasilakos, "A Survey of Millimeter Wave (mmWave) Communications for 5G: Opportunities and Challenges", *Wireless Networks (Springer)*, Vol. 21 (8), 2015, pp 2657–2676.

[3] Cisco Visual Networking Index, "Forecast and methodology, 2016-2021", *White paper*, San Jose, USA, 2016.

[4] J. Wells, "Faster Than Fiber: The Future of Multi-Gb/s Wireless," *IEEE Microwave Magazine*, Vol. 10 (3), 2009, pp. 104–112.

[5] IEEE Standards Assossiation, "IEEE 802.15.3c-2009 - IEEE Standard for Information technology-- Local and metropolitan area networks-- Specific requirements-- Part 15.3: Amendment 2: Millimeter-wave-based Alternative Physical Layer Extension", New York, 2009.

[6] Y. Ghasempour, C.R. da Silva, C. Cordeiro and E.W. Knightly, "IEEE 802.11 ay: Next-generation 60GHz communication for 100 Gb/s Wi-Fi", *IEEE Communications Magazine*, Vol. 55 (12), 2017, pp.186-192.

[7] T. Jasny, "New Approaches in the New Chapter of Telecommunications," *IEEE Communications Magazine*, Vol. 49 (10), 2011, pp. 20-22.

[8] N.J. Gomes, M. Morant, A. Alphones, B. Cabon, J.E. Mitchell, C. Lethien, M. Csörnyei, A. Stöhr and S. Iezekiel, "Radio-over-fiber transport for the support of wireless broadband services", *Journal of Optical Networking*, Vol. 8 (2), 2009, pp.156-178.

[9] D. Wake, A. Nkansah, P. Assimakopolous, N. Gomes, M. Violas, L. Zhansheng, S. Pato, F. Ferreira, G. De Valicourt, R. Brenot and F.V. Dijk, "Design and Performance of Radio Over Fibre Links for Next Generation Wireless Systems Using Distributed Antennas", *IEEE Future Network and Mobile Summit*, Italy, June 2010, pp. 1-9.

[10] C. Liu, L. Zhang, M. Zhu, J. Wang, L. Cheng and G.K. Chang, "A novel multi-service small-cell cloud radio access network for mobile backhaul and computing based on radio-over-fiber technologies", *Journal of Lightwave Technology*, Vol. 31 (17), 2013, pp.2869-2875.

[11] J. Yu, Z. Jia, L. Yi, Y. Su, G.K. Chang and T. Wang, "Optical millimeter-wave generation or up-conversion using external modulators", *IEEE Photonics Technology Letters*, Vol. 18 (1), 2006, pp.265-267.

[12] J. Yu, Z. Dong, X. Xiao, Y. Xia, S. Shi, C. Ge, W. Zhou, N. Chi and Y. Shao, "Generation, Transmission and Coherent Detection of 11.2 Tb/s (112x100Gb/s) Single Source Optical OFDM Superchannel", *Optical Fiber Communication Conference*, California, 2011, pp. 1-3.

[13] M. Maier, "WDM Passive Optical Networks and Beyond: the Road Ahead" *IEEE/OSA Journal of Optical Communications and Networking*, Vol. 1 (4), 2009, pp.1-16.

[14] S. Xiao and A. M. Weiner, "Four-user~3-GHz-spaced subcarrier multiplexing (SCM) using optical direct-detection via hyperfine WDM", *IEEE Photonics Technology Letters*, Vol. 17 (10), 2005, pp.2218-2220.

[15] D. Wake, "Trends and prospects for radio over fibre picocells", *International Topical Meeting on Microwave Photonics* , Awaji, Japan, 2002, pp. 21-24.

[16] N.J. Gomes, U. Habib, S. Noor, A.E. Aighobahi and P. Assimakopoulos, "Support of Multi-antenna and Multi-user Systems Using Radio Over Fiber", *Asia Communications and Photonics Conference*, China, 2017, pp. Su4E-1.

[17] G. Ntogari, T. Kamalakis and T. Sphicopoulos, "Analysis of Indoor Multiple-Input Multiple-Output Coherent Optical Wireless Systems", *Journal of Lightwave Technology*, Vol. 30 (3), 2012, pp.317-324.

[18] P. Cao and J.S. Thompson, "Practical multi-user transmission design in millimeter wave cellular networks: Is the joint SDMA-TDMA technique the answer?", *IEEE 17th International Workshop on Signal Processing and Advances in Wireless Communications (SPAWC)*, 2016, pp.1-5.

[19] F. Sohrabi and W. Yu, "Hybrid digital and analog beamforming design for large-scale antenna arrays", *IEEE Journal on Selected Topics on Signal Processing*, Vol. 10 (3), 2016, pp.501-513.

[20] J. Wang, H. Zhu, N.J. Gomes and J. Wang, "Frequency Reuse of Beam Allocation for Multiuser Massive MIMO Systems", *IEEE Transaction on Wireless Communications*, Vol. 17 (4), 2018, pp. 2346-2359.

[21] M. Steeg, N. Yonemoto, J. Tebart and A. Stohr, "Substrate-Integrated Waveguide PCB Leaky-Wave Antenna Design Providing Multiple Steerable Beams in the V-Band", *MDPI Electronics*, Vol. 6(4), 2017.

CHAPTER 2
BACKGROUND STUDY AND LITERATURE REVIEW

2.1. Introduction

Chapter 1 presented a brief overview of millimetre-wave (mmW) based multi-antenna and multi-user transmission with a focus on the advantages of using radio-over-fibre transport for such systems. The need for mmW multiple-input-multiple-output (MIMO) operation to improve coverage and data rate for mmW transmission, and single RF chain based design to serve multiple users were also discussed.

In this Chapter, RoF techniques for the generation and transport of mmW signals are discussed in detail with an explanation of different RoF modulation techniques. Following that, a detailed description of mmW MIMO systems, which improve the capacity and coverage of mmW based networks, is presented. A review has been performed of experimental setups reported in previous works for mmW MIMO systems using different types of RoF transport. Finally, an overview of multi-user transmission to support large numbers of users and state-of-the-art techniques used in recent work in this domain is presented, covering techniques to generate multi-user data, transporting the data over the RoF link and transmission at mmW frequencies.

2.2. RoF supported millimetre-wave (mmW) systems

Millimetre-wave (mmW) communication is considered to be a key enabling technology for the future wireless systems to provide multi Gb/s data rate services [1]. The availability of large bandwidth can meet the demands of service quality for bandwidth-hungry applications and simultaneously support the large number of users that need to be connected to the same network. While mmW transmission has been a topic of considerable interest in recent research due to the spectrum scarcity at microwave frequency bands, the high wireless transmission loss at mmW frequencies is a major bottleneck. Deployment of a large number of Remote Antenna Units (RAUs) to provide sufficient coverage for mmW systems is required, which also enables reuse of the spectrum at short distance intervals [2]. Thus the cost of a RAU is a major design consideration and it depends on several factors such the type of fronthaul and number of components required for mmW transmission. RoF technology can provide a promising solution to transport low frequency or mmW signals from CU to RAU with the advantages of centralized access, low cost transportation and support for high data rates [3] to address the key requirements of the future mobile systems.

The transport of wireless signals over optical fibre at the physical layer can be performed through digital or analog methods. The RF signal can be transported in three ways as shown in Fig. 2.1, depicting the RoF modulated signal configurations for the downlink system: baseband-over-fibre (digital), IF-over-fibre (analog) and RF-over-fibre (analog). Baseband-over-fibre offers the advantages of immunity towards distortions, maturity and robustness of digital components [4] but requires additional components at the RAU including Digital-to-analog converter (DAC), oscillators and mixers. By contrast, the Analog RoF is easy to implement, low-cost and is a more transparent method for integrating optical and wireless transmission than its digital counterpart [5]. The IF-over-fibre technique is based on low-bandwidth components for modulation and photonic mixing stages, as compared to RF-over-fibre, but requires an additional upconversion stage at the RAU to transmit RF signals where the requirements for RF LO are comparatively simpler than baseband-over-fibre technique.

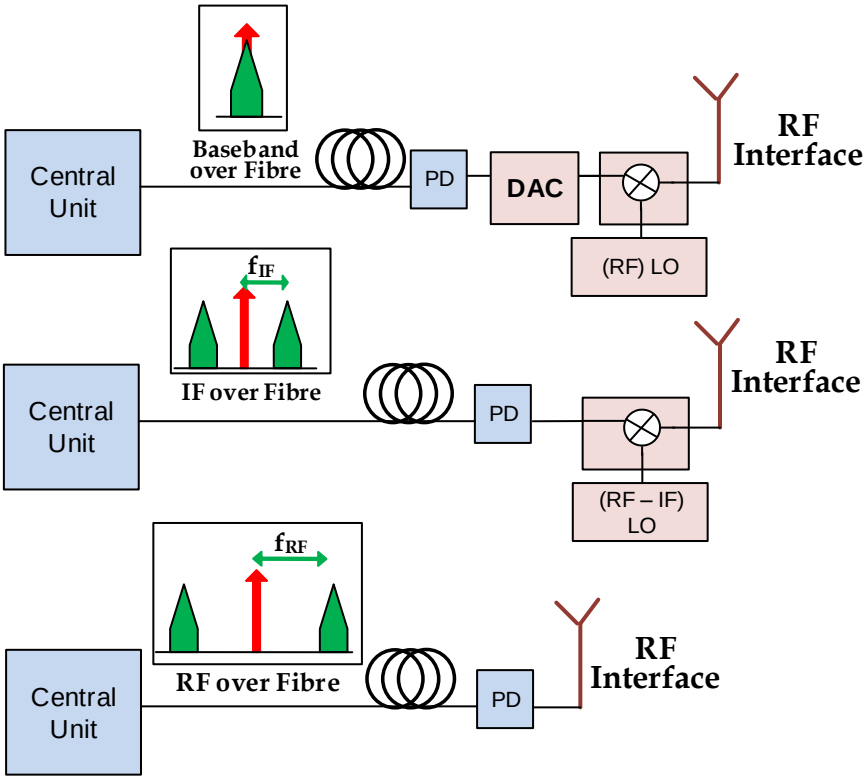

Figure. 2.1 Downlink system architecture and optical spectrum for different RoF configurations

2.2.1. Different Schemes for Photonic Generation of mmW

The two main approaches for intensity modulation direct detection (IMDD) based optical modulation in RoF systems are direct modulation and external modulation. In direct modulation, as the name suggests, the RF signal is directly modulated on to the optical carrier as shown in Fig. 2.2a. The signal directly modulates semiconductor lasers, which are commercial off-the-shelf (COTS) devices with low-cost, but are usually of lower bandwidth and require additional components to avoid wavelength drift. For high bandwidth applications, external modulation is preferred, which involves separate generation of the optical carrier and modulation of data as shown in Fig. 2.2b, where a Mach-Zehnder Modulator (MZM) is indicated in this case for the external modulation of the RF over optical link.

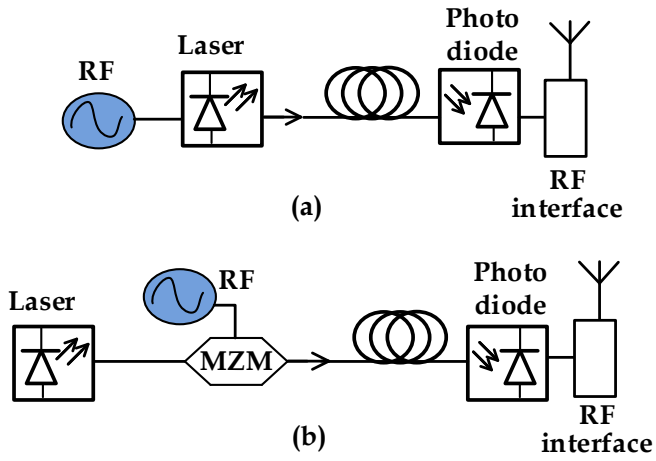

Figure. 2.2 (a) Directly modulated Laser based system (b) External modulation using MZM based system

Optical generation of mmW provides several advantages such as low-cost, flexibility for variable frequencies and availability of ultra-large bandwidth for transport from the CU (to support high data rates). Photomixing of two optical wavelengths, separated by mmW frequency difference f_{mmW}, using a high bandwidth photodiode generates a stable and continuous mmW signal with centre frequency at f_{mmW}. The two optical tones can be generated in several ways at the CU and then transported to the RAU for direct photonic upconversion. A simple method consists of optical heterodyning of two laser sources where the frequency separation between the wavelengths of the two lasers is selected to be f_{mmW}. An optical coupler can be used to combine the two wavelengths and resultant signal can be transported to the RAU using Single Mode Fibre (SMF) as shown in Fig. 2.3a. After direct photonic upconversion, the photodiode generates a signal at f_{mmW}. Though the scheme provides a simple mechanism, the two optical lines, being generated from different sources, are likely to be not correlated and have different phases, which produces high phase noise in the generated mmW signal. Of the two main approaches of the IMDD based methods, external modulation is preferred due to bandwidth limitations of directly modulated lasers, as high modulating RF signal are involved in the generation of the mmW signal. An optical phase modulator (PM) or MZM can provide a simple system architecture to generate the mmW signal. Fig. 2.3b shows the generation of an optical two-tone signal using a MZM which is driven by a RF source with frequency $f_{mmW}/2$. The double sideband modulation generates two sidebands which are separated by f_{mmW}; the MZM is biased at its minimum transmission point which provides maximum suppression of

the middle, carrier wavelength. The two-tone signal (with suppressed carrier) is transported to the PD to generate a mmW signal centred at f_{mmW}.

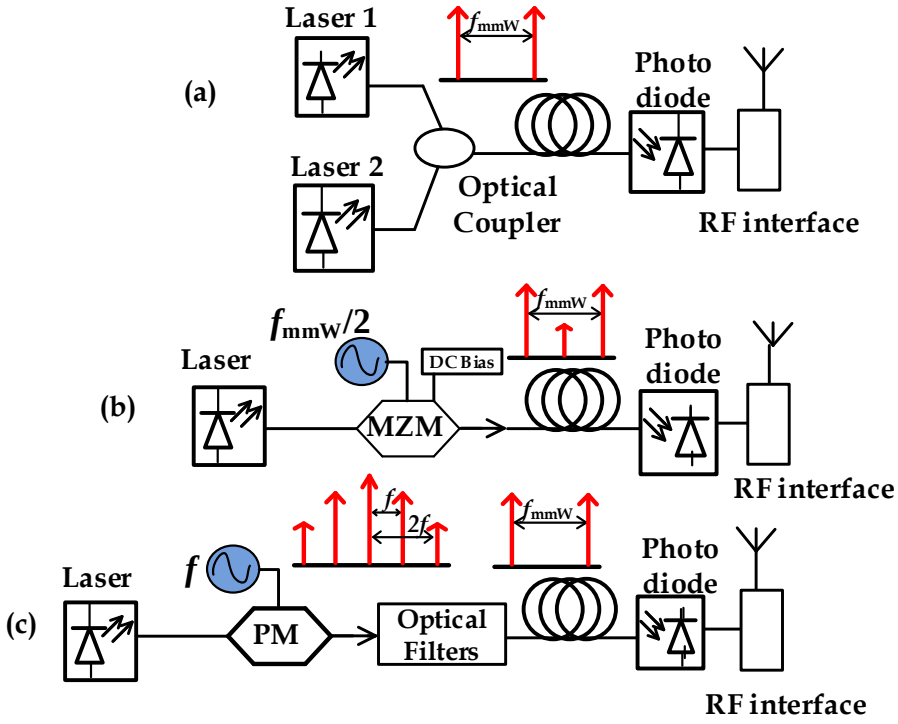

Figure. 2.3 Optical two-tone signal generation using (a) Optical Heterodyning (b) MZM biased at minimum transmission point (c) PM and optical filters to select the desired sidebands

Another scheme to photonically generate mmW frequencies involves an optical phase modulator (PM) followed by optical filters. As shown in Fig. 2.3c, the PM generates a set of multiple sidebands which are separated from each other by the applied RF frequency f and set of optical filters can be used to select the desired sidebands, and hence the mmW frequency. First order sidebands can be selected to achieve optical two tones separated by f_{mmW} when the PM is driven by RF signal with frequency of $f_{mmW}/2$. Similarly, second order sidebands can be spaced by f_{mmW} by driving the PM with an RF signal at $f_{mmW}/4$. Use of Dense Wavelength Division Multiplexing (DWDM) filters is a simple technique to obtain the desired frequency-spaced optical sidebands as shown in [6] where the output of a continuous wave laser was modulated by a PM with a 30 GHz RF signal. The 60GHz-separated upper and lower first order sidebands from the output of PM were filtered using a DWDM filter and combined using a 3dB optical coupler to obtain a 60 GHz spaced two-tone signal. The data signals at an Intermediate Frequency (IF) were modulated using an MZM and direct photonic upconversion was performed at the

RAU. The phase noise measurements on the generated mmW signals showed comparable temporal drift to that of the 30 GHz RF signal from the commercial signal generator which was used to modulate the PM. The high quality of mmW signal was due to high coherence between the optical wavelengths in the two-tone signal, as both were generated from the same laser source. Error Vector Magnitude (EVM) values for different QAM formats were under the limits indicated by wireless communication standards, which showed the capability of the generated mmW signal for data modulation, and the EVM results were found to be stable for over 128 minutes of measurement time.

Another design for optical generation of a two-tone optical signal consists of two cascaded optical filters in which one performs bandstop filtering and the other bandpass filtering. Fig. 2.4 shows the block diagram of the setup used in [7] where a 15 GHz pure sinusoidal signal was coupled with a pulse pattern generator generating downstream data at 1.25Gb/s and the combined RF signal was used to gain switch a directly modulated gain switched laser (GSL) biased at 43mA. The spectrum is shown in the inset as 15 GHz spaced optical comb lines, all of which were data modulated by the 1.25Gb/s stream. The output of the DFB laser consisting of nine spectral components, covering a spectral range of 120 GHz, was passed through a set of bandstop and bandpass filters to obtain a 60 GHz spaced two-tone optical signal. The first filter was used to supress the three optical comb lines in the centre, followed by a bandpass filter which only allowed two 60 GHz separated wavelengths. A suppression ratio (minimum) of 15dB was achieved with the cascaded filters between the two-tone signal wavelengths and unwanted suppressed optical comb lines. The output of the cascaded filters was amplified with an EDFA and transported over a SMF to the RAU, where a high bandwidth PD generates the data-modulated 60 GHz signal.

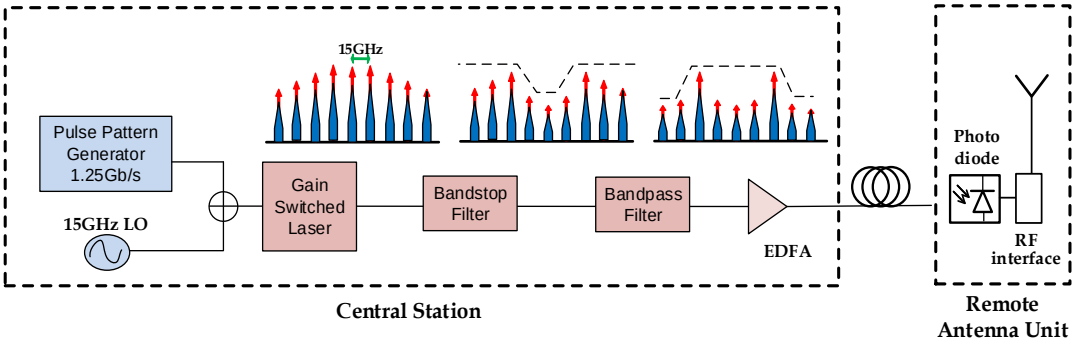

Figure. 2.4 Block diagram for setup used in [7] for generation of optical 60 GHz two-tone signal using cascaded operation of optical filters

A range of mmW frequencies can be generated by such techniques using tunable optical filters as demonstrated in [8] where 75 to 140 GHz mmW signals were generated using a PM and set of DWDM filters. A tunable laser source was modulated by a PM driven by different RF signals during the experiment, to generate a range of mmW frequency signals. The output of the PM was passed through an optical 200 GHz channel spaced DWDM thin film bandpass filter, followed by a 100 GHz DWDM filter bandstop filter. The central wavelength of the two cascaded filters was kept the same but different bandwidths were used such that the resultant optical filter had two passbands separated by the desired mmW frequency.

2.3. Line-of-Sight (LOS) based Multiple-input Multiple-output (MIMO) systems

Multiple-input-multiple-output (MIMO) has been incorporated in the latest standards (e.g LTE and IEEE 802.11n) [9] and has also been proposed for the next generation standards in mobile communication [10]. It provides increased reliability and capacity without additional power as compared to the conventional single-input-single-output (SISO) system. MIMO involves transmission of multiple signals which travel through different propagation channels and are received by multiple antennas as shown in Fig. 2.5, for a general MIMO configuration which involves M transmitting and N receiving antennas. The captured signals are processed at the receiver to achieve the advantages of MIMO transmission which involve either spatial diversity or spatial multiplexing [11], or both under certain conditions [12], which depends on the channel state [13].

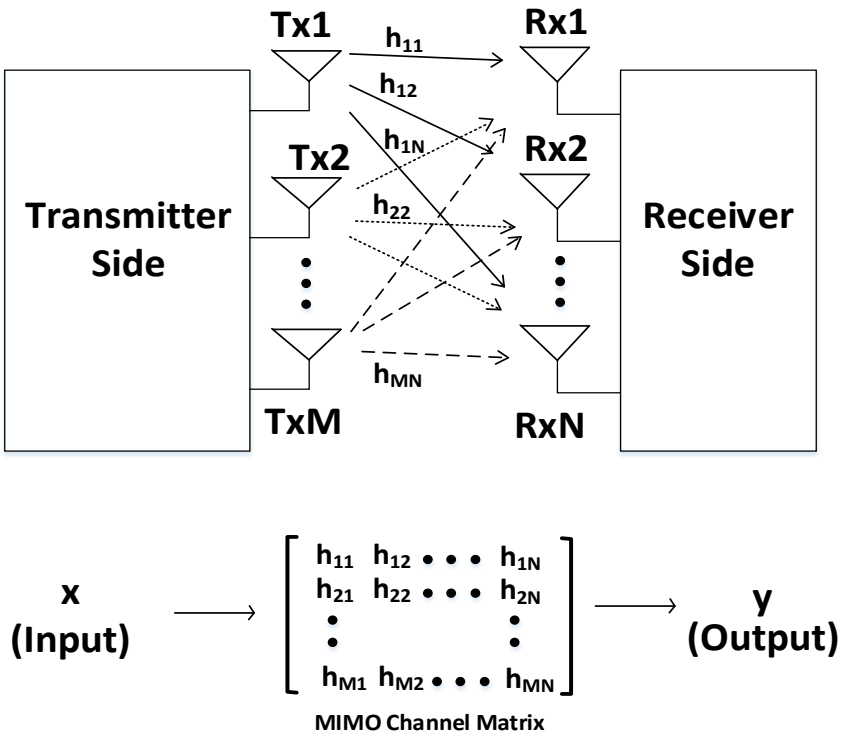

Figure. 2.5 Schematic of a MxN MIMO configuration with *M* transmitting and *N* receiving antennas

Considering the general form of MIMO represented in Fig. 2.5, for the 2x2 case (*M*=2, *N*=2), the relation between the received signals y_1,y_2 and transmitted signals x_1,x_2 can be given in the form of the following equation:

$$\begin{bmatrix} y_1 \\ y_2 \end{bmatrix} = \begin{bmatrix} h_{11} & h_{12} \\ h_{21} & h_{22} \end{bmatrix} \begin{bmatrix} x_1 & x_2 \end{bmatrix} \tag{2.1}$$

where h_{11}, h_{12}, h_{21} and h_{22} are the coefficients of the channel matrix *H* which is estimated at the receiver from the channel state information (CSI). The channel estimation can be performed through a number of methods including the use of preambles which are a defined set of symbols, known to both transmitter and receiver.

2.3.1 Spatial Diversity and Spatial Multiplexing in MIMO

Spatial diversity works on the principle that MIMO signals travel through different channel paths before they are received. The processing of different versions of the same transmitted signal improves the channel estimation, thus resulting in improvement in the performance of the link. It also enhances reliability of the link as more than one transmission path is available in this case and if one signal suffers from severe channel conditions, there is a possibility that another one will not and

the receiver will have at least one signal with good quality. However the capacity of the system remains the same as the same data is used for different transmission signals [14]. Such spatial diversity can be of different types: transmit diversity, receiver diversity or it can involve both depending on the implementation, i.e, the number of antennas on the transmitter or receiver side. Using transmit diversity, the antennas at the transmitter side are placed in a way that the signals emanating from them are made independent of each other and follow different spatial paths for propagation. The receiver diversity is usually implemented with multiple antennas at the receiver side and achieved when different versions of the same signal are available at the receiver, with having small delays or phase difference. Multiple antennas at the receiver are useful, as simultaneous drop outs at two receiving antenna locations is very unlikely. Combining diversity techniques such as Maximal-ratio combining (MRC) [15], selection combining [16] and switching combining [17] can be used to process the multiple received signals, in order to minimize the impact of channel effects. Another type of diversity involves multiple antennas at both transmitter and receiver side which provides higher order of diversity, such as using two receive antennas to perform 2x2 MIMO operation using Alamouti Space-time-block-coding (STBC) [18].

Spatial multiplexing provides improvement in the overall capacity, and thus data rates, by transmitting different data through multiple transmission paths which are combined at the receiver to achieve multiplexing gain. The most common type of combining technique at the receiver side employs the Zero-forcing algorithm [19] which is a linear detection technique to achieve spatial multiplexing. The diversity order increases with the increase in number of receiving antennas, however the maximum possible diversity is achieved when all channel coefficients are independent to each other.

2.3.2. Decorrelation of MIMO channels in LOS scenario

MIMO can improve the performance of the wireless transmission through multiple signals travelling through different paths but the performance of MIMO operation highly depends on the level of decorrelation among the multiple MIMO signals. In case of non-Line-of-Sight (non-LOS) transmission for MIMO operation, the received signals are decorrelated because they undergo reflections (single or multiple) from different objects. Thus, in the presence of a rich multipath

environment, the correlation among different signals in terms of amplitude and phase is low, as received signals travel through different channels. Thus, optimum MIMO performance can be achieved when received signals are completely decorrelated from each other. In contrary, high correlation is present among the signals in LOS based transmission and in the worst case, all components in the MIMO channel matrix in (2.1) will be identical. In that case the capacity of a MIMO system will become equal to that of a SISO system [20]. As mmW systems suffer from high wireless transmission loss, a strong LOS component is required to achieve necessary system performance. The separation between the antennas is an important factor for LOS MIMO operation as the decorrelation between the signals can be introduced by changing the physical spacing among the transmitting or receiving antennas (or both), and studies have shown that MIMO gain can be obtained in LOS transmission [21], [22] with an appropriate geometric arrangement of antennas. A combination of MIMO and mmW communication can provide a promising solution for multi Gb/s data rates with increased coverage, reliability and capacity. It has been shown that mmW MIMO can exploit the legacy benefits of conventional MIMO using spatial diversity and spatial multiplexing techniques applied to either transmitter or receiver side [23]. The decorrelation among the LOS MIMO channels is obtained by generating a static phase shift between the different received signals, by changing the spacing between the transmit (or receive) antenna units [24]. The phase of the channel coefficient h_{MN} (for MxN MIMO) varies with the wavelength (at which MIMO operation takes place) [25] as well as being dependent on the geometry, which includes both the separation between the transmit/receive antennas and the wireless transmission distance.

The correlation among the MIMO channels can be represented by the condition number (CN) of the channel matrix *H*. CN is defined as the ratio of the maximum to minimum singular values of the channel matrix [26]. Small values of CN represents good amount of decorrelation among the MIMO channels while higher values indicates ill-conditioned channel matrix, thus can be used to indicate the capability of the MIMO channel. Experimental work on LOS MIMO at mmW shows that low values of CN requires optimal spacing between the transmitting antennas which changes with the transmission distance [27].

2.3.3. Analog RoF Fronthaul for mmW MIMO

The antenna separation required to obtain optimum MIMO performance in LOS transmission can be obtained through geometrical analysis. The optimum spacing will provide minimum level of decorrelation among the MIMO channels and thus providing maximum capacity that can be achieved. For a MxN MIMO system, let d_{Tx} be the separation between the transmitting antennas and d_{Rx} between the receiving antennas as shown in Fig. 2.6. The transmit antennas can be tilted by θt and receive antennas by θr to provide in the plane of transmission. Then for MIMO operation with N number of antennas, operating at frequency having wavelength of λ and at wireless transmission distance D, the smallest optimum performance from the LOS operation of MIMO can be achieved when the following condition is met [28],[29]:

$$d_{Tx}d_{Rx} = D\lambda / \mathrm{Max}(M,N)\cos\theta_t \cos\theta_r \tag{2.2}$$

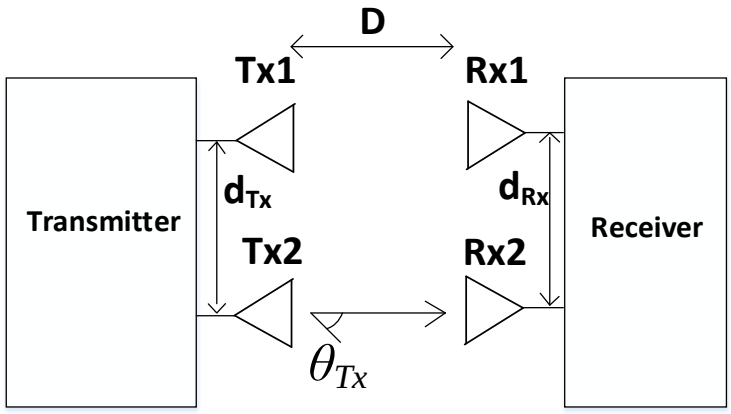

Figure. 2.6 2x2 LOS MIMO configuration

As the optimum antenna spacing increases with transmission distance, larger transmit antenna spacing will be required for longer distances (with a fixed receive antenna spacing). Using RF cables (especially at mmW frequencies, if required) to achieve the required spacing between different antennas will affect the system performance with bending and twisting of RF cables. For this reason, a flexible front haul which can provide larger spacings is required that can support low cost, low loss and high data rate at the mmW. Analog RoF fronthaul can provide a promising solution with flexibility to achieve any transmit antenna spacing, in order to achieve optimum results with MIMO operation and thus has been considered in this thesis, as will be discussed later.

2.3.4. System architecture for RoF based millimetre-wave MIMO systems

Different RoF transport schemes can be used for mmW MIMO systems, as experimentally demonstrated in recent work. The two MIMO data signals can be generated from independent sources which are transported over two RoF links. Alternatively, single data signal can be used by transporting it over a single SMF, using an optical splitter at the RAU end and introducing decorrelation in one of the RoF link to achieve two MIMO channels. In former case, where two MIMO signals are generated at the CU, [30] reports the use of single laser source for RoF transport of MIMO signals by generating an optical two-tone signal and splitting it to modulate the two MIMO signals. A software defined radio (SDR) was used to generate the two MIMO data streams at 0.74 GHz IF and space-frequency block coding (SFBC), derivation of traditional STBC Alamouti algorithm, is applied to achieve transmit diversity. Optical two-tone signal was generated by modulating the optical carrier with a 29.24 GHz RF signal using a PM. The two 58.48 GHz separated first order sidebands from the output of the PM were filtered out using a set of two inter-leavers and then combined using an optical coupler. The resultant optical two-tone signal was amplified using EDFA and divided into two paths to upconvert the two data signals. The data streams were modulated over the 58.48 GHz separated two-tone wavelengths using a set of identical MZMs and transported to the RAUs using a pair of 50m SMF. At each RAU, a 60 GHz bandwidth PD performed mixing of the data modulated optical signals and the generated mmW signal was amplified before transmission using 15dB gain horn antenna. At the receiver end, the received signal was amplified and downconverted to IF using mmW envelope detector. Another SDR was used to perform equalization and SFBC decoding at the receiver end. This technique requires use of two inter-leavers and passing both wavelengths (of the two-tone signal) from the MZM for data modulation which introduces considerable optical loss to the data modulated two-tone signal, transported from CU to RAU. RoF transport of the two low frequency MIMO signals generated at the CU can be performed using a pair of modulating lasers. After the IF-over-fibre transport to the RAU, the MIMO signals at intermediate frequency (IF) can be upconverted to mmW frequencies using a set of similar integrated transmitters as reported in [31].

Alternatively, a single data signal can be generated at the CU which is modulated onto an optical carrier to perform RoF transport over a single fibre. In [32], a 2x2 60 GHz MIMO system supported by RoF transport presents such a system where baseband IQ data was generated from an AWG. The signal was upconverted to 25 GHz by using an IQ mixer and 25 GHz LO as shown in Fig 2.7. A composite RF signal was formed by adding a 35.5 GHz LO to the data modulated signal. The optical two-tone signal was generated by driving an MZM with the composite RF signal. The output of the MZM was amplified using an EDFA and transported over single SMF to the RAU where a 3dB optical splitter was used to transport the optical signal to two antenna units. The decorrelation in optical path for one of them was introduced by using an additional 1km of SMF. A set of similar 60 GHz PDs was used to generate the two MIMO signals which were transmitted using a pair of 24dB gain horn. The received signals were downconverted using a 56 GHz LO to be captured by the oscilloscope. In [33], a similar example is demonstrated where the generated IQ signal was upconverted to 22 GHz and coupled with a pure sinusoidal 38.5 GHz RF signal to form a composite signal which was then used to drive a MZM, biased at minimum transmission point, to generate four set of wavelengths with suppressed carrier. The output of the MZM was amplified by 20dB and passed through an inter-leaver to supress one data modulated sideband and an unmodulated wavelength to produce 60.5 GHz separated two-tone signal. The two-tone signal comprising of a data modulated sideband and an unmodulated wavelength was split in two paths for the two transmitting antennas. A 1.5km SMF was added to one optical path to decorrelate the two signals for the two RAUs.

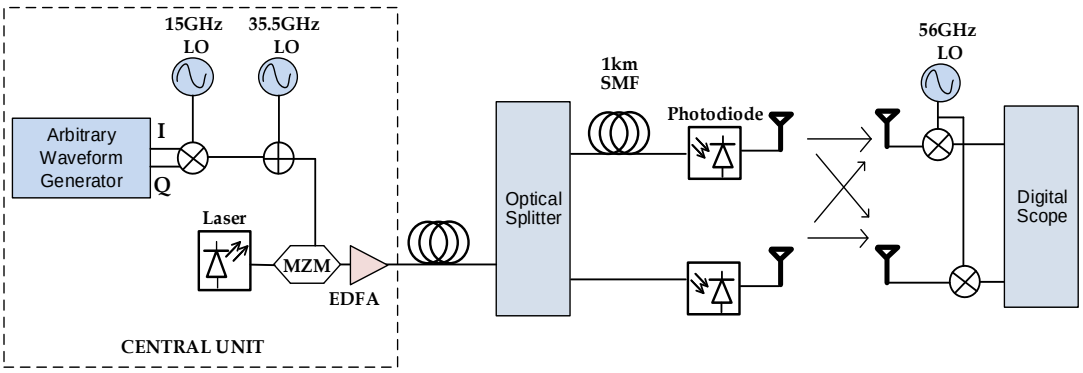

Figure. 2.7 Experimental setup used in [32] for 2x2 MIMO using IQ generation of data and direct photonic upconversion

Optical Time Division Multiplexing (OTDM) [34] can also be used to transport two separately generated MIMO signals over a single fibre link from the CU to the RAUs. In [35], two OFDM signals for MIMO operation were generated and multiplexed in time domain at the Central Office (CO) and after RoF transport over a SMF, an optical switch was used to perform de-multiplexing. At the CO, a 30 GHz LO was used to drive a PM to generate 60 GHz separated sidebands with the optical carrier in the middle. A set of MIMO signals with 400MHz bandwidth were generated in MATLAB and combined to single TDM signal by using 0.5 GHz clock sequence. The output of the PM was passed through an MZM for data modulation and optical interleavers was used to select the two 60 GHz separated sidebands. The optical two-tone signals was amplified and transported over 25km of SMF, after which it was split in to two paths and optical switches were used to de-multiplex data signal for each transmitting antenna unit which comprised of a 60 GHz PD, a RF amplifier and a horn antenna. The use of TDM requires complex processing at the receiver end which was emulated by individual measurement of channel coefficients and performing offline MIMO processing afterwards. For such type of setup, the two MIMO signals can be transported over single SMF at the cost of additional complexity at the CO, transmitting units and receiver end.

2.4. Multi-user 60 GHz Transmission for Future Systems

In addition to improvement of coverage at mmW, design considerations for future mobile communication systems should also include multi-user transmission as the number of users are growing at a rapid rate [36]. Especially in case of large outdoor events or traffic jams where large number of people are concentrated in a small region [37]. To support large number of users from a RAU, multiple RF chains and large numbers of antennas are required [38]. The cost of overall system, especially in design of RAU where multiple high cost mmW components are required per RF chain [39], is thus an important consideration for the future mobile systems.

Multiple access schemes such as Time Division Multiple Access (TDMA) or Frequency Division Multiple Access (FDMA) allows the limited spectrum to be shared among the users by assigning different time slots or different frequencies to the users, respectively. Spatial Division Multiple Access (SDMA) can be used to take advantage of the spatially located users and serve them at the same time and

frequency. Multi-user MIMO is one of the state-of-the-art technique to serve several users using SDMA [40]. MU-MIMO operation is performed by using a large number of antennas at the transmitter side [41], hence will require same amount of RF chains at the RAU. Thus the cost and complexity of the RAU and the amount of signal processing that is required at the user end is a major issue. Using one transmit antenna per user at the RAU is a minimum design requirement for such systems, where the number of RF chains can be reduced to some extent by performing optimization through hybrid beamforming [42]. In addition to the high cost of required components for multiple RF chains for such systems, using same frequency for multiple users increases the risk of interference which requires complex techniques for suppression of inter-user interference [43]. In contrast to that, the combination of FDM and SDMA can provide the advantages of both frequency and spatial diversity at the same time. The antennas which can perform FDM to SDMA conversion at the RAU can be used as key components to enable multi-user transmission using separate frequency for each user [44]. Such antennas provide transmission of a range of frequencies to different directions by generating multiple beams with distinct central frequency, each of which is directed towards a particular angular location.

RoF can provide simultaneous transport of multiple RF signals to the RAU through different multiplexing-over-fibre techniques such as wavelength division multiplexing (WDM) or Subcarrier Multiplexing (SCM). Multiple channels can be used to carry data for different users, which is generated at the CU and transported over a single fibre. At the RAU, use of directive steerable antennas can then be used to direct each channel towards a particular spatial location.

2.4.1. Multiplexing-over-fibre techniques

Optical fibres are capable of transporting extremely high data rates (up to TB/s) but the practical speeds are limited by the non-linear effects and bandwidth of the electronic components in the transmission system [45]. Transport of multiple signals over the single fibre can increase the capacity of the system which can be accomplished in time or frequency domain. Optical TDM over RoF transport [34] can be performed by either encoding data signal on an optical pulse stream or by generating TDM signal in electric domain and modulating it over a CW laser. In

both cases, an ultra-fast optical clock is required at the receiver to recover the data which needs to be synchronized with the CU. The cost and complexity involved in such systems can be reduced by using frequency domain techniques for multiplexing. The simultaneous transmission of multiple channels can be obtained through WDM or SCM. Channel multiplexing through WDM is performed using several optical sources to provide multiple distinct wavelengths [46]. Each wavelength is modulated with data and the subsequent optical signals are multiplexed using a WDM multiplexer such as an Arrayed Waveguide Grating at the transmitter as shown in Fig. 2.8. The combined wavelengths are transported over a single fibre from the CU to the RAU where a de-multiplexer is employed to separate each channel's wavelength.

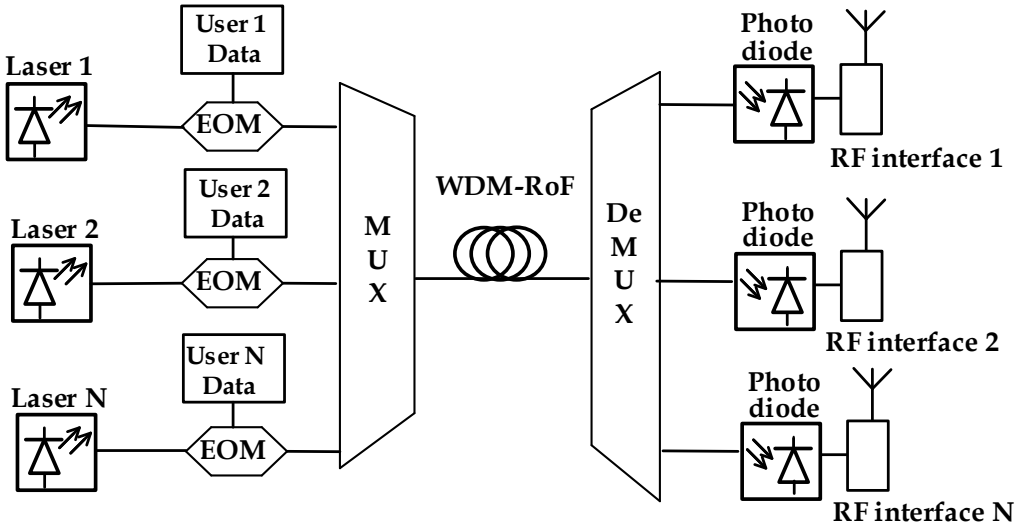

Figure. 2.8 WDM-RoF based Multi-user transmission

The ITU-T recommendation for DWDM supports channel spacing from 12.5GHz to 100GHz (and multiples of 100GHz) [47]. Smaller channel spacings can be achieved using electrical domain generation and filtering of channels, such as in SCM. Also, an important issue related to WDM systems is the carrier wavelength (or frequency) stability, as it changes with the operating temperature of the lasers [48]. Additional components and complex techniques are required for stabilization such as electrical feedback locking [49] or optical phase locked loop [50]. In comparison to WDM, SCM is a technique in which multiple RF channels are generated at different carrier frequencies and are added together using a power combiner to form a composite RF signal. At the receiver end, each channel is separated using a bandpass filter, centred at subcarrier frequency, and demodulated

[51]. SCM can be used for multi-user transmission by using individual subcarrier for a particular user's data and modulating the composite RF signal over a single wavelength as shown in Fig. 2.9. After RoF transport, a single PD performs the photo-mixing and the set of subcarriers are sent to RAUs where a bandpass filter is used to select a particular subcarrier. The filtered SCM subcarrier is upconverted to mmW frequency using a high frequency LO and RF mixer at each RAU [52]. Alternatively, the generated SCM signal consisting of multiple IF user signals can be transported over mmW separated optical two-tone signal [53]. The photonic upconersion from the PD at the RAU generates the subcarriers at mmW frequencies.

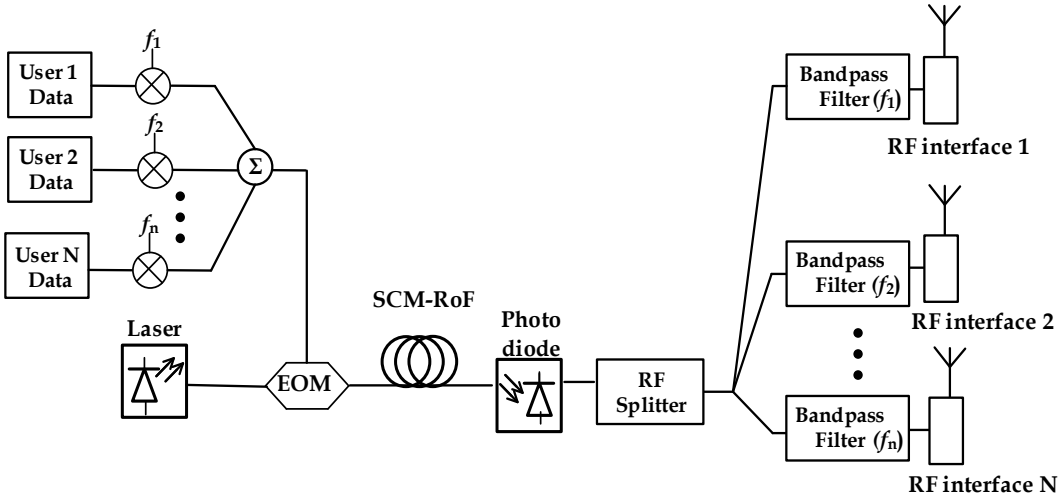

Figure. 2.9 SCM-RoF based Multi-user Transmission

In SCM, the stability of RF oscillators and the high frequency selectivity of RF filters allows a large number of data channels to be placed within a specific bandwidth [54]. Thus SCM offers a low cost and highly bandwidth efficient multiplexing-over-fibre scheme as compared to the WDM. Also the RF oscillators are more stable than optical lasers and channel selectivity of RF filters is better than WDM filters. SCM and WDM can be used together to achieve high spectral efficiency and ultra-large capacity in a multi-user network as proposed in the [55]. The simulation model is shown in Fig. 2.10 where 16-QAM modulated 100MB/s data was generated for each user and signal for the first user was upconverted using 625MHz LO. Different SCM subcarrier spacings were used during the analysis. The composite SCM signal was modulated over an optical carrier using MZM. The same set of SCM subcarrier frequencies were used to generate another set of users

which were modulated over a different wavelength and modulated optical signals were combined to obtain the WDM signal. WDM channel spacings of 50, 100, 200 GHz were used to analyse the effect of performance limitations of such system. The SCM-WDM signal was amplified using EDFA and transported over a single fibre link. At the other end, a de-multiplexer was used to direct each optical carrier towards the intended station. Similar set of SCM subcarrier LOs were used to recover each user signal.

Other multiplexing schemes such as polarization multiplexing (PoMUX) can be used in addition to SCM-WDM based system, to further enhance the capacity of the system as demonstrated in [56] where WDM based multi-user transmission system with four DFB lasers (each modulating a SCM signal of four users) with 50 GHz channel spacing uses PoMUX to form 32 channels.

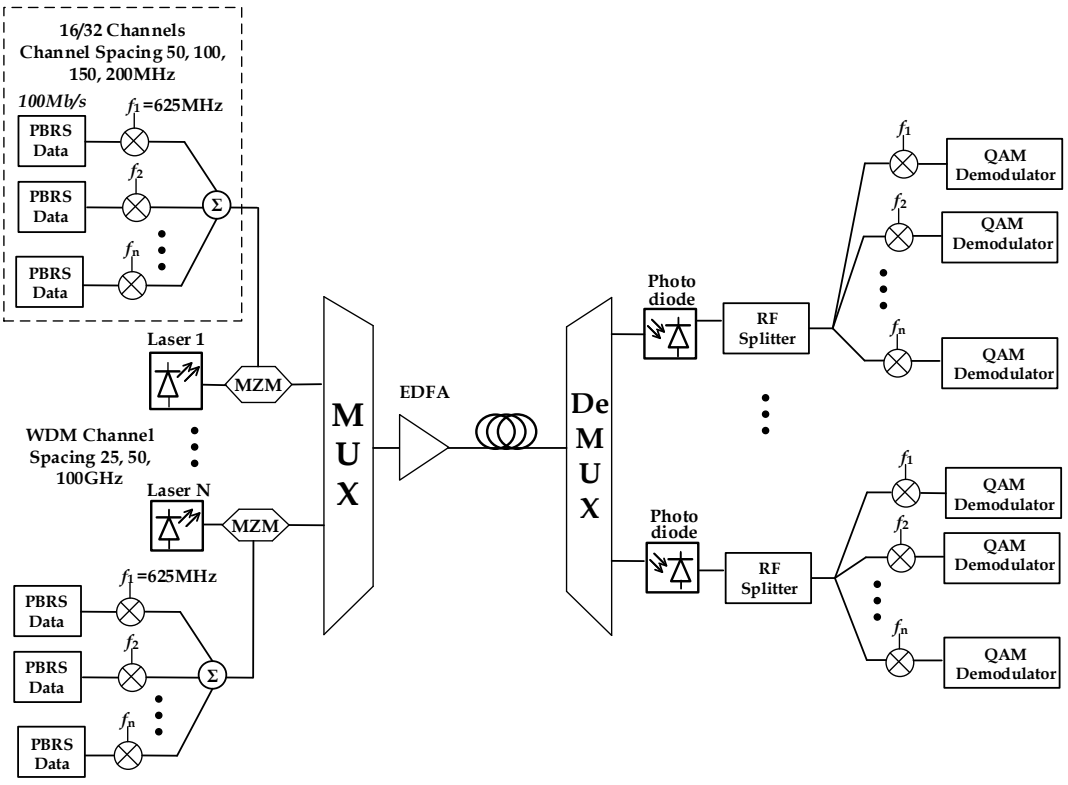

Figure. 2.10 Simulation configuration used in [34] for SCM-WDM based Multi-user Transmission

2.4.2. Antenna Beamsteering for Multi-user transmission

After RoF transport of data channels at the RAU, the transmission to the intended user for each channel needs to be performed. Conventional high gain antennas at mmW can mitigate the transmission loss but beamsteering characteristics are required to allow user mobility or to serve a large number of users in a dense user

environment, by directing beams towards different spatially distributed users. By using frequency-selective directive antennas [57] which can generate beam towards different spatial locations, depending on the frequency of the input signal, a low-cost and low-complexity solution to provide SDMA can be obtained. The Leaky Wave Antenna (LWA) reported in [58] is an example of such an antenna which has been used for experimental work on multi-user transmission in this thesis. Such antennas change the angle of transmission with the carrier frequency as shown in Fig. 2.11. The conversion of multiplexing-over-fibre to SDMA at the RAU to achieve spatial-frequency diversity can be achieved by feeding the RoF transported composite signal, comprising of several data channels, to the antenna. Thus multiple channels are transmitted in different angular locations, towards the intended users, and the overall multi-user transmission is achieved using single RF chain.

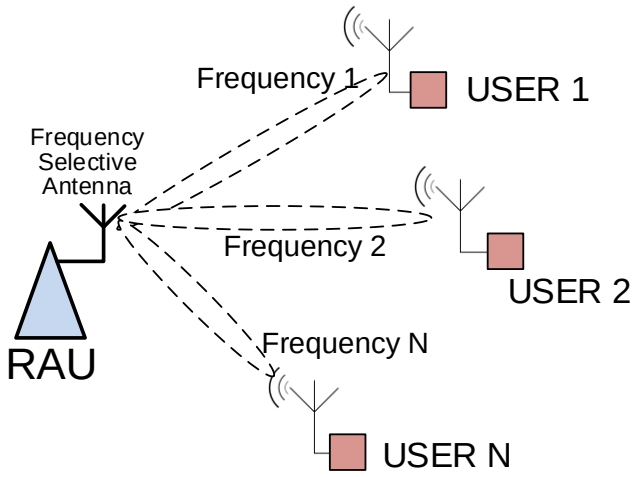

Figure. 2.11 Transmission to different spatial locations using single Frequency-selective antenna

2.5. Summary

This chapter presented a detailed description of different RoF transport configurations and modulation schemes for future mmW based systems. Different RoF configurations were presented and it was discussed that Analog RoF provides lower cost and complexity to support mmW transmission, than its digital counterpart. Also, it was discussed that direct modulation method is useful for low frequency applications where upconversion to mmW is performed at the RAU and external modulation technique is more suitable where high frequency is modulated at the CU. Different techniques for photonic generation of mmW were discussed and the experimental setup reported in previous work was reviewed to explore the feasibility of each approach. High quality and stable mmW can be generated through the generation of an optical two-tone signal from a single laser source and performing direct photonic upconversion at the RAU, but it requires high bandwidth modulators and PDs along with set of optical filters.

In addition, it was discussed that issues related to coverage at mmW can be addressed using multi-antenna (MIMO) operation exploiting spatial diversity and spatial multiplexing. The importance of antenna spacing to achieve decorrelation of MIMO channels in LOS operation has been explained and it was discussed that larger spacings are required for longer transmission distances for optimum MIMO performance, for which RoF fronthaul can be used as a flexible, low cost and low loss technique. System architecture for RoF transport and mmW generation to perform MIMO was reviewed as stated in the recent work, explaining different techniques for generation and transport of MIMO channels to the two RAUs.

Finally, a discussion on multi-user transmission at mmW to serve a large number of users with low cost and low complexity RAU design has been performed. Frequency domain multiplexing-over-fibre techniques, WDM and SCM, were explained to provide RoF transport of data for multiple users from CU to the RAU. It was discussed that SCM can offer better spectral efficiency and performance, due to legacy robustness of RF oscillators and frequency selectivity of RF filters, as compared to WDM technique. Transmission of multi-user data from a single RAU using frequency-selective beam steerable antenna was also discussed, which can convert the multiplexing-over-fibre transport to SDMA. Such antennas direct

different data channels at distinct frequencies towards multiple spatially distributed users. The multi-user operation was performed using multiple RF chains or multiple antennas in previous work but it is discussed that combination of frequency and spatial diversity in a multiplexing-over-RoF supported frequency-selective beamsteering antenna system can serve multiple users at mmW frequencies using single RF chain and single transmit antenna, as a low-cost low-complexity solution.

REFERENCES

[1] S. Rangan, T. S. Rappaport and E. Erkip, “Millimeter-wave cellular wireless networks: Potentials and challenges”, *Proceedings of the IEEE*, Vol. 102 (3), 2014, pp. 366–385.

[2] R. Magueta, D. Castanheira, A. Silva, R. Dinis and A. Gameiro, "Hybrid iterative space-time equalization for multi-user mmW massive MIMO systems." *IEEE Transactions on Communications*, Vol. 65 (2), 2017, pp.608-620.

[3] N. J. Gomes, P. P. Monteiro, and A. Gameiro, “Next Generation Wireless Communications Using Radio over Fiber”, *John Wiley & Sons*, Inc., 2012.

[4] C. Lim, A. Nirmalathas, D. Novak and R. Waterhouse, “Optimisation of baseband modulation scheme for millimetre-wave fibre-radio systems”, *Electronics Letters*, Vol. 36 (5), 2000, pp. 442-443.

[5] L. Kazovsky, W. Shing-Wa, T. Ayhan, K. M. Albeyoglu, M. R. N. Ribeiro, and A.Shastri, "Hybrid Optical-Wireless Access Networks," *Proceedings of the IEEE*, Vol. 100 (5), 2012, pp.1197-1225.

[6] P. Shen, A. Nkansah, J. James and N.J. Gomes, "Multilevel modulated signal transmission for millimeter-wave radio over fiber system", *IEEE International topical meeting on Microwave photonics (MWP)*, Australia, 2008, pp.27-30.

[7] H. Shams, P. M. Anandarajah, P. Perry and L. P. Barry, "Photonic generation and distribution of a modulated 60 GHz signal using a directly modulated gain switched laser", *21st Annual IEEE International Symposium on Personal, Indoor and Mobile Radio Communications*, Instanbul, 2010, pp.1032-1037.

[8] P. Shen, J. James, N.J. Gomes, P.G. Huggard and B.N. Ellison, "Low-cost, continuously tunable, millimeter-wave photonic LO generation using optical phase modulation and DWDM filters", *IEEE Photonics Technologies Letters*, Vol. 20 (23), 2008, pp.1986-1988.

[9] K. Issiali, V. Guillet, G. E. Zein andG. Zaharia, "IEEE 802.11 ac multi-user MIMO capacity and impact of antenna array geometry based on indoor measurements", *IEEE 26th Annual International Symposium on In Personal, Indoor, and Mobile Radio Communications (PIMRC)*, 2015, pp.726-730.

[10] S.A. Busari, K.M.S. Huq, S. Mumtaz, L. Dai, and J. Rodriguez, "Millimeter-wave massive MIMO communication for future wireless systems: A survey", *IEEE Communications Surveys & Tutorials*, Vol. 20 (2), 2017, pp.836-869.

[11] A.E Aighobahi and N.J. Gomes, "Capacity and Error Performance Verification of Multi-Antenna Schemes in Radio-over-Fiber Distributed Antenna System", *Journal of Lightwave Technology*, Vol. 34 (40), 2016, pp.4779-4785.

[12] A. Lim and V.K. Lau, "On the fundamental tradeoff of spatial diversity and spatial multiplexing of MISO/SIMO links with imperfect CSIT", *IEEE Transactions on Wireless Communications*, Vol. 7 (1), 2008, pp.4186-4190.

[13] C.B. Chae, A. Forenza, R.W. Heath, M.R. McKay and I.B. Collings, "Adaptive MIMO Transmission Techniques for Broadband Wireless Communication Systems" *IEEE Communications Magazine*, Vol. 48 (5), May 2010, pp. 112-118.

[14] A. Lozano and N. Jindal, "Transmit diversity vs. spatial multiplexing in modern MIMO systems", *IEEE Transactions on Wireless Communications*, Vol. 9 (1), 2010, pp.186-197.

[15] Y. Jing, "Combination of MRC and distributed space-time coding in networks with multiple-antenna relays", *IEEE Transactions on Wireless Communications*, Vol. 9 (8), 2010, pp.2550-2559.

[16] L.C. Lin, M. Guo and K.T. Wong, "Two-branch selection in wireless space-diversity reception: an upper bound for its output power", *IEEE Transactions on Communications*, Vol. 60 (2), 2012, pp.537-546.

[17] A.B. Narasimhamurthy and. C. Tepedelenlioğlu, "MIMO receive switched diversity with imperfect channel", *IEEE 43rd Asilomar Conference on Signals, Systems and Computers*, California USA, 2009, pp.1392-1396.

[18] P. Mishra, G. Singh, R. Vij and G. Chandil, "BER analysis of Alamouti space time block coded 2× 2 MIMO systems using Rayleigh dent mobile radio channel", *IEEE 3rd International Advance Computing Conference (IACC)*, 2013, pp. 154-158.

[19] C. Wang, E.K. Au, R.D. Murch, H.W. Mow, R.S. Cheng and V. Lau, "On the performance of the MIMO zero-forcing receiver in the presence of channel

estimation error", *IEEE Transactions on Wireless Communications*, Vol. 6 (3), 2007, pp.805-810.

[20] L. Hanlen and A. Grant, "Capacity analysis of correlated MIMO channels", *IEEE Transactions on Information Theory*, Vol. 58 (11), 2012, pp.6773-6787.

[21] T. Halsig, D. Cvetkovski, E. Grass and B. Lankl, "Measurement results for millimeter wave pure LOS MIMO channels", *IEEE Wireless Communications and Networking Conference (WCNC)*, 2017, pp. 1-6.

[22] B.S. Kim, M.S. Kang, K.S. Kim, W.J. Byun, M.S. Song and H.C. Park, "18 GHz 2× 2 analog LOS MIMO test-bed system with fully controlled ICM", *IEEE International Conference on Information and Communication Technology Convergence (ICTC)*, 2016, pp. 1023-1025.

[23] W. Roh, J.Y. Seol, J. Park, B. Lee, J. Lee, Y. Kim, J. Cho, K. Cheun and F. Aryanfar, "Millimeter-wave beamforming as an enabling technology for 5G cellular communications: Theoretical feasibility and prototype results", *IEEE Communication Magazine*, Vol. 52 (2), 2014, pp. 106–113.

[24] L.S. Joon, M.G. Kyeong and L.W. Yong, "Capacity analysis of MIMO channel with line-of-sight and reflected paths for millimeter-wave communication", *IEEE 4th International Conference on Signal Processing and Communication Systems (ICSPCS)*, 2010, pp.1-5.

[25] I. Sarris and A. R. Nix, "Design and performance assessment of high-capacity MIMO architectures in the presence of a line-of-sight component", *IEEE Transactions on Vehicular Technology*, Vol. 56 (4), 2007, pp.2194-2202.

[26] Q.H. Abbasi, H. El Sallabi, E. Serpedin, K. Qaraqe and A. Alomainy, "Condition number variability of ultra wideband MIMO on body channels", *IEEE International Workshop on Antenna Technology (iWAT),* 2016, pp.167-169.

[27] Y. H. Cho and J. J. Kim, "Line-of-Sight MIMO Channel in Millimeter-Wave Beamforming System: Modeling and Prototype Results", *IEEE 81st Vehicular Technology Conference (VTC Spring)*, Glasgow, 2015, pp. 1-5.

[28] F. Bohagen, P. Orten and G. Oien, "Modeling and analysis of a 40 ghz mimo system for fixed wireless access", *IEEE 61stVehicular Technology Conference (VTC)*, Sweden, 2005, pp. 1691–1695.

[29] J. Onubogu, K. Ziri-Castro, D. Jayalath, and S. Hajime, “Experimental evaluation of the performance of MIMO-OFDM for vehicle-to-infrastructure communications”, *EURASIP Journal on Wireless Communications and Networking*, 2015, Vol. 183, pp.1–19.

[30] L. Cheng, M.M.U. Gul, F. Lu, M. Zhu, J. Wang, M. Xu, X. Ma and G.K. Chang, "Coordinated Multipoint Transmissions in Millimeter-Wave Radio-Over-Fiber Systems", *Journal of Lightwave Technology*, Vol. 34 (2), 2016, pp. 653-660.

[31] D. Cvetkovski, E. Grass, T. Hälsig and B. Lankl, "Hardware-in-the-loop demonstration of a 60GHz line-of-sight 2× 2 MIMO link", *17th IEEE International Conference on Smart Technologies (EUROCON)*, MACEDONIA, 2017, pp. 631-636.

[32] C.H. Ho, W.R. Jiang, R. Sambaraju, W.Y. Lee, T.H. Lu, C.Y. Wang, H. Yang, C.T. Lin, C.C. Wei, S. Chi and A. Ngoma, "Performance Evaluation of a 60 GHz RoF System Employing MIMO and OFDM Modulation", *IEEE Journal on Selected Areas in Communications*, Vol. 31 (12), 2013, pp. 780-787.

[33] C.T. Lin, A. Ng’oma, W.Y. Lee, C.C. Wei, C.Y. Wang, T.H. Lu, J. Chen, W.J. Jiang and C.H. Ho, "2× 2 MIMO radio-over-fiber system at 60 GHz employing frequency domain equalization", *Optics Express*, Vol. 20 (1), 2012, pp. 562-567.

[34] T. Tashiro, K. Miyamoto, K. Hara, T. Taniguchi, J.I.Kani, N. Yoshimoto, K. Iwatsuki, T. Nishiumi, T. Higashino, K. Tsukamoto and S. Komaki, "Broadband ubiquitous network based on RoF-DAS over WDM-PON", *IEEE Optical Fiber Communication Conference and Exposition and the National Fiber Optic Engineers Conference (OFC/NFOEC)*, 2011, pp. 1-3.

[35] M. Zhu, S.H. Fan, L. Zhang, C. Liu, T. Wang and G.K. Chang, "High Speed MIMO-OFDM Wireless Data Transport in 60-GHz Radio-over-Fiber System Multiplexed by Optical TDM", *Optical Fiber Communication Conference and Exposition (OFC/NFOEC)*, 2013, pp. 1-3.

[36] A.A. Dulaimi, X. Wang and C.Lin I, "5G Networks: Fundamental Requirements, Enabling Technologies, and Operations Management", *John Wiley & Sons*, 2018

[37] A. Osseiran, J.F. Monserrat, and P. Marsch, "5G mobile and wireless communications technology", *Cambridge University Press*, 2016.

[38] M. Vu and A. Paulraj, "MIMO wireless linear precoding", *IEEE Signal Processing Maganize*, Vol. 24 (5), Sep. 2007, pp. 86–105.

[39] T. S. Rappaport, J. N. Murdock, and F. Gutierrez, "State of the art in 60-GHz integrated circuits and systems for wireless communications," *Proceedings of the IEEE*, Vol. 99 (8), 2011, pp. 1390–1436.

[40] P. Kela, X. Gelabert, J. Turkka, M. Costa, K. Heiska, K. Leppänen and C. Qvarfordt, "Supporting Mobility in 5G: A comparison between Massive MIMO and Continuous Ultra Dense Networks", *IEEE International Conference on Communications (ICC)*, May 2016.

[41] E. Aryafar, N. Anand, T. Salonidis and E.W. Knightly, "Design and experimental evaluation of multi-user beamforming in wireless LANs", *16th Annual International Conference on Mobile computing and networking (ACM)*, 2010, pp.197-208.

[42] F. Sohrabi and W. Yu, "Hybrid digital and analog beamforming design for large-scale antenna arrays", *IEEE Journal on Selected Topics in Signal Procssing*, Vol. 10 (3), 2016, pp.501-513.

[43] K. Takinami, H. Motozuka, T. Urushihara, M. Kobayashi, H. Takahashi, M. Irie, T. Sakamoto, Y. Morishita, K. Miyanaga, T. Tsukizawa and N. Saito, "A 60GHz hybrid analog/digital beamforming receiver with interference suppression for multiuser gigabit/s radio access", *IEICE Transaction of Electronics*, Vol. E99-C (7), 2016, pp. 856-865.

[44] T.A. Milligan, "Modern Antenna Design", Second edition, *Wiley-IEEE press*, 2005.

[45] G.P. Agrawal, "Multichannel systems" in Fibre-optic communications systems, Third edition, *John Wiley and Sons*, 2002.

[46] B. Xu and M.B. Pearce, "Multiuser detection for WDM fiber-optic communication systems", *IEEE International Symposium on Information Theory*, 2002, pp.474.

[47] International Telecommunications Union, Tech Recommendation, "Spectral grids for WDM applications: DWDM frequency grid", G. 694.1, 2012.

[48] A. Asmari, J. Hodgkinson, E. Chehura, S.E. Staines and R.P. Tatam, "All-electronic frequency stabilization of a DFB laser diode", *Optics Express*, Vol. 25 (10), 2017, pp.11679-11691.

[49] M. Funabashi, H. Nasu, T. Mukaihara, T. Kimoto, T. Shinagawa, T. Kise, K. Takaki, T. Takagi, M. Oike, T. Nomura and A. Kasukawa, "Recent advances in DFB lasers for ultradense WDM applications", *IEEE Journal of selected topics in quantum electronics*, Vol. 10 (2), 2004, pp.312-320.

[50] V. Ferrero and S. Camatel, "Optical phase locking techniques: an overview and a novel method based on single side sub-carrier modulation", *Optics Express*, Vol. 16(2), 2008, pp.818-828.

[51] C. Sierens, D. Mestdagh, G.V.D. Plas, J. Vandewege, G. Depovere and P. Debie, "Subcarrier Multiple Access for Passive Optical Networks and Comparison to Other Multiple Access Techniques", *IEEE GLOBECOM*, Arizona, 1991, pp.619-623.

[52] S. Liu, Y.M. Alfadhli, S. Shen, H. Tian and G.K. Chang, "Mitigation of Multi-user Access Impairments in 5G A-RoF-based Mobile Fronthaul utilizing Machine Learning for an Artificial Neural Network Nonlinear Equalizer", *Optical Fiber Communications Conference and Exposition (OFC)*, 2018, pp. 1-3.

[53] L. Zhang, M. Zhu, C. Ye, C. Liu, S.H. Fan, Z. Li, X. Hu, Y. Su and G.K. Chang, "Multi-service, multi-band, and MIMO data distribution over 60-GHz RoF system for gigabit wireless local area networks", *In Asia Communications and Photonics Conference (ACP)*, China, 2012, pp. ATh2C-2.

[54] R. Hui, B. Zhu, R. Huang, C.T. Allen, K.R. Demarest and D. Richards, "Subcarrier multiplexing for high-speed optical transmission", *Journal of Lightwave Technology*, Vol. 20 (3), 2002, pp.417-427.

[55] K. Kim, J. Lee and J. Jeong, "Performance limitations of subcarrier multiplexed WDM signal transmissions using QAM modulation", *Journal of Lightwave Technology*, Vol. 27 (18), 2009, pp.4105-4111.

[56] J. Fan, Y. Shao and N. Chi, "Novel 32× 1.25-Gb/s WDM-PoMUX-IDMA Multiuser RPON Scheme and Its EXIT Analysis", *IEEE Photonics Technology Letters*, Vol. 24 (21), 2012, pp.2183-2186.

[57] E.R. Castillo, P. Harati, I. Kallfass, P. Hugler, C. Waldschmidt and S. Shiba, "Spatial-Frequency-Scanning Data Transmission for mmW Multi-User Wireless Communication Systems", *47th European Microwave Conference*, Nuremberg, Germany, Oct 2017, pp. 220-223.

[58] M. Steeg and A. Stöhr, "High data rate 6 Gbit/s steerable multibeam 60 GHz antennas for 5G hot-spot use cases", *IEEE Photonics Society Summer Topical Meeting Series (SUM)*, 2017, pp.141-142.

CHAPTER 3
ANALYSIS OF RADIO-OVER-FIBRE TRANSPORTED MILLIMETRE WAVE SYSTEMS THROUGH SIMULATIONS AND EXPERIMENTS

3.1. Introduction

This chapter describes the simulations of the RoF transported mmW communication systems in an optical communication simulation software, Virtual Photonics Inc ® (VPI), and the experimental implementation of RoF transport setup, which have been considered in this thesis for mmW MIMO and multi-user transmission. The VPI software package provides modelling for a large variety of optical and RF components used in the entire downlink system from Central Unit (CU) to the Remote Antenna Unit (RAU), and from RAU to the user end. It allows the characterization of components through sets of parameters that can be varied according to the experimental responses. Initial characterization of available components (MZM, RF amplifiers, EDFA, Photodiode, Optical Phase modulator) is performed through experiments, which are then modelled in the VPI environment, according to their actual responses, to be used in downlink system simulations. The objective of these simulations is to test and investigate the performance of different models for RoF transport and mmW generation (25 GHz and 60 GHz) which will require different sets or combinations of optical and RF components. VPI provides a series of suitable analyzers/visualizers including optical spectrum analyzer, RF spectrum analyzer, and constellation diagram plotter to analyze the signals at different stages. It also allows performing sweeps to analyze the performance for a range of parametric values. Simulation results for SISO transmission models have been verified by carrying out experiments using the same set of components.

Simulation models are then extended to 2x2 MIMO transmission models which have been used in the mmW MIMO experiments, as explained in the next chapter.

3.2. Component Modelling in VPI

VPI provides a wide range of module parameters for the components to design and characterize them according to their actual response. The set of global parameters provides the common settings for various parameters (such as time resolution or sampling rate). The time and frequency resolution for the simulation is set by the parameters TimeWindow and SampleRateDefault. There are a few restrictions on the values of these two parameters. As the VPI simulator runs with the FFT algorithm [1], the number of samples *N* should be a power of two (2^n). The relation between the SampleRateDefault, TimeWindow and *N* can be given as:

$$N = \text{TimeWindow} * \text{SampleRateDefault} \tag{3.1}$$

3.2.1. OFDM signal Generation and Demodulation

The block diagram of a general OFDM generator is shown in Fig. 3.1 which uses a Quadrature Amplitude Modulation (QAM) encoder to map the input data bit stream to complex symbols (I+jQ), each representing a specific point on the constellation diagram. The IQ symbols are mapped to orthogonal subcarriers using the IFFT operation. The generated I and Q time-domain sample are passed through Digital-to-Analog converters and the resultant waveforms are upconverted by using a RF LO. At the receiver end, the signal is downconverted to baseband and the FFT operation is performed to recover the QAM modulated symbols.

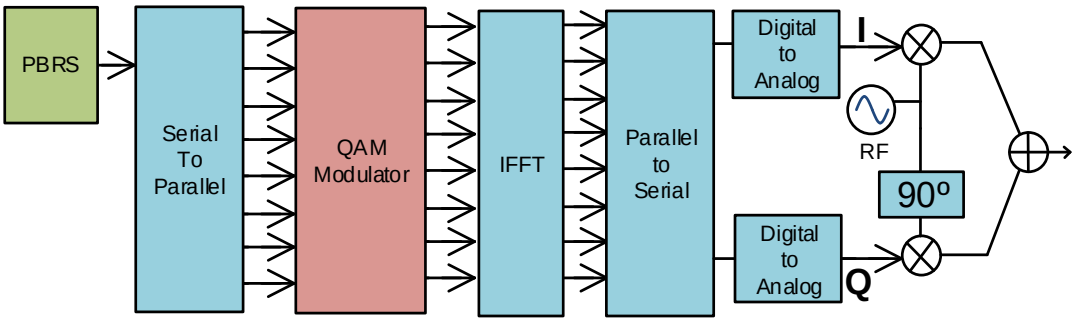

Figure. 3.1 Block diagram for OFDM Signal Generation and Upconversion

In VPI, the OFDM signal generator module comprises of a Pseudo Random Binary Sequence (PRBS) generator whose output is modulated using an OFDM coder block as shown in Fig. 3.2. The OFDM coder produces I and Q baseband streams

which are passed through a set of similar pulse shaping filters. An RF generator is modelled as a Sine Function generator, which is split using a fork, with one output used by a 90° phase shifter in order to obtain a cosine signal, these two signals upconverting the I and Q streams to an Intermediate Frequency (IF) as shown in Fig. 3.2. The upconverted signals are combined to obtain an OFDM signal centred at the IF. The OFDM block provides a set of parameters to allow selection of the QAM modulation level, baud rate, number of subcarriers, percentage of cyclic prefix, centre frequency for IF upconversion etc. For an IF of 1.5 GHz, using 16-QAM modulation, filter type of Square Root Raised Cosine and bandwidth of 512MHz, the generated signal is shown in Fig. 3.3, as observed by using a spectrum analyser in VPI. The demodulator block consists of downconversion stage, followed by a set of low pass filters. The baseband I and Q signals are converted to symbols and transmission performance is evaluated using a DSP block.

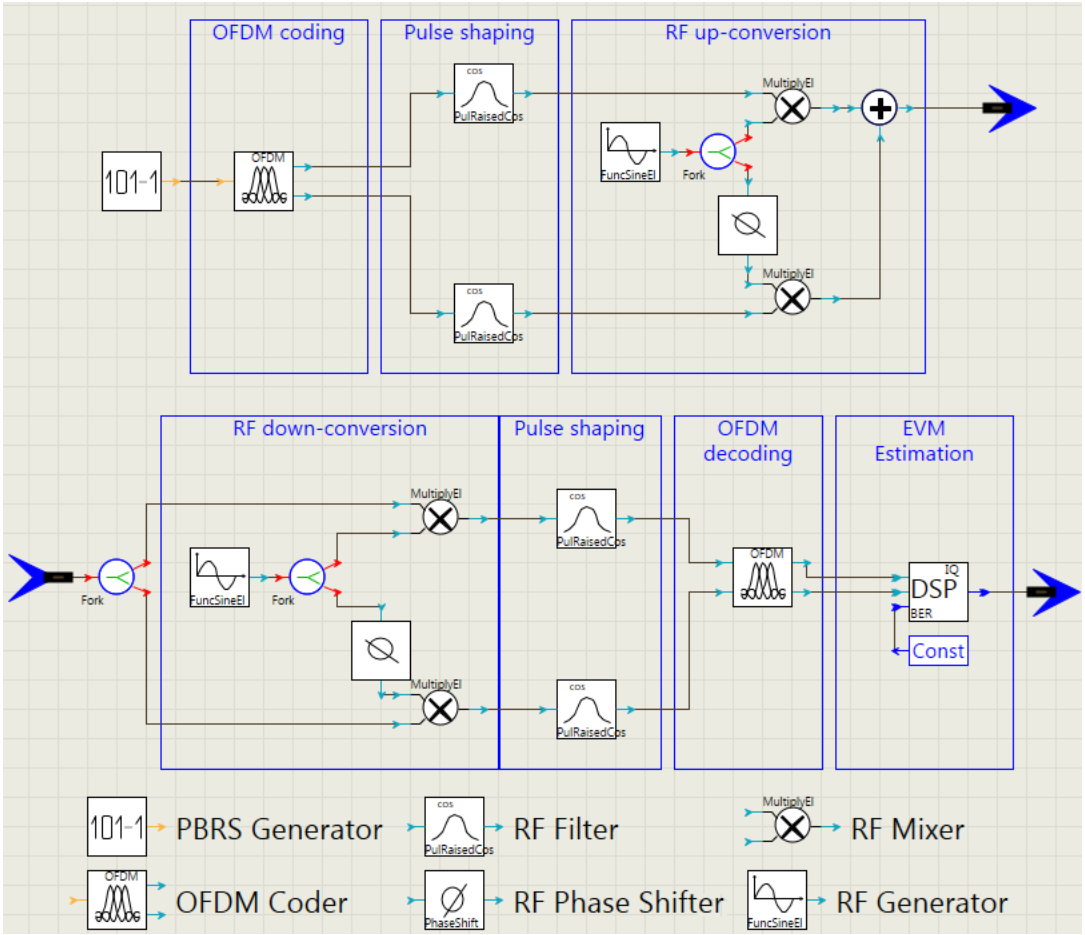

Figure. 3.2 VPI model for OFDM Signal Generation and Upconversion to IF

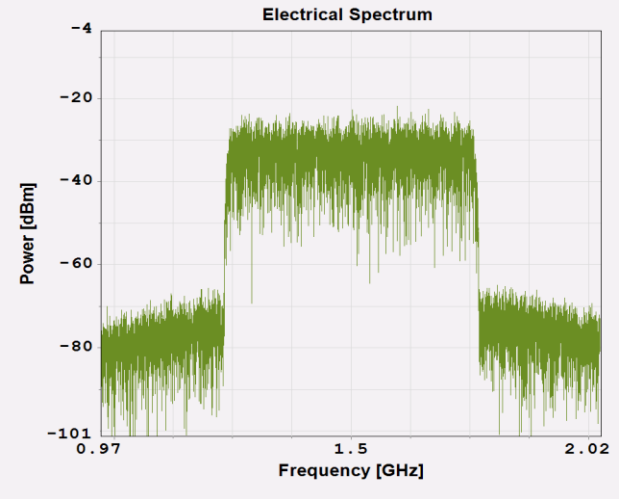

Figure. 3.3 RF spectrum of 512MHz OFDM signal centred at 1.5 GHz IF

3.2.2. Error Vector Magnitude

The figure of merit used in this thesis for the system performance is error vector magnitude (EVM). EVM is a standard metric for performance measurement in wireless and wireline communication systems with phase-amplitude or quadrature-amplitude modulation. EVM represents the effective distance of the received symbols from the ideal constellation points [2]. Fig.3.4a shows the ideal constellation points for a 16-QAM modulation format, in which each symbol consists of 4 bits resulting in a total of 16 possible points (2^4) on the constellation plane. For a received signal vector *E*r shown in Fig.3.4b, the EVM is the measure of deviation vector E_{error} of the received vector from the ideal vector *E*i. The difference values are averaged over a considerable number of symbols to increase the accuracy of the results. The EVM for the overall transmission system is commonly presented as a percentage.

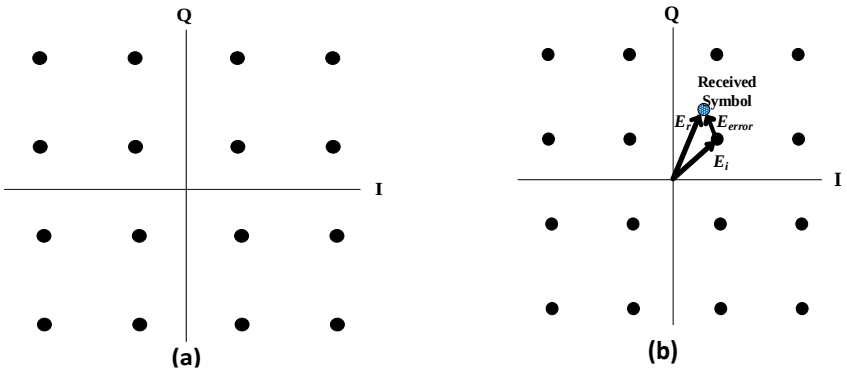

Figure. 3.4 (a) Ideal constellation diagram for 16-QAM modulation (b) Error vector between received symbol and ideal constellation point

For K number of unique symbols, the mathematical expression for the EVM [3] can be given as:

$$\mathrm{EVM}_{\mathrm{RMS}}\ (\text{in }\%) = \sqrt{\frac{\frac{1}{K}\sum_{k=0}^{K-1}\left|S_k - S_{0,k}\right|^2}{\frac{1}{K}\sum_{k=0}^{K-1}\left|S_{0,k}\right|^2}} \times 100 \tag{3.2}$$

where S_k and $S_{0,k}$ represents the normalized k_{th} measured symbol and normalized ideal constellation vector for that particular symbol, respectively. The EVM (represented as a percentage) from (3.2) and Signal-to-Noise Ratio (SNR) are related to each other [4] by following equation:

$$\mathrm{SNR}(dB) = -20\log_{10}(\mathrm{EVM}/100) \tag{3.3}$$

The minimum requirement for EVM for different modulation formats in LTE [5], [6] are given in Table. 3.1. However these requirements are for relatively small bandwidth signals and for the transmitter side. For an end-to-end system, the requirement would be higher than these values. In this thesis, for performance measurements, we have used the transmitter requirement for EVM for different modulation formats to compensate for the increase in bandwidth in our system compared to LTE and/or to allow for the addition of another power amplifier before the transmitting antenna to achieve much longer wireless distances.

Table. 3.1 Transmitter side EVM Requirement for LTE

Modulation Scheme	EVM Requirement for Transmitter	SNR (dB)
4-QAM	17.5%	15.14
16-QAM	12.5%	18.06
64-QAM	8%	21.9

3.2.3. Noise Figure of components

VPI does not provide a direct input value for the Noise figure F of optical or RF components. Instead, the noise figure is modelled as a Current Noise Spectral Density, I_n. The relation between the two can be derived and stated as [7], [8]

$$F = 10\log_{10}\left(1+\frac{RI_n^2}{2kT}\right) \tag{3.4}$$

The unit for I_n is $amps/\sqrt{Hz}$. T denotes the room temperature, R is the termination resistance and k is the Boltzmann constant. For T=290 K, k=1.38×10^{-23} J/K and R = 50Ω, the I_n can be calculated for a component with a specific noise figure. The I_n is calculated for the three amplifiers which are available for the experiments and will be used for the downlink setup later in this chapter, using the noise figure from their datasheets. The I_n becomes 12.62×10^{-12} $amps/\sqrt{Hz}$ for the low noise amplifier having 3dB noise figure (used before capturing the data with the oscilloscope), 18.6×10^{-12} $amps/\sqrt{Hz}$ for the amplifier having 5dB noise figure (used at the Mobile Unit) and 25.34×10^{-12} $amps/\sqrt{Hz}$ for the power amplifier having 7dB noise figure (used at the RAU).

3.2.4. MZM Response

The characterization of the MZM is an important step as the output power level of the transmitted signal and EVM performance changes with the bias point of the MZM in the setup. The experimental response of the MZM with respect to bias voltage can be found by measuring the output power of the MZM for a voltage sweep from 0v to 5.5v. For this purpose, the output of the MZM (EOspace AX-OK5-10-PFU) is measured using an optical power meter. Fig. 3.5 shows the optical output power as the bias voltage changes with a step size of 0.1v. The MZM in the VPI is modelled to have a Vπ of 5V and the response from the VPI simulations is also shown in Fig. 3.5 by running a sweep of bias voltage.

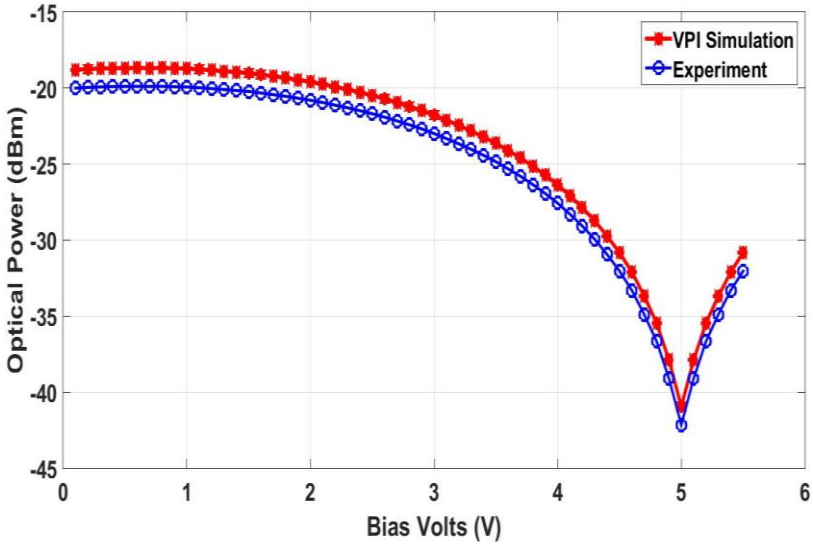

Figure. 3.5 VPI simulation and Experimental results of MZM response versus Bias Voltage

3.3. Phase Modulator and Sideband Filtering based mmW generation and transmission

3.3.1. Downlink System Modelling in VPI

Optical Phase Modulator (PM) based mmW generation techniques were discussed in the previous chapter which involved generation and filtering of mmW separated optical sidebands. Here the complete downlink system is modelled in VPI and performance analysis is performed. The OFDM data signal is generated with FFT of 512, cyclic prefix 0.125 and bandwidth of 512MHz. The EVM of the generated signal (without modulation over an optical carrier) captured directly by the receiver was made to be 3% (as observed by connecting the transmitter and receiver directly with a small RF cable during the experiments) by adding noise to the receiver in the VPI, in order to model the noise of the real time oscilloscope (to be used in the experiments). This is accomplished by using the model of RF amplifier with 7dB noise figure (I_n = 25.34×10^{-12} $amps/\sqrt{Hz}$) for the amplifier used just before the oscilloscope. At the Central Unit (CU), a continuous wave laser source centred at 192.8867 THz (corresponding wavelength 1554.24nm) with 3.1622 mW output power (5dBm) is used with Relative Intensity Noise (RIN) of -150dB/Hz. The output of the laser is modulated using a PM after passing it through a polarization controller. The insertion loss of the polarization controller (0.5dB) and PM (6dB) is realized in VPI by the insertion of an optical attenuator before the phase modulator,

as shown in Fig. 3.6. The phase modulator is driven by an RF signal generator with frequency of 23.5 GHz and amplitude of 15dBm. The output of the PM is shown in Fig. 3.7 where the main optical carrier with the first order and second order sidebands are shown to have 23.5 GHz spacing. The power in the side bands depends on the modulation depth for the PM, which depends on the RF input power to the PM. The PM can be driven with a high RF power signal to obtain maximum optical amplitude for the sidebands. The output of the PM is passed through two optical filters to obtain the optical carrier (centred at 192.8867 THz) and first side band. The carrier (which has higher optical power than the first sideband) is modulated by an OFDM signal at an IF of 1.5 GHz (data rate of 2Gb/s) using an MZM biased at minimum transmission point. The minimum transmission point provides maximum suppression of the unwanted optical carrier and allows maximum amplification of the data-modulated sidebands from the EDFA [9]. The output of the MZM is combined with the filtered first order sideband (unmodulated) using a 3dB optical coupler to form the two-tone signal. Single wavelength modulation has been used here as only one sideband of the optical two-tone signal, instead of using both sidebands for data modulation which can be termed as double wavelength modulation. In this thesis, single wavelength modulation has been used because it provides better performance than double wavelength modulation for the mmW generation through optical two-tone signal technique, as only one sideband suffers from the loss of data modulator (MZM) [10]. The data modulated two tone signal is amplified using a 25dB gain EDFA and transmitted over 2.2km of single mode fibre to the Remote Antenna Unit (RAU).

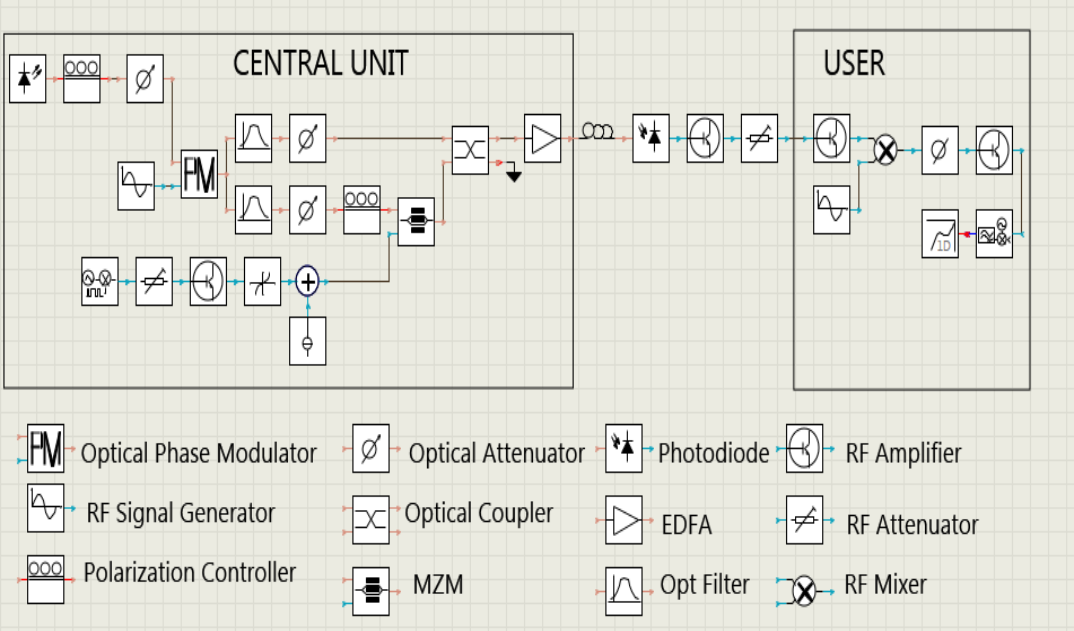

Figure. 3.6 VPI System Model for 25 GHz generation using Sideband filtering and Photonic Upconversion

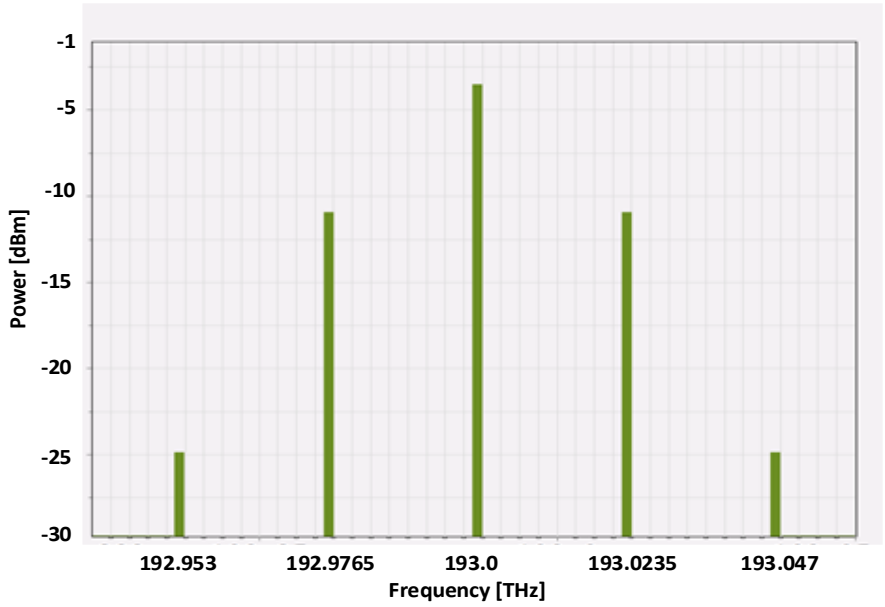

Figure. 3.7 Optical Spectrum of output of Phase Modulator driven by an RF signal of 23.5 GHz

The set of parameters used for components at the RAU and mobile unit are summarized in Table. 3.2. The RAU consists of a high bandwidth photodiode with 0.5A/W responsivity for direct photonic upconversion. The two tone signal produces a 23.5 GHz signal with two data modulated sidebands at 22 GHz and 25 GHz. The output of the photodiode is amplified by a 35dB gain power amplifier with noise figure of 7dB. For the transmission frequency of 25 GHz over a distance of 7m, the total free space path loss is 77.8dB [11] which is compensated by the

Table. 3.2 Set of simulation parameters for the RAU and Mobile user

Unit	Component	Simulation Parameters
Remote Antenna Unit	Photodiode	Responsivity 0.5A/W, Noise density $10\times10^{-12}\ amps/\sqrt{Hz}$
	mmW Power Amplifier	35dB Gain, 7dB Noise Figure
	Transmit Antenna	20dB gain horn antenna
Mobile Unit	Receive Antenna	20dB gain horn antenna
	mmW Amplifier	25dB gain, 5dB Noise Figure
	LO for downconversion	23.5GHz LO, +7dBm power
	Low noise amplifier	10dB gain, 2dB noise figure

gains of the transmit antenna, receive antenna and an amplifier at the receiver end. For a pair of standard gain horn antennas with 20dBi gain each, the wireless transmission loss in line of sight scenario would be 32.8dB. An RF attenuation of 32.8dB is included in the VPI simulations to model this. The MU consists of an amplifier with 25dB gain (5dB noise figure), and a downconverter which mixes the amplified data modulated signal with a 23.5 GHz LO. The output of the mixer is amplified by 19dB using an amplifier (2dB noise figure) and demodulated for EVM analysis. Fig. 3.8 shows the constellation of the 16-QAM modulated generated signal (before MZM modulation) and the constellation for the received signal (after the demodulation at the MU). From VPI simulations, the EVM at the receiver end is found to be 9.7% which shows the feasibility of the system for mmW generation and transmission up to 7m.

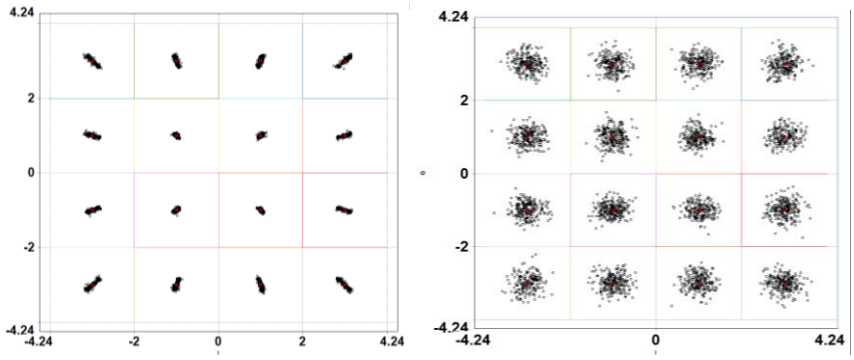

Figure. 3.8 Constellation for 16-QAM modulated data for (left) back-to-back (right) and end-to-end system

The minimum EVM after transmission over the end-to-end system was obtained when the MZM was biased at its minimum transmission point. It is an important setting to be used in the experiments later on as Fig. 3.9 shows the system performance as the bias voltage of the MZM is changed.

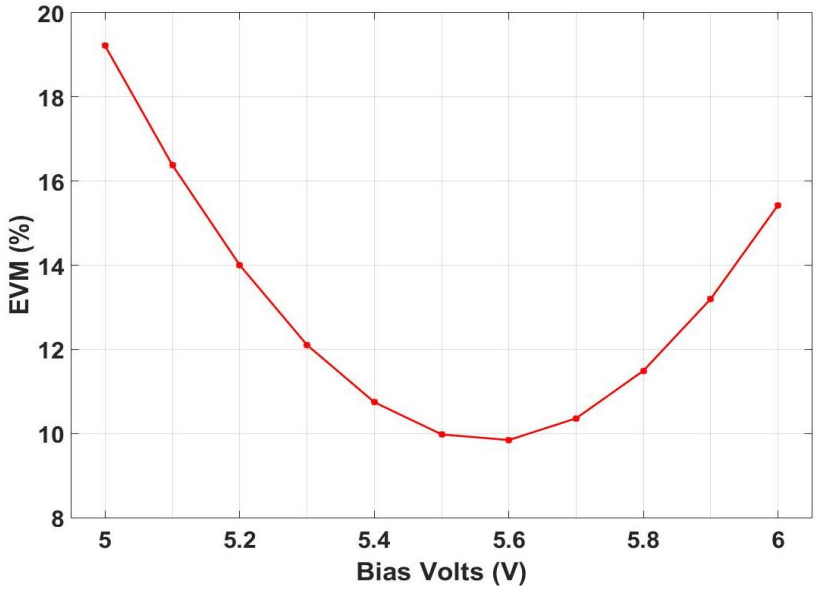

Figure. 3.9 VPI Performance analysis for EVM versus MZM Bias Voltage

3.3.2. Experimental verification of the simulation model

The simulation results are verified by performing experiments for photonic generation of the 25 GHz data modulated signal, RoF transport and wireless transmission for 7m. The experimental setup is shown in Fig. 3.10 where a tunable continuous wave laser (Agilent 8164A) operated at 1554.218nm with power level of 5dBm is used to generate the 23.5 GHz separated optical lines using an optical phase modulator (Sumitomo T.PM1.5-40). An RF signal with frequency of 23.5 GHz is generated by a signal generator (Agilent E8244A) at 2dBm (cable loss is 1.5dB) and is amplified by 15dB to provide an input to the phase modulator. The 23.5 GHz separated side bands are filtered using a Tunable Thin Film DWDM filter with 25 GHz channel spacing. The main optical carrier (filtered) at 1554.218nm is passed through a polarization controller (PC) and used for data modulation. OFDM data symbols mapped with 16-QAM with signal bandwidth of 610 MHz (data rate of 2Gb/s) are generated in MATLAB. An Arbitrary Waveform Generator (AWG) Tektronix AWG7122C is used to generate the analogue waveform and upconvert the baseband OFDM signal to an IF of 1.5 GHz at the central unit. The IF OFDM signal is modulated onto the optical carrier using a Mach Zender Modulator biased

at null point. The Vπ of the MZM (EOspace AX-oK5-10-PFU-PFUP-UL-S) was 5.5V. A 3dB optical coupler is used to couple the output of the MZM with the unmodulated 23.5 GHz separated optical line. The output of the coupler is amplified using an EDFA by 25dB and passed through an optical filter to remove Amplified Spontaneous Emission (ASE) noise before transmission over a single mode optical fibre with length of 2.2km.

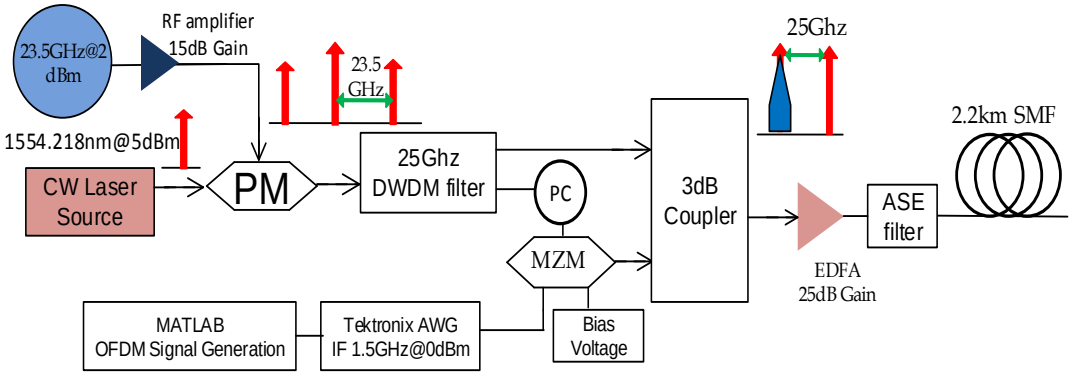

Figure. 3.10 Experimental Setup for Photonic Generation and Transmission of 25 GHz Data Modulated mmW from CU to the RAU

The experimental setup for the RAU and MU are shown in Fig. 3.11 where the optical signal after the RoF transmission is passed through a 40 GHz bandwidth photodiode after the RoF transport to obtain the data modulated 25 GHz signal through direct photonic upconversion. The output of the photodiode is amplified using a 35dB gain amplifier (Nordon N07-1726) and transmitted using a 20dBi horn antenna (Flann Microwave FMI 20240 standard gain horn antenna with FMI waveguide to SMA adapter). After wireless transmission over 7m, the signal is received using an identical 20dBi horn antenna. The signal received at the MU is amplified using a 35dB gain amplifier (Quinstar Technology QLW24403546) and then downconverted to the IF of 1.5 GHz by mixing it with an LO of 23.5 GHz as shown in Fig. 3.11. The output of the mixer (MITEQ DB1826LW1) is amplified using a 19dB gain amplifier (SHF AG Berlin SHF-824). The signal at 1.5 GHz IF is captured using a Tektronix Oscilloscope (DPO 72304DX) using a sampling rate of 100GS/s. The captured data is processed further in MATLAB for manual time alignment and EVM analysis. The EVM after end-to-end transmission was found to be 10.2%.

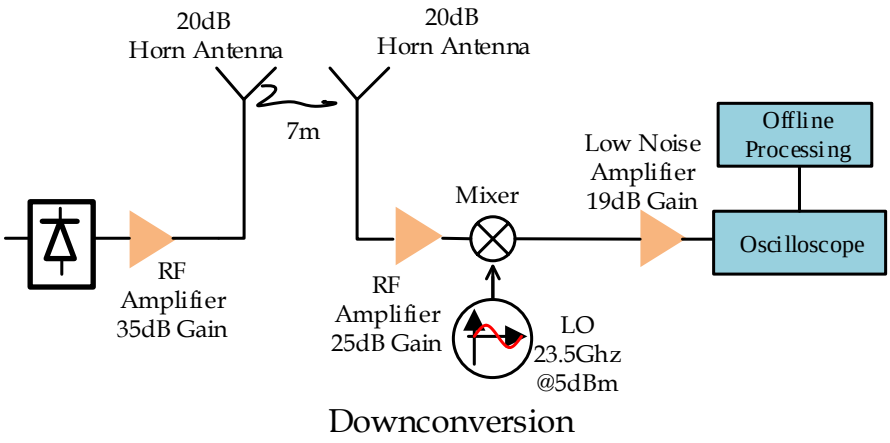

Figure. 3.11 Experimental Setup for RAU Transmission and reception at the MU

3.4. MZM based Double-sideband suppressed carrier technique for mmW Generation

As described in the previous chapter, an MZM modulated by an RF of frequency *f* and biased at minimum transmission point can be used to generate mmW with frequency 2*f*. The two tone signal is obtained by the suppression of the optical carrier due to the use of the minimum transmission point. An MZM based mmW generation setup is presented in this section to be compared with the phase modulator and sideband filtering based mmW generation technique.

3.4.1. VPI Downlink model for MZM based mmW generation

Fig. 3.12 shows the VPI system model in which a CW laser (193.5 THz frequency with 5dBm output power) provides the optical input to a MZM (MZM-1) biased at minimum transmission point. The sine generator produces a 11.75 GHz signal to modulate the optical carrier. The output of MZM-1 comprising of a suppressed carrier and two first order sidebands, which are 23.5 GHz apart, as shown in Fig. 3.13, is amplified by 5dB using an EDFA (EDFA-1), whose output is filtered using a pair of optical filters with 6dB loss and the filtered upper sideband is used for data modulation while the lower sideband is left unmodulated. The data modulation is performed by using a second MZM (MZM-2) biased at minimum transmission point and an OFDM (16-QAM modulation) signal with 512MHz bandwidth is used at an IF of 1.5 GHz. The output of the MZM-2 and unmodulated lower sideband (from the output of the optical filter) are combined together using a 3dB coupler. The composite signal, shown in Fig. 3.14, is amplified by 25dB using EDFA-2 and

transported to the RAU using 2.2km of SMF. The architecture of the RAU is the same as that described previously for the model for mmW generation. A photodiode provides direct photonic upconversion to generate a data modulated 25 GHz signal (along with other spectral components) which is amplified and passed through an RF attenuator to emulate the path loss of 32.8dB (assuming 20dB gain for transmitter and 20dB for receiver antenna) from the wireless transmission. The mmW signal is amplified at the receiver end and downconverted by using a 23.5 GHz LO. The IF signal at 1.5 GHz is amplified by 19dB and is demodulated for EVM analysis. The EVM at the receiver end was 9.22% from the simulation results.

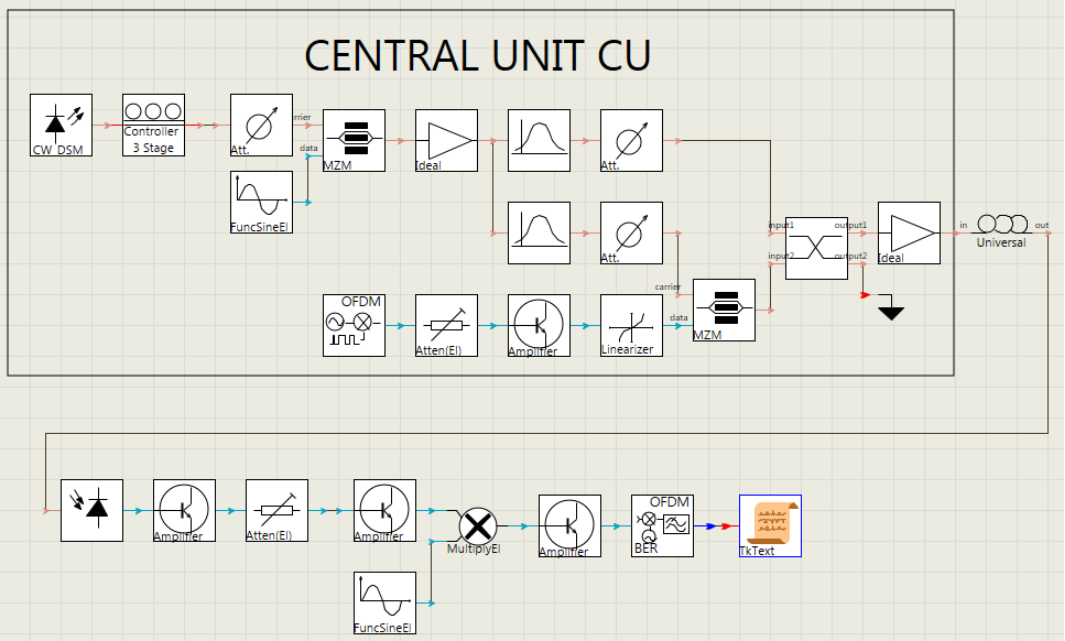

Figure. 3.12 Downlink System in VPI for MZM based mmW Generation

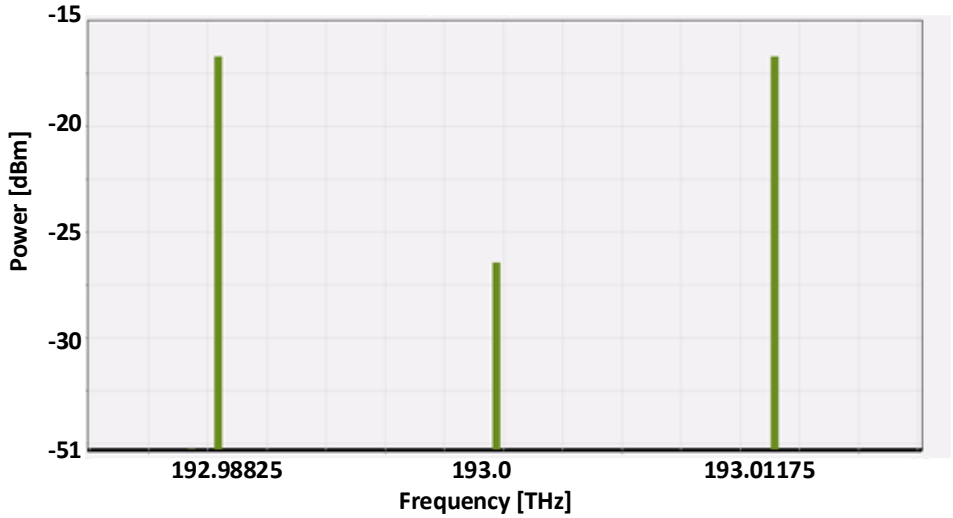

Figure. 3.13 Output Optical Spectrum of the MZM driven by 11.75 GHz RF signal and biased at minimum transmission point

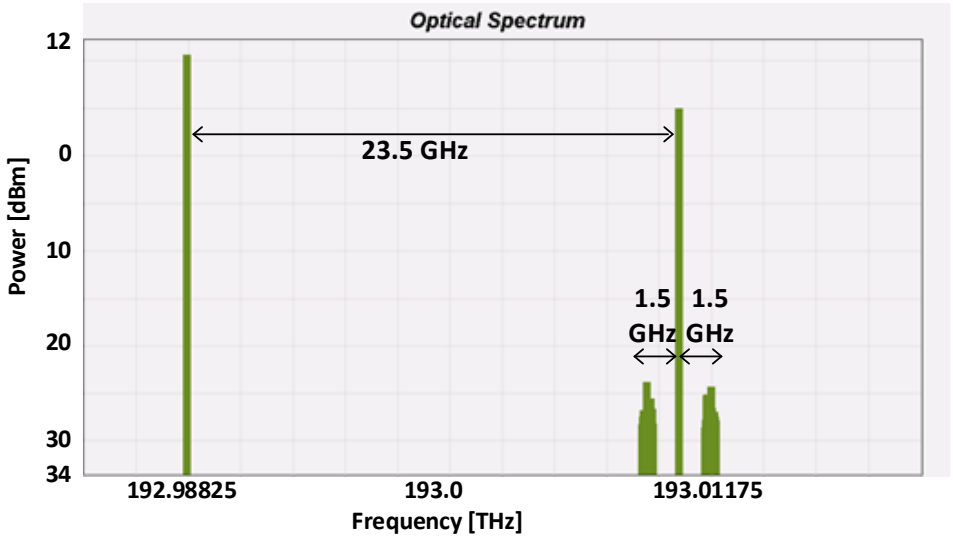

Figure. 3.14 Optical Spectrum of data modulated two tone signal transported to the RAU

3.4.2. Comparison with PM based mmW generation technique and limitations for experimental work

As PM based technique uses the main carrier (with high optical power) and one sideband for 25GHz transmission, additional optical gain of 5dB is required in the case of MZM based downlink system after the first MZM (MZM1), in order to achieve same performance as of PM based downlink system. Fig. 3.15 shows the performance comparison of the two mmW generation techniques as simulated in the VPI. The MZM based technique has also been analysed without the additional 5dB EDFA gain (after the MZM1 as used in the VPI model shown in Fig. 3.12) to

show the need for optical amplification in MZM based setup. The use of optical filters in the MZM based mmW generation setup can be avoided by using double wavelength modulation, in which the output of MZM1 is directly used as an input to MZM2 and both sidebands are modulated with data. For double wavelength modulation, the MZM2 is biased at quadrature point to obtain the optimum performance [10]. The RoF transport consists of two data modulated sidebands which results in a number of spectral components after the photomixing at the RAU (which also affects the efficiency of photodetector). The performance of double wavelength modulation can be seen in Fig. 3.15 which has been degraded as additional RF spectral components are received by the EVM analysis block. A mmW RF filter after the photodiode is used to improve the performance as can be observed from the results.

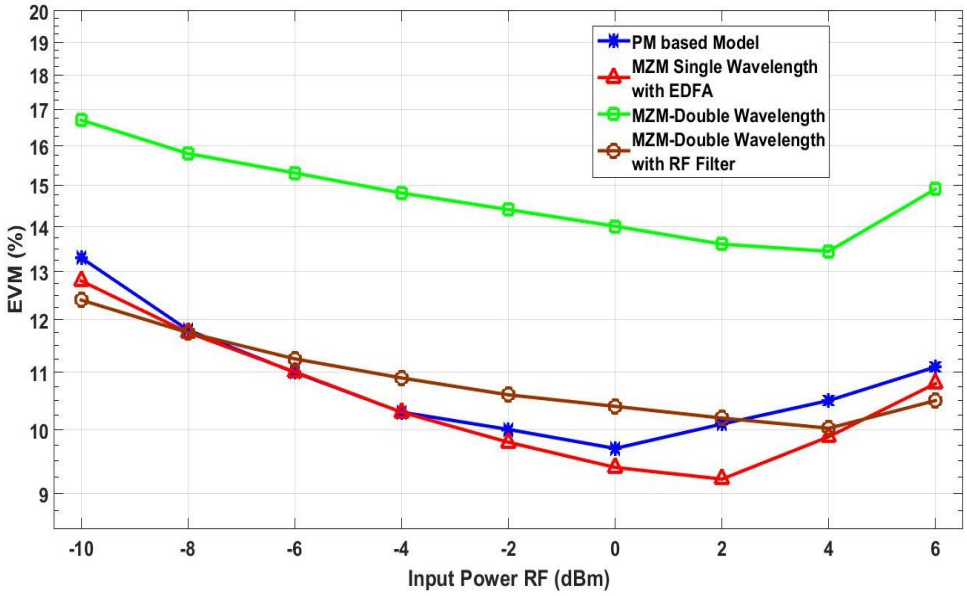

Figure. 3.15 EVM performance for different system configurations using MZM based mmW generation technique versus PM based mmW generation model

The experimental implementation of the model using the MZM for mmW generation is not attainable due to unavailability of second EDFA and mmW bandpass filter, as well as due to the the low bandwidth of the available MZM (10GHz) to produce a two tone signal with 23.5 GHz spacing. The AWG can generate IF signals up to 3.5 GHz and sideband generation from the MZM with spacing lower than 23.5 GHz can be used but the insertion loss of the DWDM filter (25 GHz spacing) increases as the spacing between the filtered sidebands deviates from 25 GHz. Generation of mmW can be performed with a low bandwidth MZM

using cascaded operation of two modulators [12] or filtering of second or third order sidebands (which have very low optical power) [13] but it requires a high gain EDFA after the generation of optical two-tone signal for adequate operation because of using the lower power higher order sidebands and to compensate the loss of optical filters [14]. In addition to these, bias drifting in the MZM is a major problem which effects the amount of carrier suppression and fluctuations in the sideband power, and hence the performance of the overall system, which can be avoided by using complex techniques such as bias feedback circuits [15].

MIMO transmission will require two independent transmit and receive paths (for 2×2 operation) which will require additional optical and RF components and the practicability of the PM based mmW generation technique will be analyzed in the next section through VPI modelling.

3.5. Phase Modulator based Sideband Generation and Filtering for mmW generation for MIMO transmission

Fig. 3.16 shows the system architecture for RoF transport of two different data streams from the CU in VPI simulations. Instead of filtering two optical spectral lines from the output of the phase modulator as described in section 3.2.1, four optical lines including carrier, first order sidebands and one second-order sideband are filtered using optical filters. A pair of OFDM modulators have been used to generate two independent sets of data and these are modulated on two of the filtered sidebands. The data modulated sidebands are combined with 23.5 GHz apart unmodulated sidebands using a single WDM coupler. The combined signal is optically amplified by 30dB using an EDFA and transported over 2.2km of optical fibre. After RoF transport, a WDM filter is used to split the optical carriers for the two RAUs as shown in Fig. 3.17. Fig. 3.18 shows the spectrum received by the RAU1 which consists of a data modulated (having Data Set 1) second order sideband along with 23.5 GHz separated unmodulated carrier, and spectrum at the RAU2 consisting of data modulated main carrier (having Data Set 2) with a 23.5 GHz separated unmodulated optical line which are filtered and sent to RAU2. Each RAU receives a two tone signal, and suppressed unwanted sidebands as shown in Fig. 3.18, which is converted to a data modulated mmW signal to be transmitted. Each RAU performs direct photonic upconversion using a photodiode and amplifies

the mmW signal before the wireless transmission to its respective user. At the user end, the mmW signal is downconverted and amplified for EVM analysis.

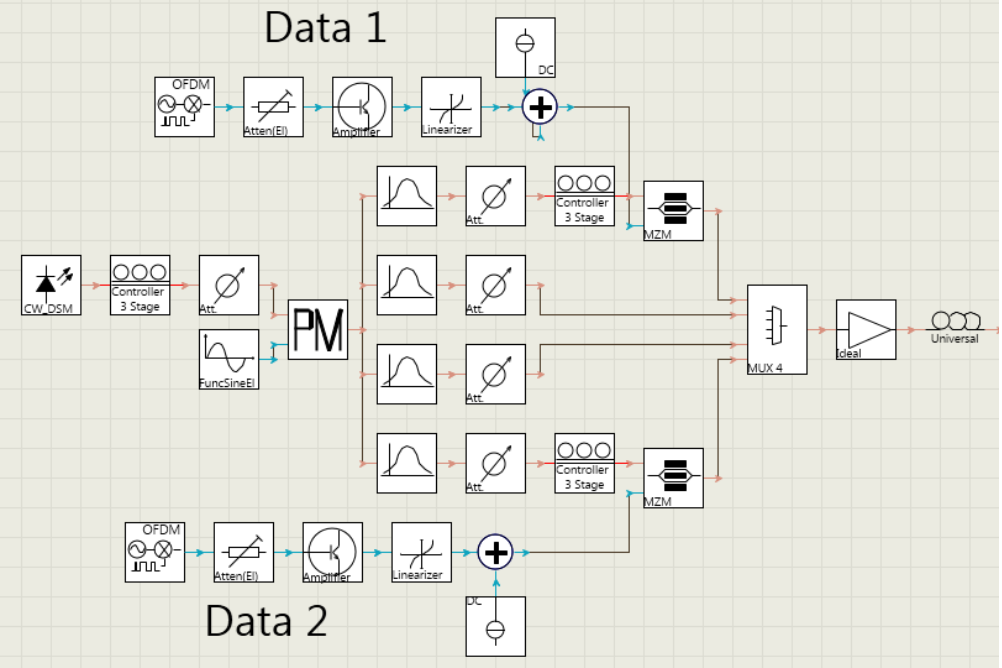

Figure. 3.16 VPI model for CU consisting of two data modulated mmW generation sets and RoF transport using single SMF

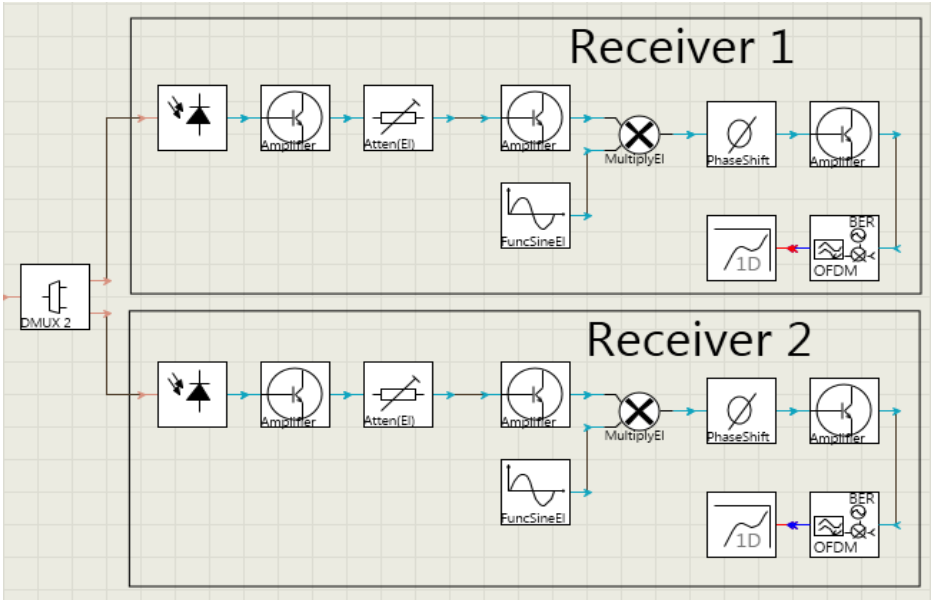

Figure. 3.17 VPI model for the two RAUs and respective users

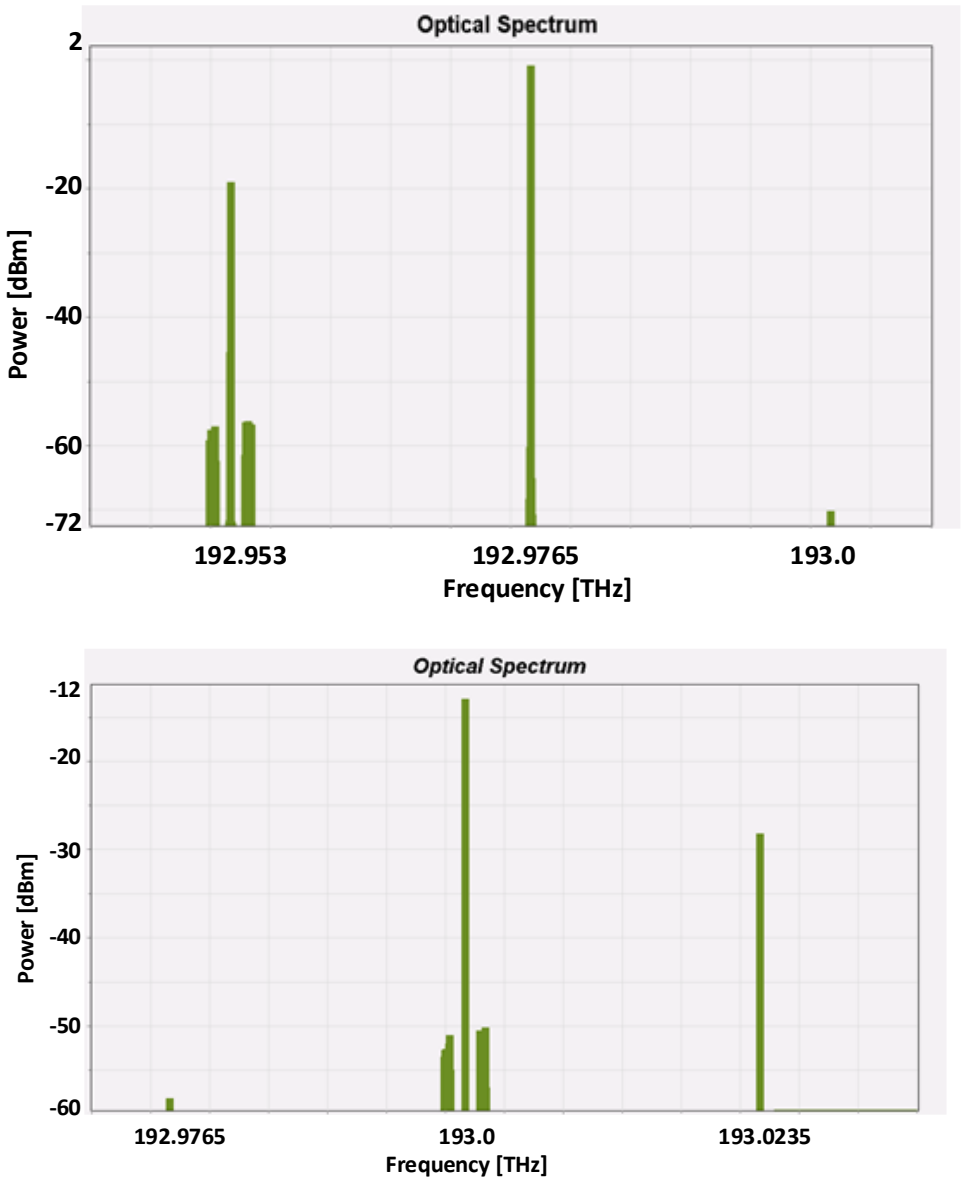

Figure. 3.18 Optical two tone Spectrum after Optical filtering of composite signal for (top) RAU1 (bottom) and RAU2

The data from the two RAUs is received by a set of receivers in the VPI simulations. Each received signal is amplified, downconverted and passed through a low frequency amplifier. The demodulation shows that data stream from RAU1 provide 11% and RAU2 provide 11.3% EVM (for 16-QAM modulated data) for their own receivers, which shows that the proposed system can be used to transmit MIMO data to provide 2×2 operation. The slight difference in the performance is due to the small difference in the optical power levels of the wavelengths that were kept unmodulated (main carrier and second order sideband from the output of the PM). The experimental setup will be explained in the next chapter.

3.6. Simulations and Experimental Setup for 60 GHz Generation and Transmission

For 60 GHz generation, the use of a sideband filtering technique using a PM is not practically achievable in the experiments undertaken due to the unavailability of the required components for an adequate power budget that would accomplish wireless transmission. The free space transmission loss at 60GHz is higher than at 25GHz and lower optical power is available in the 60GHz case because it requires the filtering of the two first-order sidebands (rather than filtering of the higher power main carrier and one first order sideband, as was the case in the 25GHz setup) from the output of the PM. In addition, the DWDM filter in the experiments is tunable with a fixed grid spacing of 25 GHz. The AWG can generate IF signals up to 3.5GHz and filtering two optical tones with frequency spacing higher than 56.5GHz spacing introduces an additional 3 to 4dB optical loss. Lastly, this technique will require a set of 60 GHz RF amplifiers equivalent to those in the 25 GHz setup: one amplifier is needed after the photodiode to amplify the signal before the wireless transmission and another one after the receiving antenna at the MU to compensate for the free space transmission loss.

Using MZM for generation of 60 GHz is not possible for experimental work due to the low bandwidth of the available MZM (10 GHz) and implementation of 60 GHz MIMO using MZM based mmW generation technique will require a greater number of additional components than the PM based downlink system, as discussed in section 3.4.2. The recent development of integrated devices at 60 GHz frequencies [16], [17] has gain a lot of interest and need is to characterize them for a complete downlink system. Although the issues related to integrated devices such as frequency offset, phase noise and linearity can affect the performance, with an additional requirement of an active LO at the RAU, their ability to provide high output power and compact design (with the development of advanced VLSI technology) makes them a practical solution to the high path loss for 60 GHz transmission and deployment of multiple integrated devices on a single RAU. The concept and functionality of such devices has been modeled in VPI for performance analysis and to show their feasibility for experimental work.

3.6.1. VPI Simulation Model for RoF Supported 60 GHz Generation and Transmission

Fig. 3.19 shows the VPI simulation model for RoF transport of an OFDM signal and its upconversion to 60 GHz and transmission at the RAU. The RoF transport has been realized in this model using a directly modulated laser which operates at 193.5 THz and provides 5dBm output power for the optical carrier. OFDM data (256MHz bandwidth, 1Gb/s data rate) is directly modulated onto the laser and transported to the RAU using 2.2km SMF. At the RAU, a low bandwidth photodiode is used to recover the OFDM centred at signal 1.5 GHz which is amplified by a 22dB low frequency amplifier to compensate the loss from the RoF transport. The amplified signal is upconverted to 61.5 GHz using an LO of 60 GHz. The generated mmW signal is passed through an RF attenuator to model the free space path loss. The path loss for a carrier frequency of 61.5 GHz after 7m of wireless transmission is 85.12dB. For a 20dB transmit antenna gain and 16dB gain receive antenna, the total loss becomes 49.12dB. At the user end, the received mmW signal is amplified by a 35dB V-band amplifier with 5dB noise figure. A 60 GHz LO is used to downconvert the mmW signal to IF, which is then amplified and demodulated for EVM analysis. The EVM at the RAU after RoF transport and before the mmW upconversion was found to be 3.5%. Fig. 3.20 shows the constellation diagram after RoF transport and for the end-to-end system transmission, including 2.2km RoF transport and 7m of wireless transmission, for which the EVM was 8.16%. This shows the feasibility of using the integrated transmitter and receiver devices for SISO transmission at 60 GHz.

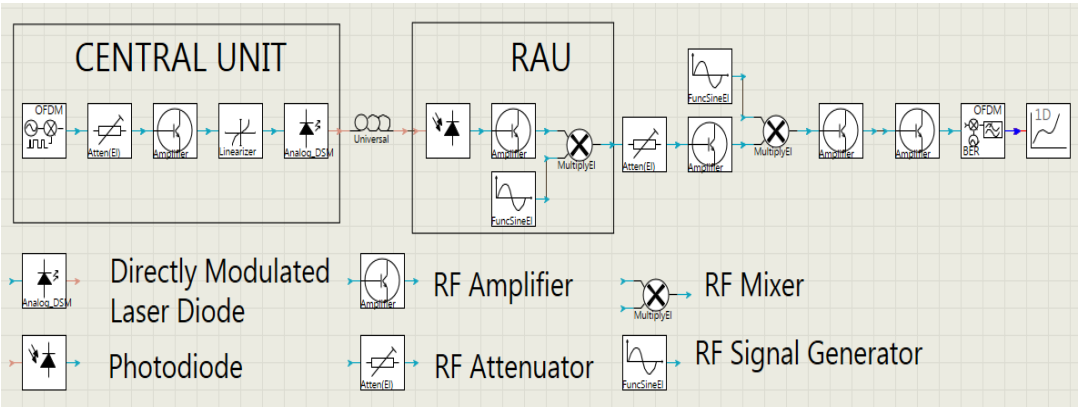

Figure. 3.19 Downlink System architecture for RoF supported 60 GHz transmission using RF upconverter at the RAU

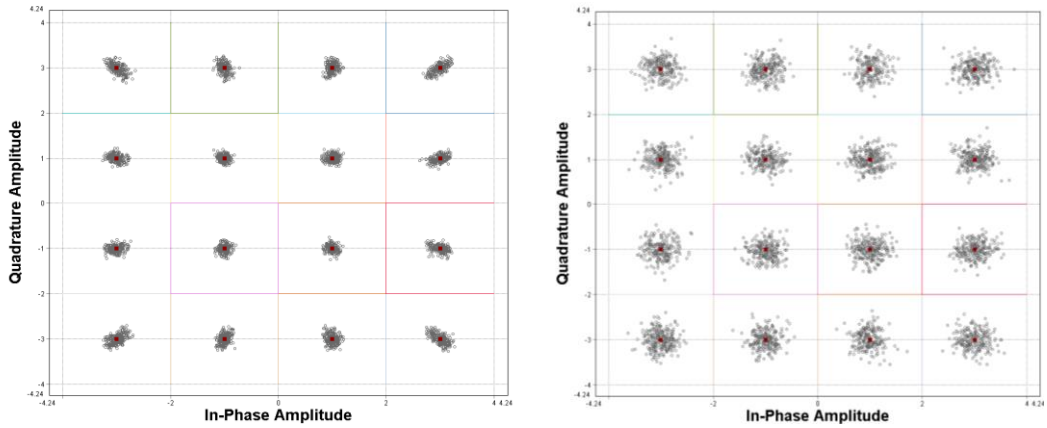

Figure. 3.20 Constellation Diagram for OFDM 16-QAM transmission from VPI simulation after (left) RoF transport (right) end-to-end system from CU to the MU including wireless transmission

3.6.2. Experimental Setup for RoF transported 60 GHz Transmission

The experimental setup for RoF transport and 60 GHz transmission system is shown in Fig. 3.21 where the OFDM signal is generated at an IF of 1.5 GHz using an AWG. The OFDM signal is modulated onto an optical carrier through direct modulation using a Distributed Feedback (DFB) Laser (Emcore 1933F) which provides 5dBm optical output power. The output of the DFB laser is connected to 2.2km of SMF for transport to the RAU, where a low bandwidth photodiode is used to recover the signal. The output of the PD is amplified by 22dB (Minicircuits ZX60-2522M) and passed through a differential balun (6dB insertion loss) before passing it to the Integrated Transmitter Module (Gotmic gTSC0020*) which uses an LO of 10 GHz to produce 60 GHz single tone signal which is then used to upconvert the input signal to 61.5 GHz. The 61.5 GHz data modulated signal is transmitted over 7m wireless distance using an 20dB gain horn antenna. At the other end, the mmW signal is received by a 16dB slot array antenna* [18] and is downconverted to IF using an integrated receiver (Gotmic gRSC0016*) which also requires an LO of 10 GHz. The signal is captured using the Tektronix Oscilloscope at 50GS/s sampling rate for offline processing, which includes carrier synchronization and demodulation for EVM analysis. The EVM was found to be 4% after the RoF transport and 12% after 7m wireless transmission for the downlink system, for 305MHz bandwidth OFDM signal (1Gb/s data rate).

*Acknowledgment: provided by Prof. Stuart Walker (University of Essex) and Dr. Terence Quinlan

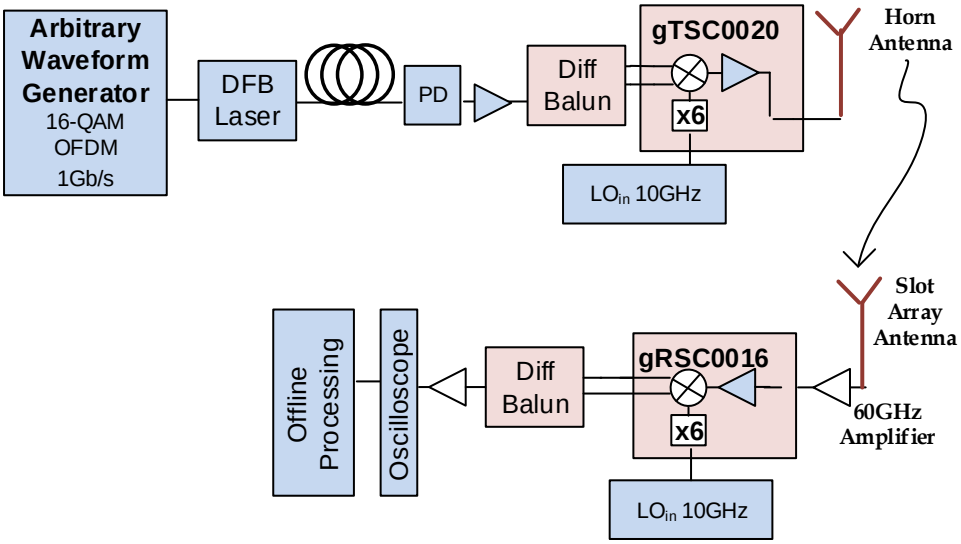

Figure. 3.21 Experimental setup for DFB laser based RoF transport and 60 GHz transmission (using Integrated Transmitter at the RAU and Integrated receiver at the User end)

3.6.3. VPI Simulation Model for RoF supported 60 GHz MIMO

The 60 GHz transmission experimental setup using a set of integrated transmitter and receiver can be extended to two independent transmission streams for MIMO transmission. The VPI system model for 60 GHz MIMO transmission, assuming the use of integrated devices, is shown in fig. 3.22, where a pair of similar directly modulated lasers is used to transport the two channels of MIMO signals to the independent RAUs. Each RAU consists of a photodiode, an RF amplifier and an upconverter to generate data modulated 61.5 GHz signal. The path loss due to the wireless transmission is modelled by adding an RF attenuator. The received signal at each MU is amplified by a V-band amplifier (30dB gain for RAU1 and 35dB for RAU2, as amplifiers of these specifications were available for the experimental work) and downconverted to IF using a 60 GHz LO and a RF mixer. The IF signal is amplified by 17dB before the demodulation block. The EVM for MU1 was 9.97% and for MU2 was 8.16% because of the different gain of the V-band amplifier at the respective RAUs. The 7dB noise figure of the integrated transmitter and 5dB noise figure of the integrated receiver are added to the simulation model, for which the receiver EVM for MU1 becomes 11.83% and for MU2 the EVM degrades to the value of 10.35%.

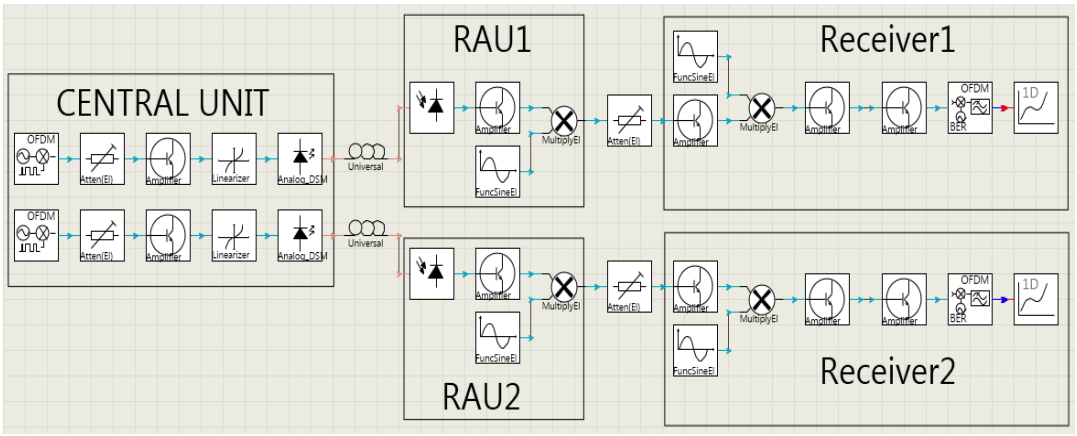

Figure. 3.22 VPI system architecture for 60 GHz for two data streams transmission

Fig. 3.23 shows the EVM results from VPI simulation for the two mobile unit where MU1 achieves the same performance as of the receiver of the single link setup, for different values of input power at the central unit. The experimental results for single link setup has also been shown which suggests comparable EVM performance of the VPI simulation results, to that of the experimental setup, and shows the validity of the simulation model of the setup for MIMO operation, which will be implemented in the next chapter for experimental work.

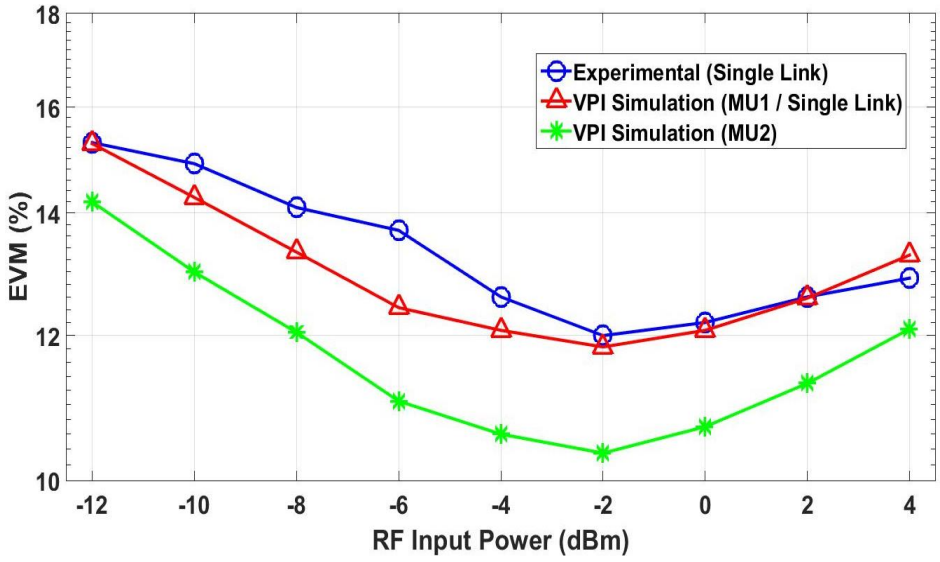

Figure. 3.23 Comparison of receiver EVM from VPI models for SISO and MIMO transmission for different input RF power levels, and SISO experimental setup using integrated transmitter/receiver at the RAU

3.7. Summary

In this chapter, VPI simulations have been carried out for different configurations of RoF transport and mmW generation. Comparison has been made between PM based and MZM based mmW generation setups using VPI simulations. Experiments were performed to analyse the practicality of the proposed setups with the available equipment and system performance. VPI modelling for SISO transmission has been extended to the transport of two data channels at mmW, which will be used in the experimental work on mmW MIMO.

The RF and optical components have been modelled in VPI according to their experimental characteristics using the extensive range of parameters that VPI provides for each component. The simulation results show that photonic generation and RoF transport of a 25 GHz signal using optical phase modulator and sideband filtering technique provides a feasible solution to carry out the experimental work. By contrast, the experimental implementation of a mmW generation setup based on two-tone signal generation through an MZM is not possible as it requires a large bandwidth MZM and additional components.

Finally, simulations were carried out for the 60 GHz transmission system using the integrated transmitter and receiver by using a low bandwidth DFB laser for the RoF transport and performing 60 GHz upconversion at the RAU using RF LO. The experimental verification is performed for the SISO transmission and the VPI modelling is extended to the transmission of two independent OFDM signals for 60 GHz MIMO operation. The experimental work performed in this chapter has only been conducted for SISO transmission with EVM performance analysis for a single receiver location. The analysis on different user locations and MIMO transmission will be presented in the next chapter.

REFERENCES

[1] Virtual Photonics Incorporated, "Photonics Module Reference Manual", *VPI*, 1999.

[2] R. Schmogrow, B. Nebendahl, M. Winter, A. Josten, D. Hillerkuss, S. Koenig, J. Meyer, M. Dreschmann, M. Huebner, C. Koos and J. Becker, "Error vector magnitude as a performance measure for advanced modulation formats", *IEEE Photonics Technology Letters*, Vol. 24 (1), 2012, pp.61-63.

[3] 3GPP TS 36.104 ver 10.7.0 Release 10, "Evolved Universal Terrestrial Radio Access (E-UTRA); Base Station (BS) Radio Transmission and Reception", ETSI TS 136 104 V9.4.0, Jul, 2012.

[4] R.A. Shafik, M.S. Rahman and A.R. Islam, "On the extended relationships among EVM, BER and SNR as performance metrics", *4th IEEE International Conference on Electrical and Computer Engineering (ICECE'06)*, Bangladesh, 2006, pp.408-411.

[5] P.T. Dat, A. Kanno and T. Kawanishi, "Performance evaluation of LTE signal transmission over a seamlessly integrated radio-over-fiber and millimeter-wave wireless link", *IEEE Globecom Workshops (GC Wkshps)*, 2013, pp.748-753.

[6] "Base Station (BS) radio transmission and reception", 3GPP TS 36.104, V.12.6.0, Feb, 2015.

[7] J. James, "Optical phase modulator and sideband filtering millimetre-wave generation for radio over fibre systems", *Ph.D dissertation*, School of Engineering and Digital Arts, University of Kent, UK, 2011.

[8] S. Sykora, "Noise Figure and Equivalent Input Noise", Stan's library, 2005 (DOI: http://dx.doi.org/10.3247/SL1Ee05.003)

[9] P.S. Devgan, "REVIEW OF IMPROVEMENTS IN RADIO FREQUENCY PHOTONICS", AFRL-RY-WP-TR-2017-0156, Sep 2017.

[10] J. James, P. Shen, A. Nkansah, Xing Liang and N.J. Gomes, "Nonlinearity and noise effects in multi-level signal millimeter-wave over fiber transmission using single and dual wavelength modulation", *IEEE Transactions on Microwave Theory and Techniques*, Vol. 58 (11), 2010, pp.3189-3198.

[11] https://www.pasternack.com/t-calculator-fspl.aspx (Free space loss calculator)

[12] M. Mohamed, X. Zhang, B. Hraimel and K. Wu, “Frequency sixupler for millimeter-wave over fiber systems”, *Optics Express*, Vol. 16 (14), 2008, pp. 10141–10151.

[13] X. Li, J. Zhang, J. Xiao, Z. Zhang, Y. Xu and J. Yu, "W-Band 8QAM Vector Signal Generation by MZM-Based Photonic Frequency Octupling", *IEEE Photonics Technology Letters*, Vol. 27 (12), 2005, pp. 1257-1260.

[14] Z. Xu, X. Zhang, and J. Yu, “Frequency upconversion of multiple RF signals using optical carrier suppression for radio over fiber downlinks”, *Optics Express*, Vol. 15 (25), 2007, pp. 16737–16747.

[15] C.T. Lin, P.T. Shih, W.J. Jiang, J. Chen, P.C. Peng and S. Chi, "A continuously tunable and filterless optical millimeter-wave generation via frequency octupling", *Optics Express*, Vol. 17 (22), 2009, pp.19749-19756.

[16] S.E. Gunnarsson, C. Karnfelt, H. Zirath, R. Kozhuharov, D. Kuylenstierna, A. Alping and C. Fager, "Highly integrated 60 GHz transmitter and receiver MMICs in a GaAs pHEMT technology", *IEEE Journal of Solid-State Circuits*, Vol. 40 (11), 2005, pp.2174-2186.

[17] S. Glisic, Y. Sun, F. Herzel, M. Piz, E. Grass, C. Scheytt and W. Winkler, "A fully integrated 60 GHz transmitter front-end with a PLL, an image-rejection filter and a PA in SiGe", *34th IEEE European Solid-State Circuits Conference (ESSCIRC)*, 2008, pp.242-245.

[18] T. Quinlan and S. Walker. "A 16.8 dBi quasi-discoidal radiation pattern antenna array for 60GHz non-line-of-sight applications", *Antennas and Propagation Conference (LAPC)*, 2014 Loughborough, 2014, pp.210-213.

CHAPTER 4
RADIO-OVER-FIBRE TRANSPORTED MILLIMETRE-WAVE MULTIPLE-INPUT, MULTIPLE-OUTPUT SYSTEMS

4.1. Introduction

Chapter 2 presented a review of mmW MIMO transmission to achieve spatial diversity and spatial multiplexing and different RoF transport schemes for MIMO signals to different RAUs. Furthermore, chapter 3 presented simulation and experimental work on modelling of several end-to-end systems for RoF transport and mmW generation with different configurations and component requirements. This chapter presents experimental work on RoF-transported mmW MIMO systems using the downlink end-to-end (from central unit to the user end) transmission systems presented in the previous chapter. RoF fronthaul is a suitable candidate for mmW communication as it provides a low-cost infrastructure and extremely low-loss transport of data over several km of distance [1]. The centralized control enabled by the RoF transport from CU to multiple RAUs is extremely useful to achieve the required coordination among the RAUs. Coverage in the mmW band for multiple user locations has been a serious issue which needs to be addressed for future communication systems. MIMO techniques have been used in various IEEE standards such as 802.11ac, WiMAX and LTE [2-4] at microwave frequencies to improve the coverage and reliability of service. Most of the experimental work which has been done so far on MIMO is based on microwave frequencies [5] which does not require Line-of-Sight (LOS) transmission and makes use of the multipath environment to achieve decorrelation among the MIMO channels. On the contrary, mmW systems suffer from high propagation loss and depend heavily on the LOS

component. Studies have shown that decorrelation among the MIMO channels in LOS communication can be achieved with optimum spacing among the transmitting or receiving units, or both [6, 7]. Thus, the optimum physical spacing between different RAUs in a distributed MIMO system requires a flexible fronthaul.

The purpose of this work is to present an Analog RoF fronthaul for mmW MIMO for future mobile systems in order to achieve spatial multiplexing and spatial diversity at several user locations. The improvement in coverage can be achieved from the well-known STBC Alamouti algorithm. Increased data rates are obtained from the multiplexing gain, where several data streams are combined to achieve a higher aggregate data rate, using the Zero Forcing algorithm. Millimeter-wave generation through the use of direct photonic upconversion or integrated RF components as discussed in chapter 3, are used here for 2×2 MIMO systems at 25 GHz and 60 GHz. The experimental work in this chapter uses different RoF transport schemes for the two MIMO systems and a performance analysis for 1Gb/s data rate is performed at several user locations to identify spatial diversity and spatial multiplexing gains. The effect of transmit antenna spacing has been analyzed in detail for various transmission distances and analog RoF fronthaul has been proposed to achieve the flexible and wider transmit antenna spacings desirable for the longer distances. An approach to measure individual channel coefficients for MIMO processing has been used to extend the analysis for distances up to 30m.

4.2. DWDM-Radio-over-Fibre Transported 25 GHz MIMO

This section describes the photonic generation and RoF transport of 25 GHz signals to perform 2×2 MIMO. A single laser source has been used to generate the mmW signals to achieve centralized control and phase correlation between the two MIMO signals. The direct photonic upconversion provides a low cost solution for the mmW generation at the RAU. Future mmW systems are anticipated to have a large number of RAUs connected to a central station [8] and low cost RAU design is a major design requirement for such systems.

4.2.1. Photonic Generation of mmW MIMO signals

Fig. 4.1 shows the experimental setup for photonic generation of two 25 GHz signals for 2×2 MIMO operation. The basic principle is the phase modulation of a single laser source and sideband filtering to achieve mmW separated optical carriers for photonic upconversion [9]. A Continuous Wave (CW) laser source (Agilent 8164A) is used to generate an optical wavelength centred at 1554.8nm with an output power of +5dBm, which is passed through a polarization controller and modulated by an optical phase modulator (Sumitomo T.PM1.5-40). The phase modulator is driven by an RF signal of 23.5GHz at +15dBm, generated by an RF signal generator (Agilent E8244A) followed by a power amplifier. The output of the optical phase modulator is shown in inset (a) of Fig. 4.1 which has the optical carrier with the sidebands. The first order sidebands have the highest power (greater than the carrier component) as the PM is overdriven by high RF power. The optical spectrum of the output of the PM is shown in Fig. 4.2 which is passed through a DWDM filter for sideband filtering. Four (23.5 GHz apart) optical lines including central carrier, upper and one lower first-order sidebands and lower second-order sideband are filtered by tuning the DWDM filter. The central carrier with upper first-order sideband and the lower first order sideband with lower second order sideband represent two sets of 23.5 GHz apart optical tones. For each pair of optical two-tone signals, single wavelength modulation is adopted in which data is modulated on one wavelength and is then combined with the 23.5 GHz-apart unmodulated wavelength. Data modulation is performed by passing the wavelength through a polarization controller (PC), followed by a Mach-Zehnder Modulator (MZM).

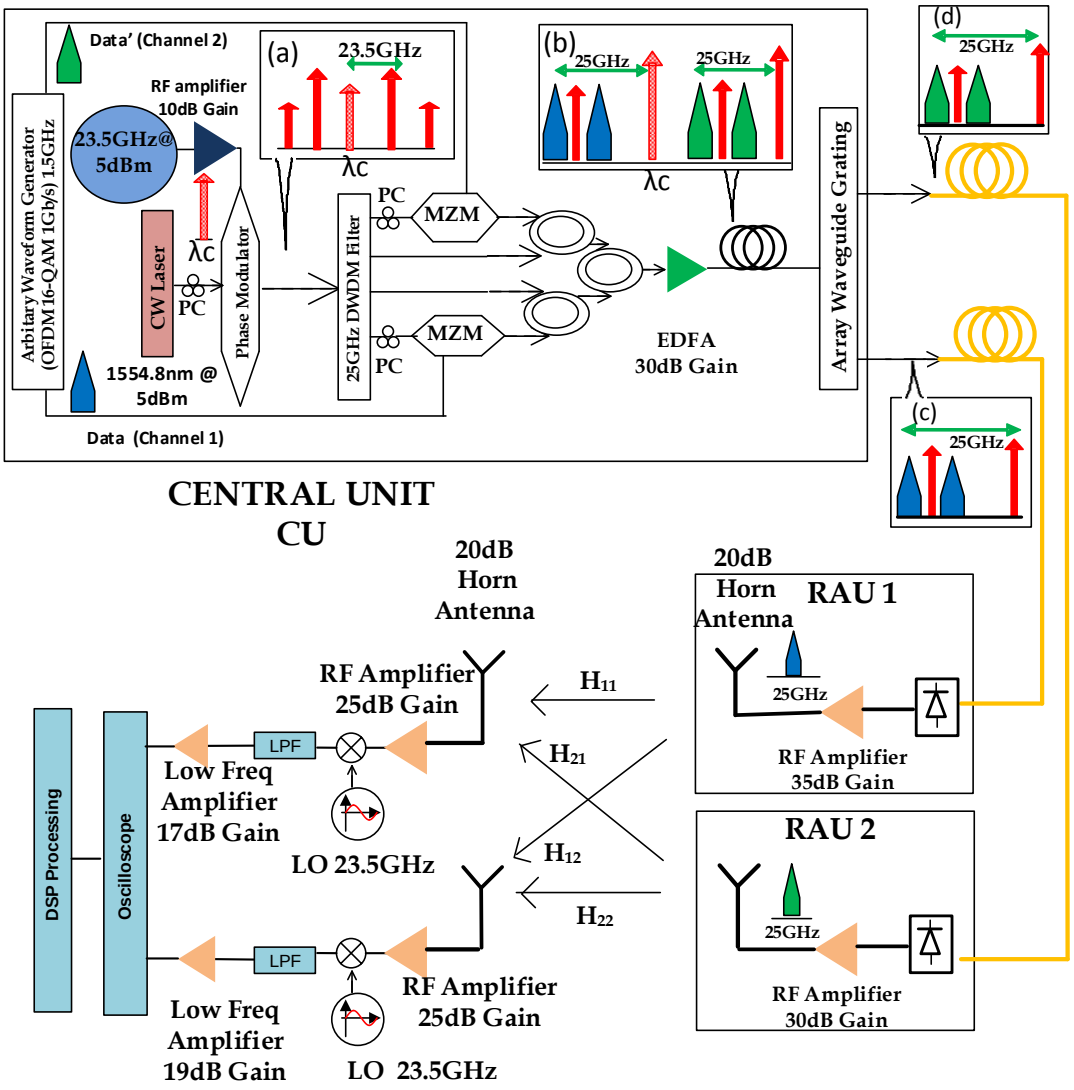

Figure. 4.1 Experimental setup for Photonic Generation of 25 GHz MIMO signals

Figure 4.2 Optical Spectrum of the PM output (Agilent Optical Spectrum Analyser 86146B)

Data signals were generated in MATLAB/Simulink software as baseband IQ signals using the OFDM signal block. 16-QAM modulation is used and OFDM symbols are generated with an IFFT size of 512, guard bands of 112 subcarriers and a Cyclic Prefix (CP) of 1/8. An OFDM-based preamble symbol is added for channel estimation. The data symbols generated in MATLAB are used by the RFXpress software running on the Arbitrary Waveform Generator (AWG) Tektronix 7122C to generate an analog waveform for each MIMO signal. The two MIMO data waveforms at an IF of 1.5 GHz are transmitted from the two channels of the AWG and each is applied to an MZM for data modulation. The first data stream is modulated over (filtered) upper first-order sideband by EOspace MZM *(*AX-oK5-10-PFU-PFUP-UL-S) biased at null point. The second data stream is modulated over the lower first-order sideband using JDSU MZM (12345) biased at the null point. The data modulated optical lines are combined with the unmodulated wavelengths using 3dB couplers and the composite signal is shown in inset (b) of Fig. 4.1 which is amplified by 30dB using an Erbium-Doped-Fibre-Amplifier (EDFA). An Array-Waveguide-Grating (*Neo-optics,* insertion loss of 5dB per channel) is used to separate the optical two-tone signals for the two Remote Antenna Units (RAU). Inset (c) and Inset (d) in Fig. 4.1 shows the two 25 GHz separated sidebands transported to RAU1 and for RAU2, respectively. Fig. 4.3 shows the optical spectrum for the output of the AWG for each RAU. The data modulated sidebands are not visible due to the minimum possible resolution bandwidth (0.5nm) of the OSA (Agilent 86146B).

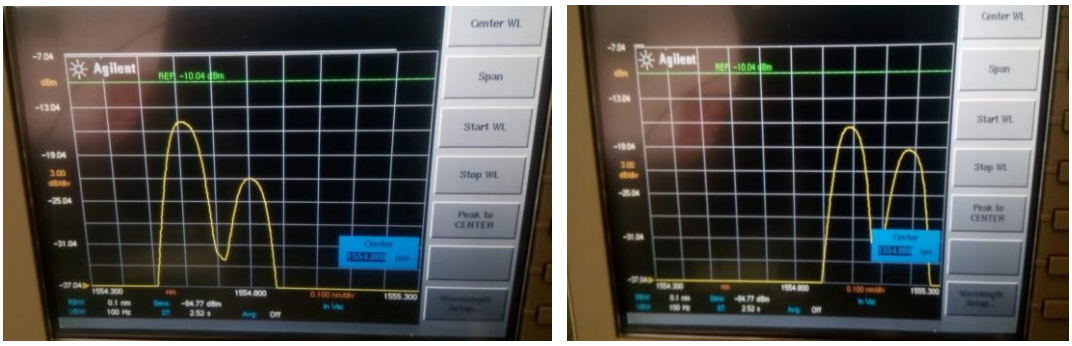

Figure 4.3 Optical Spectrum for the two-tone signal for RAU 1 (left) and RAU 2 (right)

Each optical path to the RAU consists of 2.2km of Single Mode Fibre (SMF). At each RAU, a wide bandwidth photodiode (70GHz) is used for direct photonic downconversion of the optical two-tone signal to a mmW signal. An RF power amplifier is used to amplify the data modulated 25GHz signal which is transmitted

using a 20dB standard gain horn antenna FMI 20240 (17.6GHz - 26.7GHz). The measured antenna pattern of the two horn antennas used in the experiment in the anechoic chamber is shown in Fig. 4.4; this was performed to verify that both antennas in the MIMO transmission experiment have similar antenna gain and 3dB beamwidth.

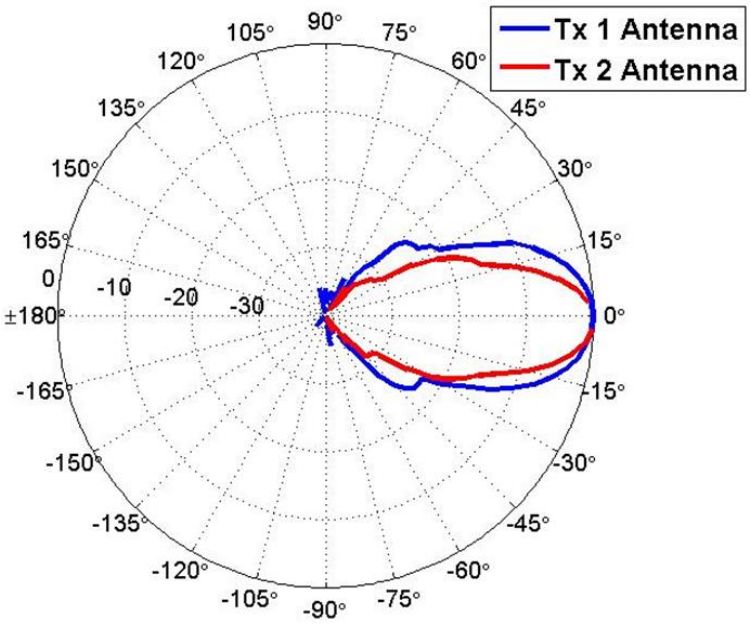

Figure. 4.4 Measured Antenna Pattern of the Two Horn Antennas at 25 GHz in Anechoic Chamber at University of Kent

After wireless transmission of 6m, two 20dB gain horn antennas are used at the receiver side. The received signal from each antenna is amplified by 25dB and is downconverted to 1.5 GHz IF using an LO of 23.5 GHz. The output of the mixer is filtered using a low pass filter (0 to 1.9 GHz) and amplified by 17dB before capturing it using a Tektronix Oscilloscope (DPO 72304DX) for offline processing. The captured signals are processed in MATLAB by first performing time alignment of the OFDM bursts with the transmitted signal using visual inspection. OFDM modulation is performed by removing CP and padded zeros. Channel estimation is performed using the preambles and the MIMO algorithm is used for signal detection/ combining afterwards. The constellation is plotted for the processed symbols and EVM is evaluated. The RF spectrum of the generated OFDM signal (centred at 1.5GHz) is shown in Fig. 4.5a. The constellation diagrams at the receiver end for the individually transmitted SISO signal (from each RAU) is shown in Fig. 4.5b and Fig. 4.5c for RAU 1 (EVM 11.9%) and RAU 2 (EVM 12.3%), respectively.

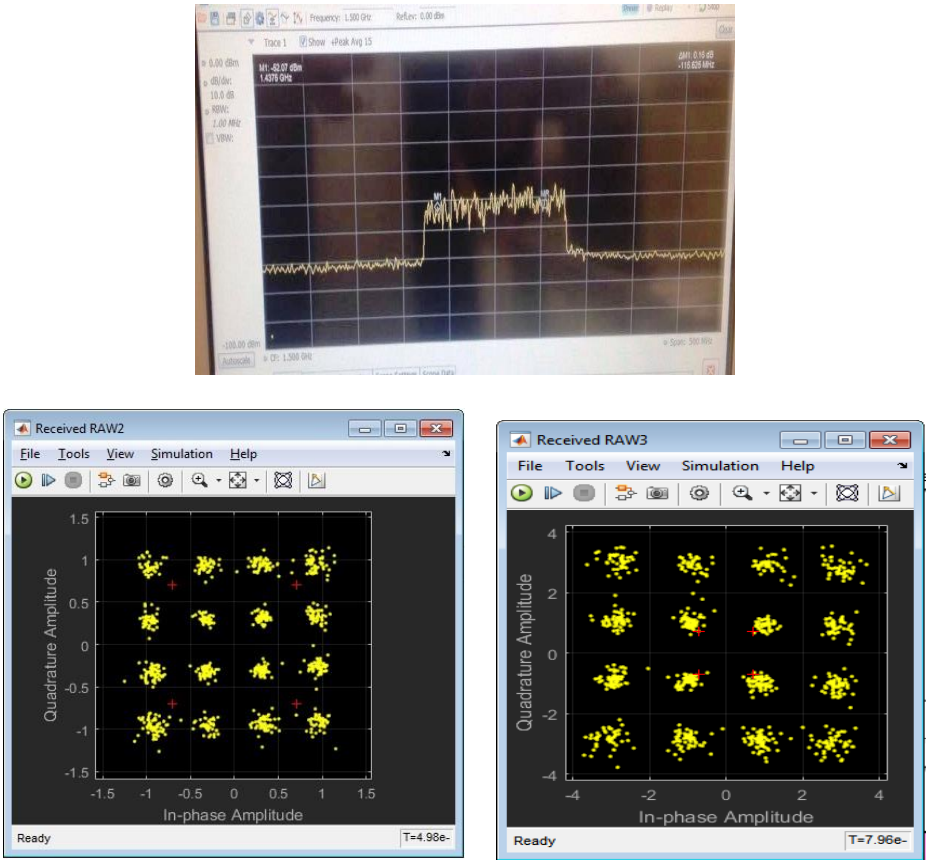

Figure 4.5 (a) RF Spectrum of the generated OFDM signal (b) Received constellation performance of RAU 1 (c) Received constellation performance of RAU 2

The characterization of the system included measurement of EVM for different bias voltages of the two MZMs. Fig. 4.6 shows the performance for the RAU 1 (having MZM 1) and RAU 2 (having MZM 2) for SISO transmission. This shows that minimum EVM is achieved at the null point for each MZM.

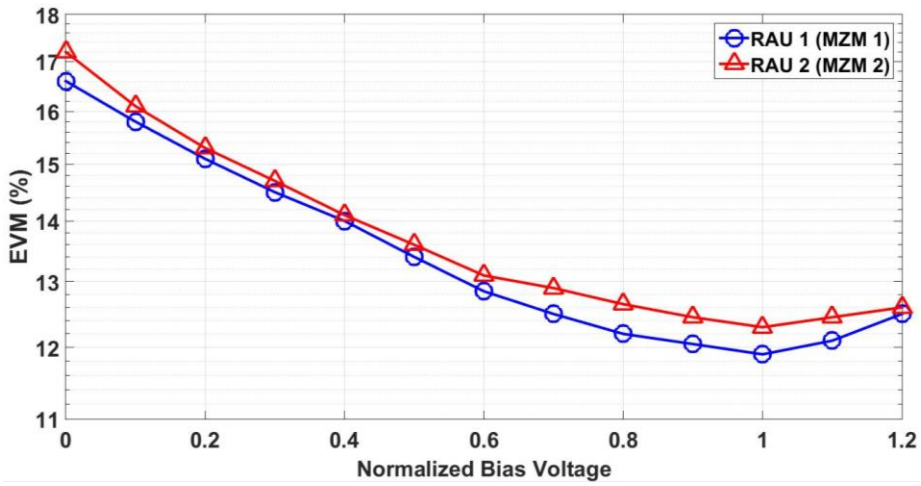

Figure 4.6 EVM Performance versus the bias voltage of the MZMs

4.2.2. Antenna Arrangement for MIMO measurements

The transmitting antennas were pointing towards the receiver (consisting of two antennas) during the experiment to ensure good signal strength from the LOS operation. The layout of the MIMO operation for the transmitting and receiving antennas is shown in Fig. 4.7 where the separation distance between the two transmitting antennas was varied for the values of 40, 60, 80 and 100cm. Different wireless transmission distances (up to 6m) were used to analyze the EVM results at six different user locations (A to F). The data is captured at all of the 30cm apart user locations over a span of 1.5m after the MIMO operation. The performance of SISO is also evaluated at each user location to be compared with MIMO results. To capture data for SISO analysis, one transmitting antenna was placed at the SISO reference point as shown in Fig. 4.7 and data was captured by placing single receiving antenna at the user location.

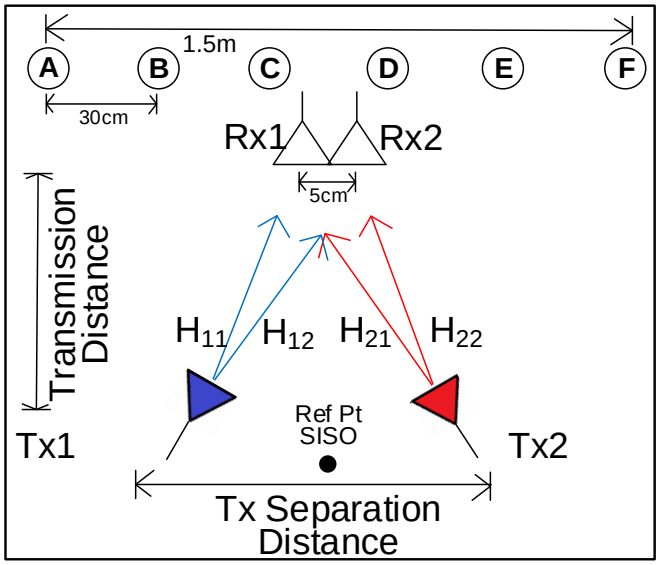

Figure. 4.7 Layout of transmit/receive antennas and user locations for measurements

4.3. 2×2 60 GHz MIMO using Integrated Transmitter and Receiver

As compared to the photonic generation of mmW described for 25GHz MIMO setup, another method to generate the mmW signals is the use of integrated RF modules. This section presents the experimental setup of RoF transported 60 GHz MIMO. IF-over-fibre transport is performed for the two MIMO signals over

separate SMF links and integrated RF modules have been used for mmW generation, as discussed in Chapter 2.

4.3.1. Experimental Setup for RoF supported 2×2 60 GHz MIMO

As shown in Fig. 4.8, each MIMO signal generated by the AWG is modulated onto an optical carrier using a DFB laser (Emcore 1935F) [10] with +5dBm output optical power (4 GHz bandwidth, maximum input power for linear operation +15dBm). After 2.2km of SMF transport, a 2.5 GHz bandwidth photodiode [11] is used at each RAU to recover the IF signal. The RF loss due to the RoF link is approximately 20dB. To compensate this loss, a 22dB gain amplifier (Minicircuits ZX22) is used after the photodiode. After RoF transport, the two 1.5GHz MIMO signals are upconverted to 61.5 GHz using a pair of integrated transmitter modules and transmitted using two similar standard 22dB gain horn antennas (V-band). After wireless transmission of 8m, a pair of slot array antennas [12] are used as a receiver. The received signals are amplified and downconverted using integrated receivers as shown in Fig. 4.8. The output from each integrated receiver at 1.5 GHz is passed through a differential balun, amplified by a low frequency amplifier and captured using the Tektronix oscilloscope.

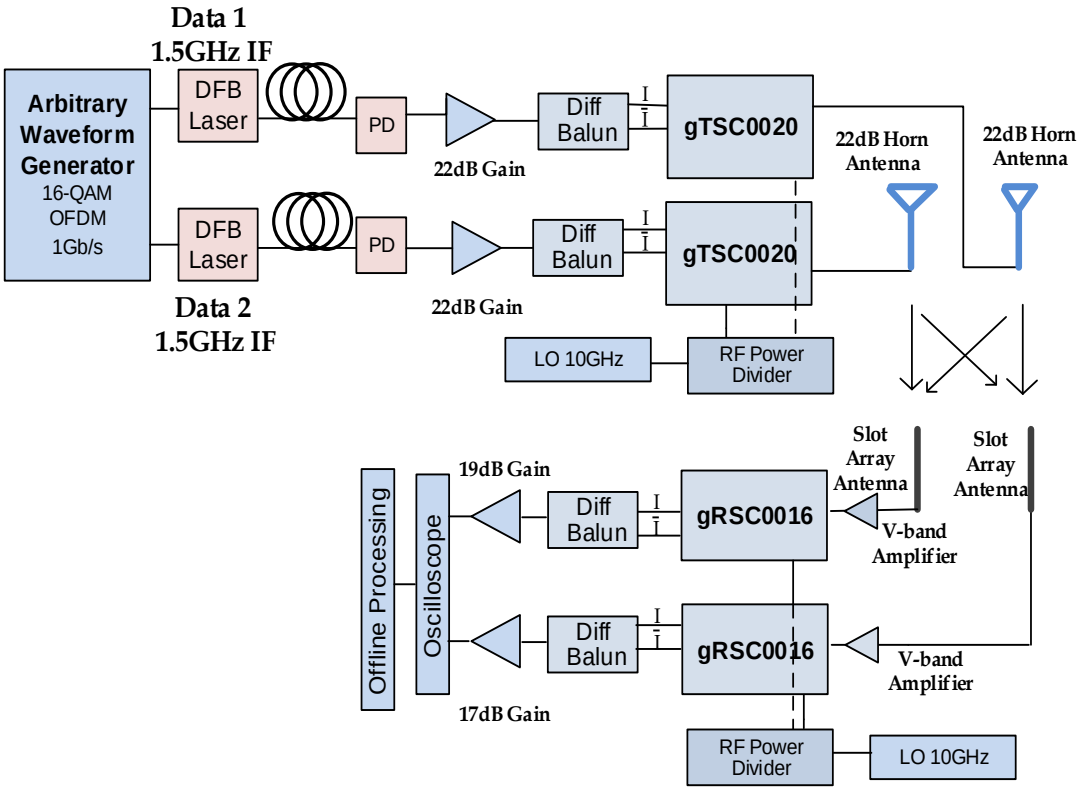

Figure. 4.8 Experimental Setup for 2×2 MIMO at 60 GHz using RoF Transport and Integrated RF Modules

Fig. 4.9 shows more details of the experimental setup where the horn antennas were placed on small tripods at the same height (1m) from the ground on the transmitter side. At the receiver side, two slot array antennas were placed on a single tripod to be used as a single receiver as shown in more detail in Fig. 4.10.

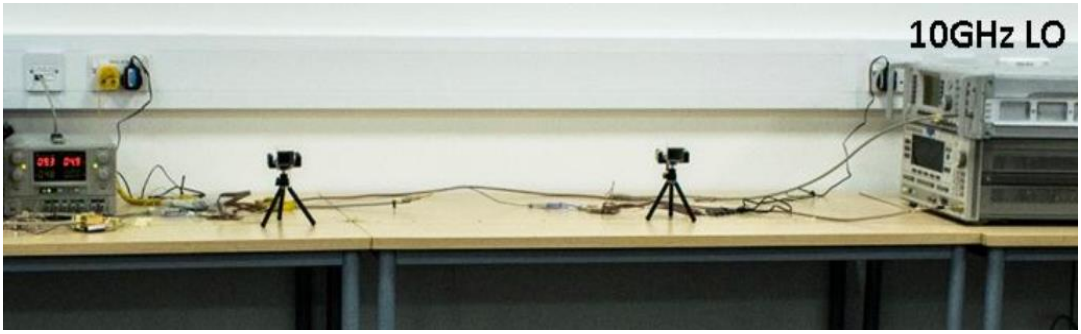

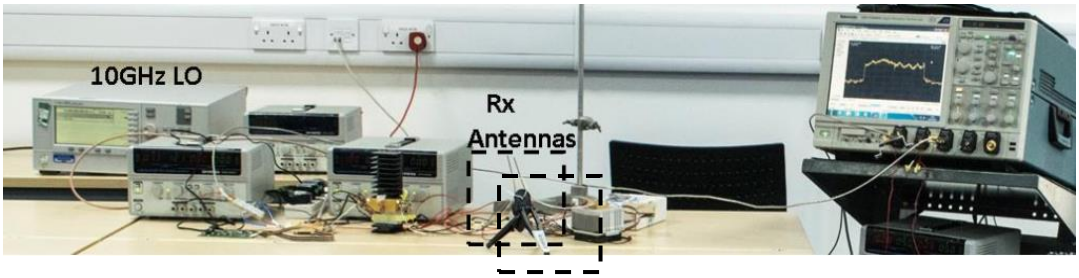

Figure. 4.9 Experimental setup for RAUs (top) Receive Side (bottom) in the Seminar Room (10m x 10m) at University of Kent

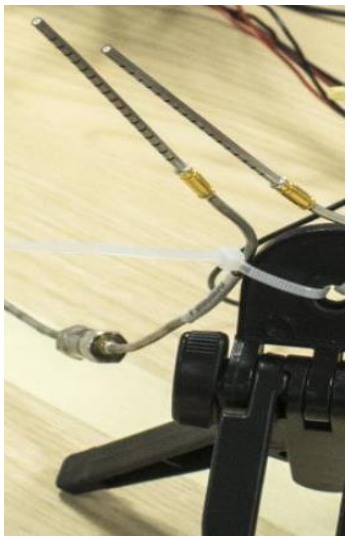

Figure. 4.10 Pair of slot array antennas at the receiver end

In order to operate the DFB in the linear region, a maximum of +5dBm IF input power was used. The 10dB back-off was used due to the high Peak-to-average power ratio (PAPR) of OFDM. Fig. 4.11 shows the EVM performance of the radio over fibre transport when the input IF power was varied up to 2dBm.

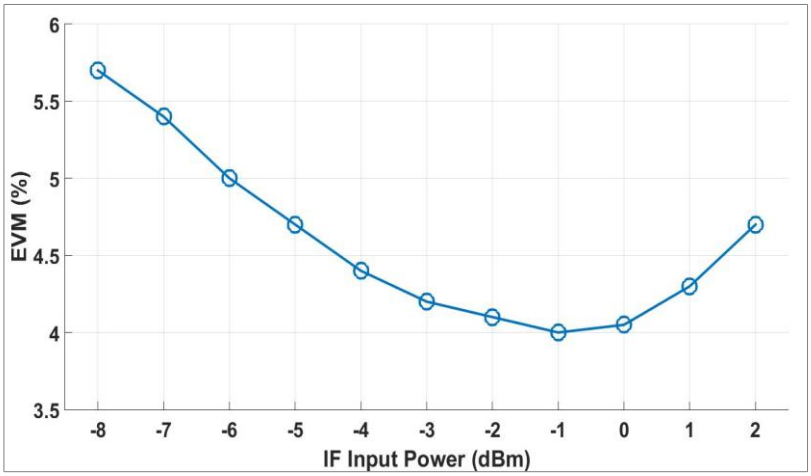

Figure. 4.11 EVM (%) plot against IF input power to the DFB laser for RoF transport

The output of the amplifier is passed through a differential balun and DC blocker (8dB loss) and is provided as an input to the 60 GHz integrated transmitter. The Gotmic gTSC0020 Integrated transmitter [13] consists of a x6 multiplier which takes a 9 GHZ to 12 GHz LO from a SMA port and upconverts the input data signal to V-band frequency. It has a power amplifier which amplifies the output of the mixer and the mmW signal is available at the MMPX connector type output port of the PCB module as shown in Fig. 4.12. The lowest EVM was obtained when power to the PCB (after the differential balun and DC blocker, with a combined 8dB loss as measured through experiments) was -5dBm. On the receiver side, the Gotmic gRSC0016 Integrated Receiver [14] is used which amplifies the input mmW signal and has a mixer to downconvert it to IF as shown in Fig. 4.12. It also uses x6 multiplier and a 10 GHz LO with +7dBm power for down-conversion, as with the Integrated Transmitter. The 10 GHz LO required by the transmitter and receiver PCB is provided by a separate set of signal generators during the experiments because the problems of synchronization and frequency offset have been compensated by using offline time alignment and use of preambles, respectively.

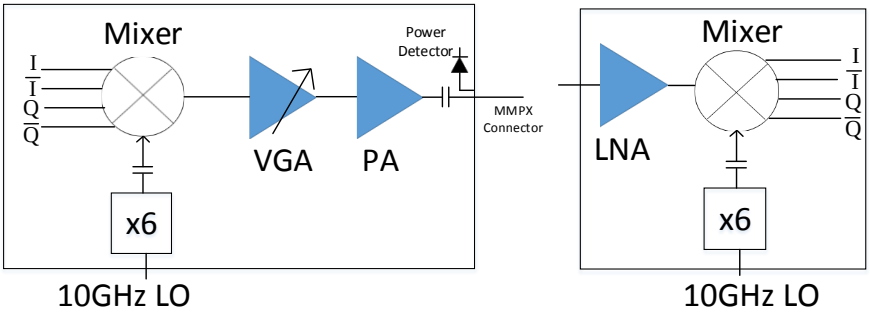

Figure. 4.12 Layout of RF Gotmic Integrated (left) Transmitter (right) Receiver

At the receiver side, a pair of slot array antennas was used. The pluggable antennas with MMPX input ports operate in the 57 GHz to 64 GHz range with 16dBi gain at 61.5 GHz [12] as shown in Fig. 4.13. Each antenna receives signals from a wider range of angles, as compared to the horn antennas, which is helpful in MIMO operation where each receiving antenna needs to be in LOS of every RAU. The low fabrication cost and small size of these antennas makes them a suitable candidate for use in future mmW systems.

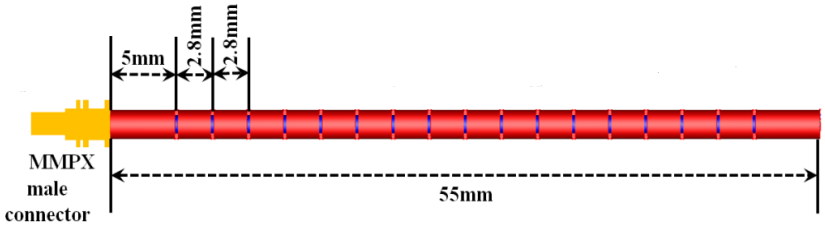

Figure. 4.13 Slot Array Antenna [12] (designed and developed at Uni of Essex)

4.3.2. Antenna Layout for measurements at various user locations

The arrangement of antennas for LOS MIMO for this work has been kept the same as that used at 25 GHz. The distance between the two receiving antennas (which comprises one receiver) has been kept constant at 2.1cm. The performance is evaluated for seven user locations over a span of 2.5m. The wireless transmission distance was limited up to 8m due to the power budget for the two RAUs. The performance of SISO is evaluated by placing one transmitting RAU at the SISO reference point as shown in Fig. 4.14. The user position M, which is in the centre of the span where user performance has been evaluated, is selected to be aligned with the SISO measurement reference point in a straight line.

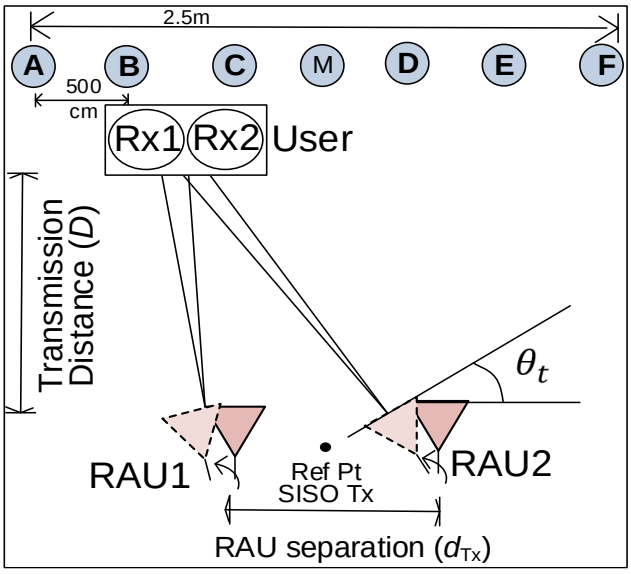

Figure. 4.14 Orientation of the RAUs and User for 2×2 MIMO Measurements

4.4. Realization of MIMO using Antenna Positioning

MIMO processing can be performed from the channel measurements by individually measuring each channel coefficient of the channel matrix, H [16].

These individual channel path measurements are processed subsequently and a MIMO algorithm, for spatial diversity or spatial multiplexing, is applied. Techniques to activate one pair of transmit-receive antennas to perform channel measurements for MIMO processing have been performed for lower frequencies [17] and can be useful for mmW MIMO where the LOS component is dominant. This section presents use of separate antenna-pair processing for MIMO measurements in a RoF supported 60 GHz MIMO in which the demonstration of performance improvement at several user locations has been performed. The results have been verified by comparing them with the MIMO setup presented in the previous section which uses two transmit and receive antennas at the same time for channel measurements. This emulated approach for MIMO processing is very useful at 60 GHz where the cost of mmW components in a large number of RF chains at the transmitter and receiver sides would be high. The MIMO measurements in the previous section were limited to 8m due to unavailability of components for two transmit RF chains. In this section, the experiments have been extended using the emulated MIMO approach to larger distances which were enabled by using the available 60 GHz amplifier before the single transmit antenna.

4.4.1. Experimental arrangement to measure channel coefficients

The experimental setup which was considered for emulated MIMO is shown in Fig. 4.15 which is similar to the setup explained for real MIMO but has only one RF chain on the transmitter and receiver side. A 60 GHz amplifier (QPI-V02030) has been added before the transmitting antenna with a variable attenuator to control the transmit power and operate the amplifier in its linear region. The measurements for channel coefficients were performed by first placing the transmit antenna at location RAU1 (shown in Fig. 4.14) and capturing the data at two receiver locations (Rx1 and Rx2). In the next step, the transmit antenna was placed at position RAU2 and data was captured at the two receiver locations. The sequential placement of antennas allows individual measurements of the channel matrix coefficients which are processed offline by an STBC Alamouti receiver or a Zero Forcing receiver, depending on the diversity scheme being used during the measurement. Using this arrangement, STBC encoded symbols in the form of Data1 and Data2 were transmitted from the positions RAU1 and RAU2, respectively, to achieve spatial diversity. For spatial multiplexing, different data at 0.5 Gb/s data rate is transmitted

from the transmit locations RAU1 and RAU2 which is then combined at the receiver using Zero Forcing processing. To analyze the effect of spatial diversity, the geometrical arrangement for the RAU spacing and user locations was kept the same as shown previously in Fig. 4.14, to compare the results from the emulated MIMO approach with the real MIMO. The experiments were performed at 6m and 8m using emulated MIMO for RAU spacings of 30cm, 60cm, 90cm and 120cm. The verification of the approach is validated by comparing the results with the real MIMO at 6m and 8m for different RAU spacings. The analysis was extended to 9m (longest distance available in the seminar room) to show the feasibility of the STBC and Zero Forcing for longer distances using the same setup and measurement environment.

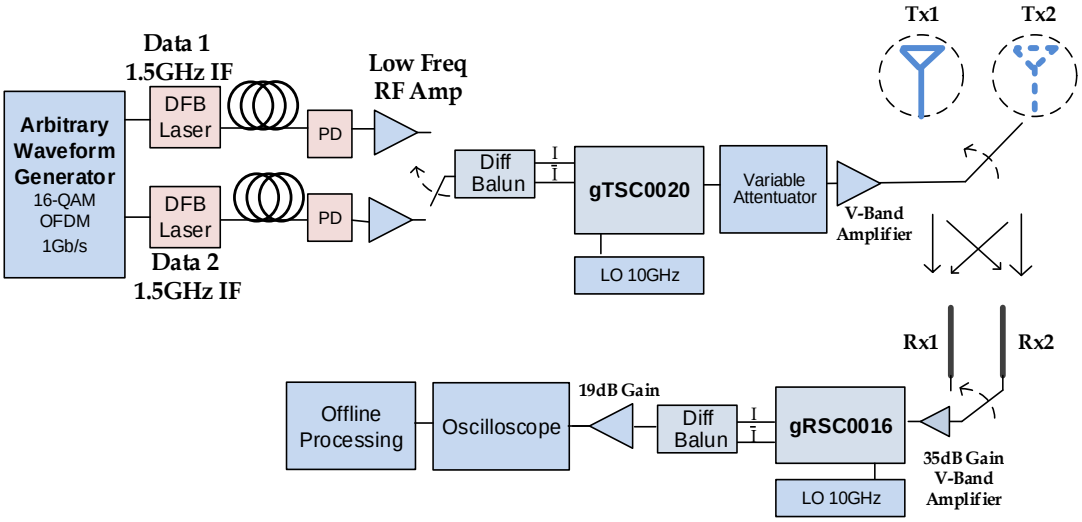

Figure. 4.15 Experimental Setup for Individual Measurements of Channel Coefficients for MIMO Processing

4.4.2. Experimental Setup for projected performance at longer distances

The performance improvement for 60 GHz system using spatial diversity and spatial multiplexing can be performed at much longer distances by using the emulated MIMO approach. The feasibility of the systems is demonstrated by performing the experiments in a 30m long corridor in the Jennison Building, University of Kent. Fig. 4.16 shows the layout of the building where CU has been placed in a room and RoF transport is used to place the RAU at two transmit locations in different corridors, which meet each other at a corner location where user was placed. The transmit antenna is used at the two locations of RAU1 and

RAU2 sequentially and data is captured for each transmit location at the user end after 25m of wireless transmission. The user is comprised of two slot-array antennas (2.1cm apart) similar to the setup used in previous section. The channel coefficients are measured and processed by the STBC Alamouti and Zero Forcing algorithms in offline processing to demonstrate the improvement in performance and feasibility of the emulated MIMO approach for 25m distance, and 30m which was the maximum possible transmission distance in the corridors. More details are shown in Fig. 4.17 which shows the pictures of the RAU consisting of an amplifier before the transmitting antenna and the user location in the corridor.

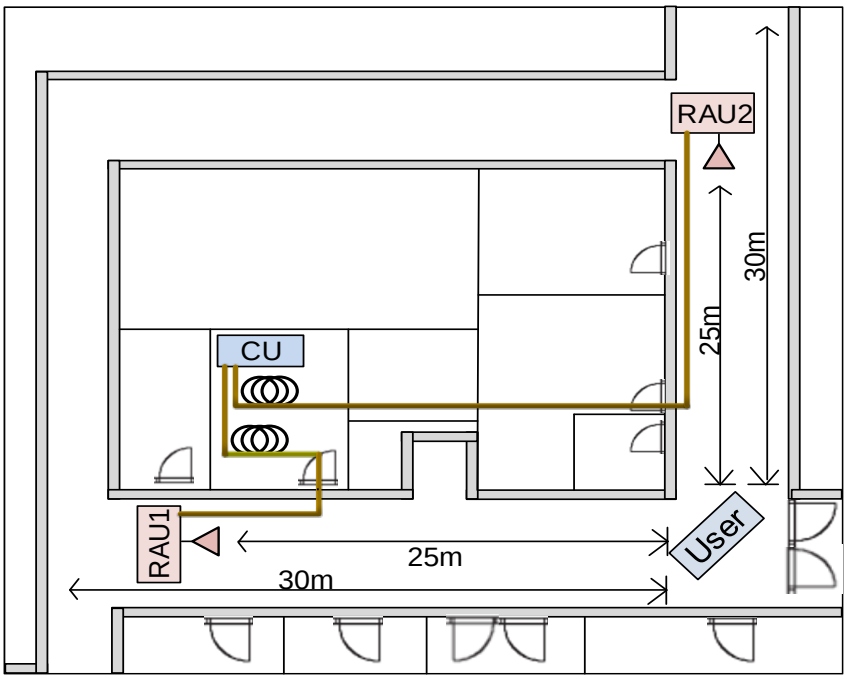

Figure. 4.16 Layout of the Measurement Location

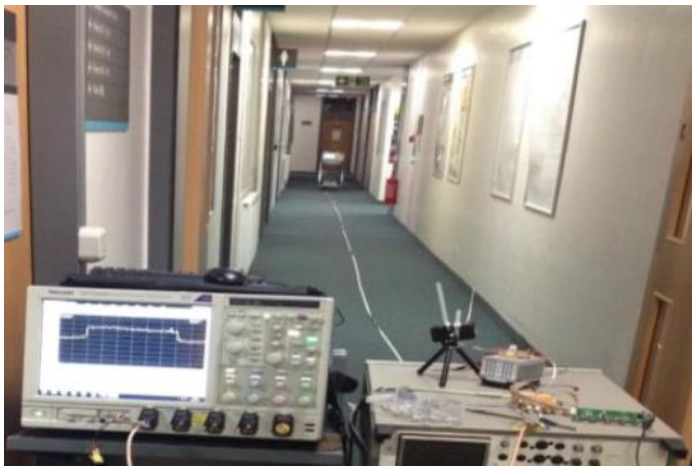

Figure. 4.17 Pictures of Measurement Location in the corridor of Jennison Building (University of Kent)

4.5. MIMO Measurement Results

This section presents the results from performing 2×2 MIMO employing Spatial Diversity and Spatial Multiplexing using STBC Alamouti and Zero Forcing, respectively. The results have been compared against the SISO performance to observe the performance improvement achieved through MIMO processing in terms of EVM or data rate.

4.5.1. Results for 25 GHz MIMO setup

The performance of SISO and MIMO with Alamouti STBC processing is shown in Fig. 4.18 for the wireless transmission distance of 3m. A data rate of 1Gb/s (305MHz bandwidth) has been used for SISO and MIMO measurements here. The separation between the two transmitting units was kept at 60cm. The individual SISO performance at each user location is higher than the 12.5% limit at a few user locations when Transmitter-1 or Transmitter-2 was used for measurements. The MIMO processing employing spatial diversity improves the performance of the systems by providing EVM below than the limit at all user locations. All six user locations receive 1Gb/s transmission with EVM below 12.5% which only occurred at two user locations (C and D) with SISO transmission.

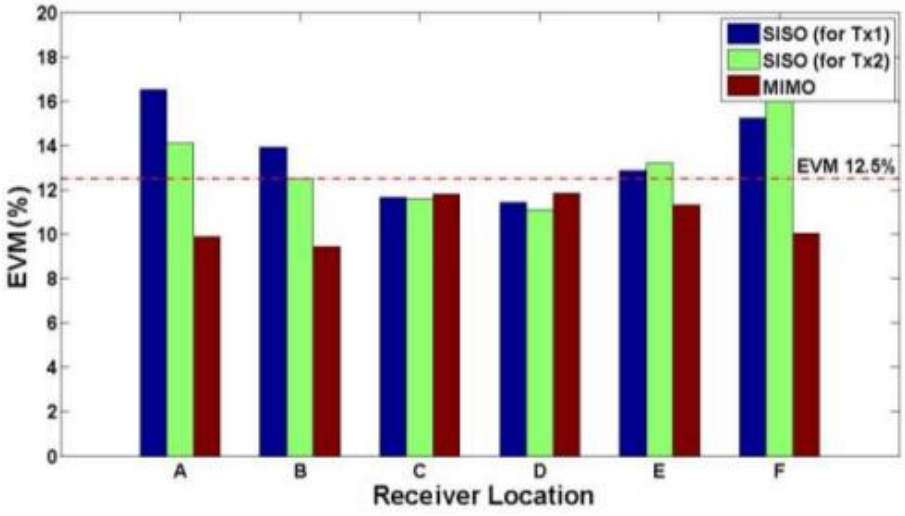

Figure. 4.18 EVM results for SISO versus STBC Alamouti MIMO transmission at 25 GHz

Fig. 4.19 shows the perforamcne of multiplexing two 0.5Gb/s data streams using the Zero Forcing algorithm after a wireless transmission of 5m. The two RAUs transmit different 0.5 Gb/s data generated by the AWG which is combined at the receiver to get an aggregate, doubled data rate. The EVM for the combined data at

1Gb/s is less than 12.5% limit at all user locations, which was not possible from SISO transmission of 1Gb/s as shown in Fig. 4.18. In Fig. 4.19, EVM results for single data at 0.5 Gb/s using SISO have been plotted for comparision because the objective of using spatial multiplexing in MIMO is to combine low data rate data streams, in order to achieve high aggregate data rate. It can be observed that both single 0.5 Gb/s and multiplexed 1Gb/s have EVM below the 12.5% threshold, except for the extreme positions of A and F where spatial diversity can be used to further reduce the EVM.

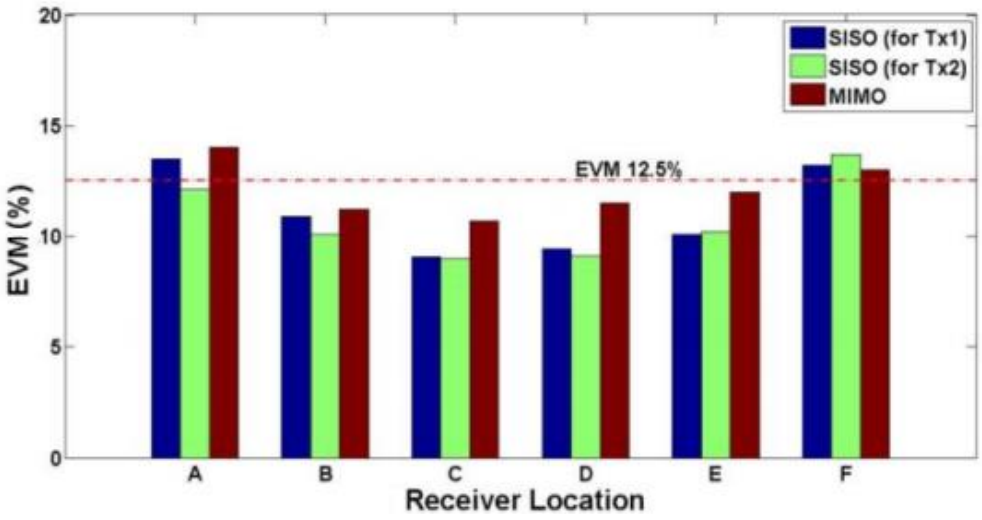

Figure. 4.19 SISO (0.5 Gb/s) versus Zero Forcing MIMO processing (1Gb/s) for 25 GHz transmission of 5m

Fig. 4.20 shows the STBC Alamouti receiver sensitivity for various transmission distances when the received power was varied from -54dBm to -38dBm. Wireless transmission of 2.5m, 3m, 3.5m and 4m were performed. It can be seen that the EVM drops below the 12.5% threshold for a received power of -50dBm and decreases further as the received power increases. For simplicity, all measurements were taken for a fixed transmitter separation of 40cm, and at one user location only. The results show that adequate amount of power budget is available to the receiver for EVM of less than 12.5% and the analysis can be extended to longer distances.

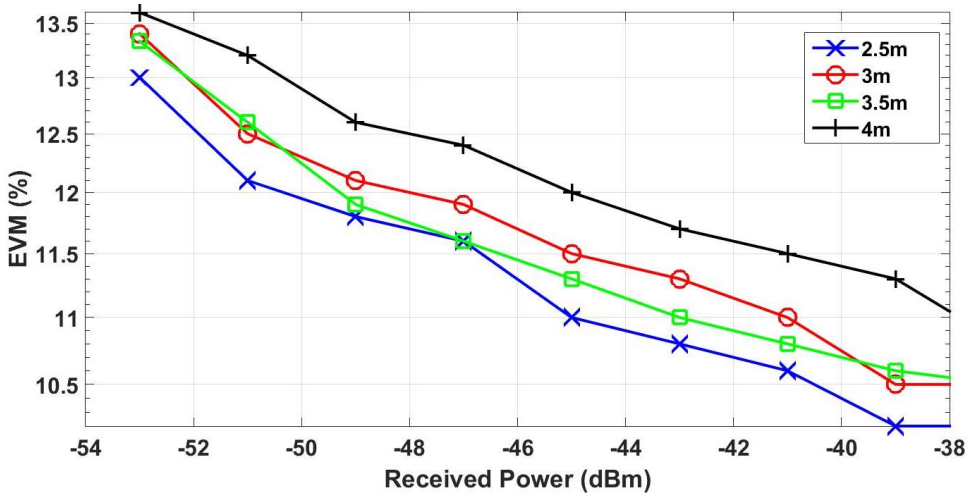

Figure. 4.20 Receiver Sensitivity for STBC Alamouti Receiver for various wireless transmission distances

4.5.2. Analysis of Different Transmit Antenna Spacing for Different Transmission Distances

As decorrelation among the MIMO channels heavily depends on the separation among the transmitting and receiving units [18], the effect of transmit antenna separation on the EVM performance in 25 GHz MIMO systems was analysed by performing the experiments for transmit antenna separation of 40cm, 60cm 80cm and 100cm. The two receiving antennas were attached together, which combined makes up the user receiver with a distance of approximately 5cm between the centres of aperture of the two antennas, during the whole work. Fig. 4.21 shows the EVM performance of Alamouti STBC for the wireless transmission distance of 3.5m for various transmit antenna separations. It can be seen that EVM values differ from each other at user locations for different values of transmit antenna separation. The lowest set of EVM was obtained when the transmit antenna separation was kept to 40cm.

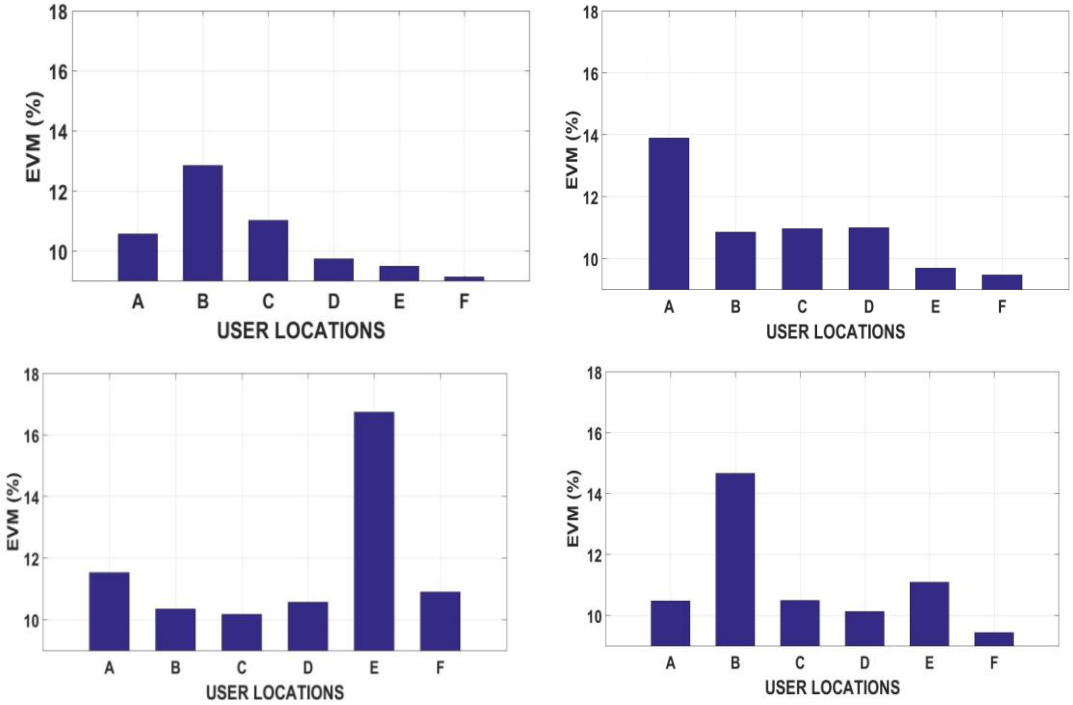

Figure. 4.21 EVM results at various user locations for transmitter separation of (top left) 40cm (top right) 60cm (bottom left) 80cm and (bottom right) 100cm for transmission distance of 3.5m

For further analysis on change in performance with the transmit antenna separation, Fig. 4.22 shows the EVM results for STBC Alamouti processing for different transmit antenna separations when the wireless transmission distance is increased to 4.5m. Comparing the results with Fig. 4.21, it can be observed that EVM for a particular transmit antenna separation changes with the wireless transmission distance for a user location. However the overall optimal performance of the system is more clearly to be best at transmit antenna separation of 60cm for 4.5m wireless distance. Hence the optimized separation between the transmit antennas needs to be adapted with the change in wireless transmission distance. This effect will be analysed in more detail for the 60 GHz setup in the following sections.

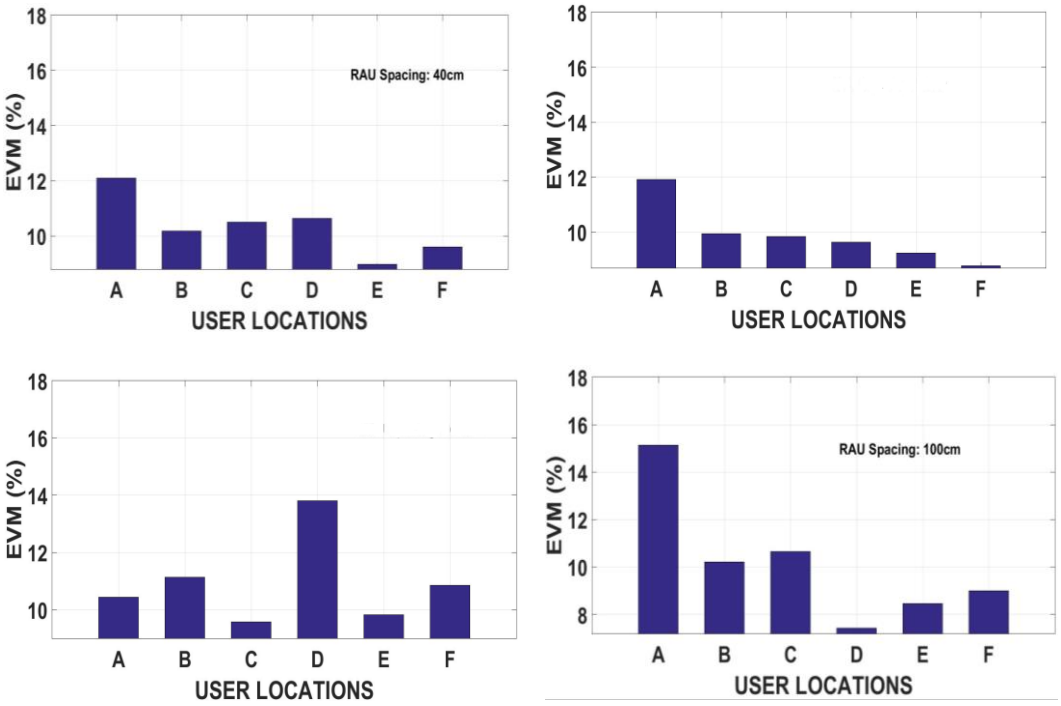

Figure. 4.22 EVM results at various user locations for transmitter separation of (top left) 40cm (top right) 60cm (bottom left) 80cm and (bottom right) 100cm for transmission distance of 4.5m

4.5.3. Distributed MIMO performance at 60 GHz

The performance improvement achieved through spatial diversity and spatial multiplexing in the distributed MIMO at 60 GHz are shown in this section for wireless transmission distances of 5m, 6m, 7m and 8m. The transmission distance was limited to 8m due to the available components for the two RF chains at the transmitter and receiver end for 2×2 operation. For Fig. 4.23 only 6m and 8m distances were selected for the results as they present results at an intermediate distance and maximum distance, respectively. Experiments were performed for transmit antenna separations of 30cm, 60cm, 90cma and 120cm, whose effect will be discussed in the later sections. The transmit antenna separation of 60cm has been used for 6m wireless distance and 120cm for 8m for the results shown in Fig. 4.23 for STBC Alamouti processing because these separations gave the lowest set of EVM values. The SISO performance at 6m is limited to few user locations and EVM becomes higher than the 12.5% limit at the locations on the edges of the measurement span (A, B, E and F). Improvement in EVM results for 6m through STBC shows that coverage can be increased to all user locations. This improvement in coverage is clearer for transmission distance of 8m where the SISO has not been

able to provide EVM below 12.5% at any user location and STBC provides a significant decrease in EVM.

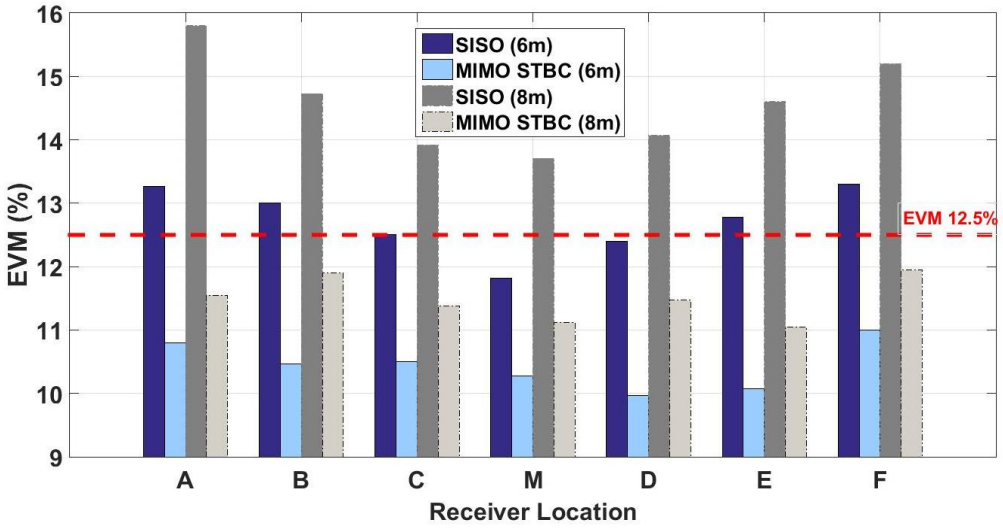

Figure. 4.23 EVM comparison of SISO (1Gb/s) versus STBC MIMO (1Gb/s) processing for 6m (RAU spacing: 60cm) and 8m (RAU spacing: 120cm)

In the next stage, results from spatial multiplexing are shown in Fig. 4.24 where two independent 0.5 Gb/s streams are combined at the receiver to achieve an aggregate data rate of 1Gb/s. The results show that SISO performance of a single 0.5 Gb/s data stream and MIMO results by combining two data streams (to achieve 1Gb/s) are below 12.5% EVM limit. The results for MIMO processing using Zero Forcing receiver have been shown for transmission distances of 6m and 8m with the transmit antenna separation of 60cm for 6m transmission and 120cm for 8m, as best results were achieved in these conditions.

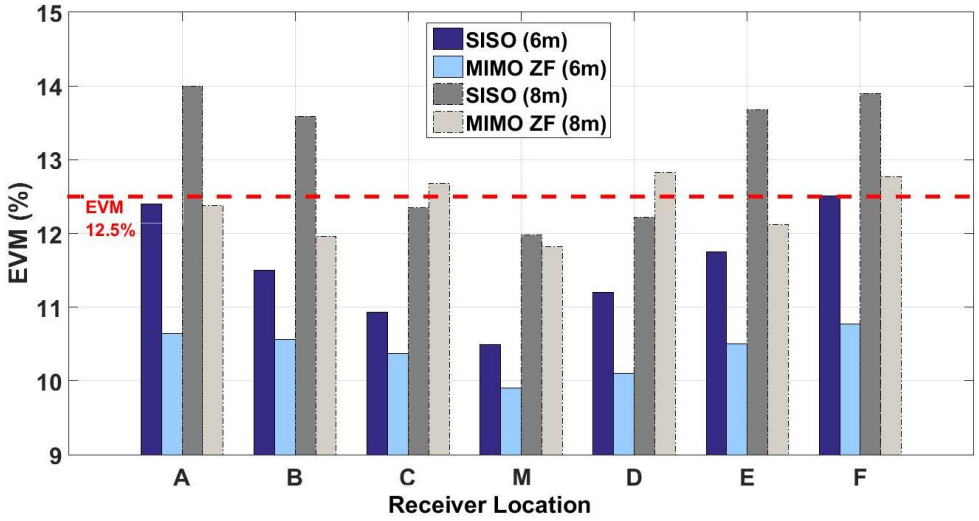

Figure. 4.24 EVM comparison of SISO (0.5 Gb/s) versus Zero Forcing MIMO (1Gb/s) processing for 6m (RAU spacing: 60cm) and 8m (RAU spacing: 120cm)

4.5.4. Analysis for Optimal Transmit Antenna Spacing

The separation distance between the transmitting units in LOS MIMO is an important parameter as decorrelation among the MIMO channels is dependent on it. Optimum performance from MIMO processing can be achieved by having the transmit antenna separation (RAU spacing) which can provide maximum decorrelation among the channels. The effect of RAU spacing on 60 GHz MIMO is analysed by performing the experiments with antenna arrangements having 30cm, 60cm, 90cm and 120cm separation between the transmitting units. The performance was analysed for these four values of RAU spacing for each wireless transmission distance (maximum up to 8m).

Fig. 4.25 shows the results after STBC processing for spatial diversity at 6m wireless transmission for various RAU spacings. For simplicity, only four user locations of one side and the middle (M) has been presented. The set of EVM for RAU spacing of 60cm provides the optimum performance as compared to the other spacings. Similarly in Fig. 4.26 which shows the results after Zero Forcing processing for spatial multiplexing at 6m distance, the RAU spacing of 60cm provides the best results as compared to the set of EVM results for 30cm, 90cm and 120cm spacings.

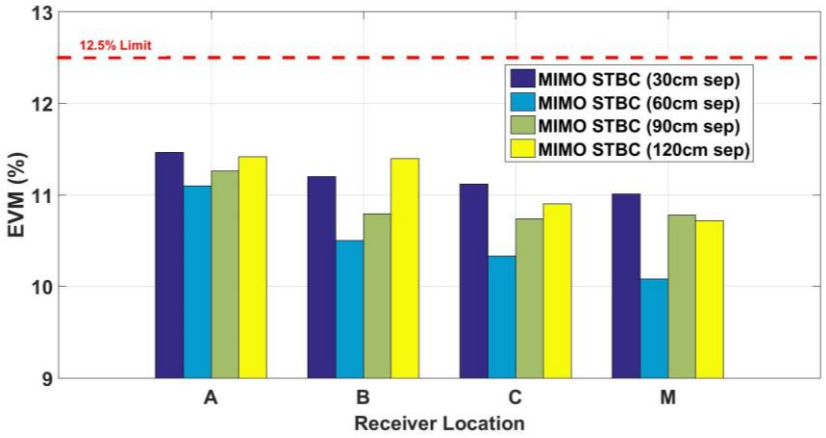

Figure. 4.25 EVM results for different RAU spacings after STBC Alamouti MIMO (1Gb/s) processing for 6m wireless transmission

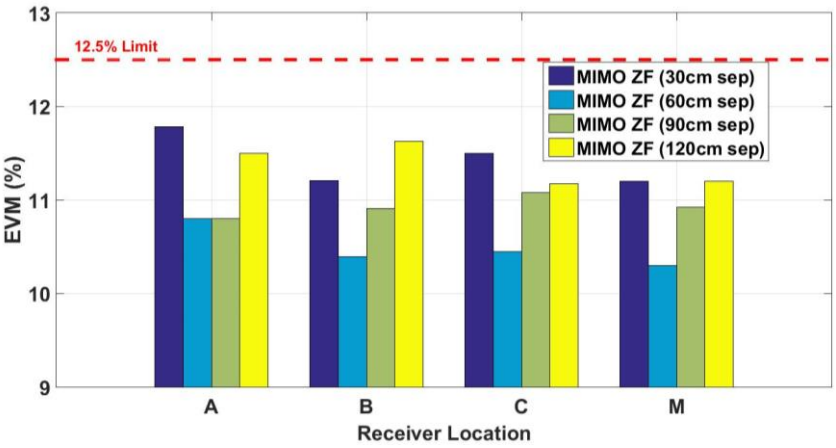

Figure. 4.26 EVM results for different RAU spacings after Zero Forcing MIMO (1Gb/s) processing for 6m wireless transmission

As the wireless transmission distance is increased, the required optimum RAU spacing increases as shown by the results in Fig. 4.27 (top) for the results from STBC and Fig.4.27 (bottom) for Zero Forcing at 8m wireless distance. The results show that the lowest set of EVM results was obtained at an RAU spacing of 120cm. Hence, larger RAU spacing is required for longer transmission distances for which the proposed RoF transport for mmW MIMO can provide the required flexibility and ease of operation.

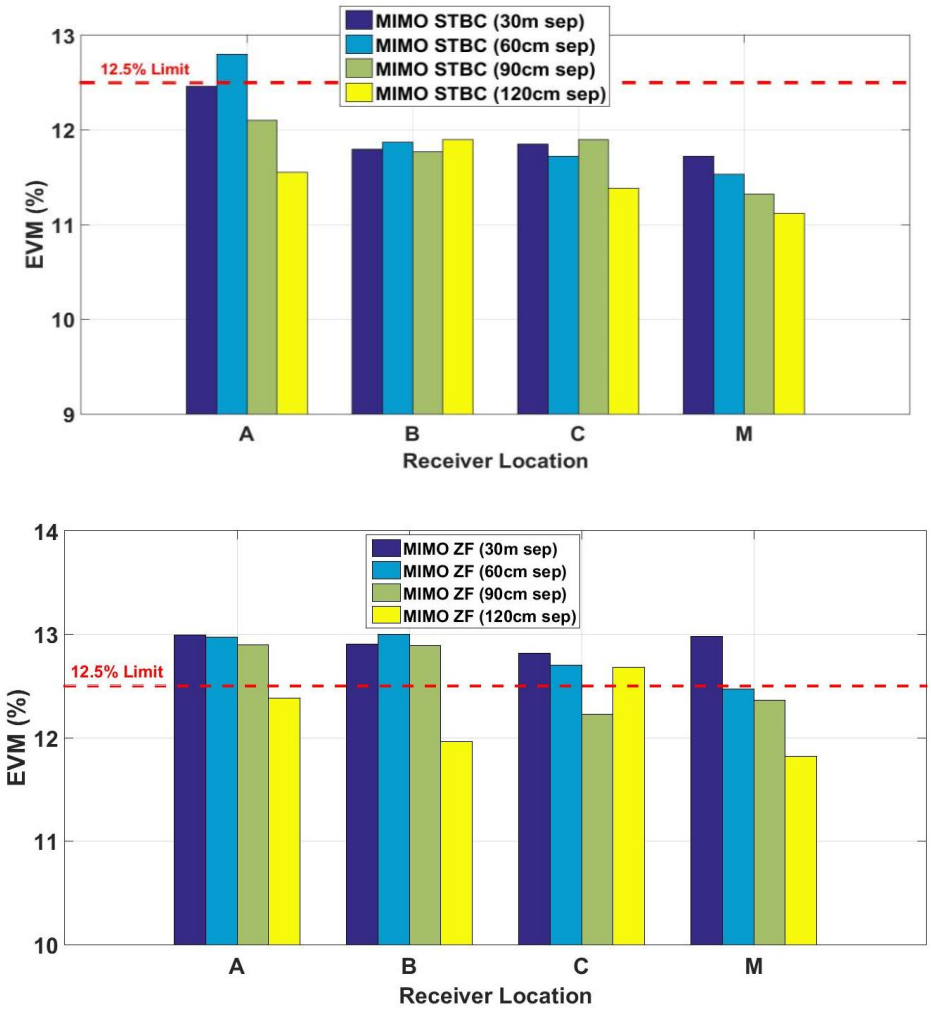

Figure. 4.27 EVM results for different RAU spacings after STBC processing (top) and Zero Forcing processing (bottom), after 8m wireless transmission

The experimental results can be compared with the theoretical optimum antenna spacing values for wireless transmission distances that have been used in the experiments. The theoretical optimum spacings are evaluated by using the condition by which maximum capacity can be obtained from the MIMO operation. i.e $HH^H = n_M I_N$. Where H represents the MIMO channel matrix and M, N represents the number of transmitting and receiving antennas, respectively. This condition is achieved when MIMO channels are orthogonal [18] and by solving the geometry of the antenna arrangements for 2×2 LOS MIMO operation for this condition; the optimum configuration [19], [20] can be obtained as:

$$d_{Tx} d_{Rx} = D\lambda / 2\cos\theta_t \cos\theta_r \tag{4.1}$$

where λ is the mmW transmission wavelength, D represents wireless transmission distance and d_{Tx}, d_{Rx} are the separation distances between the transmitting and

receiving antennas, respectively. θ_t represents the angle of tilt of the transmit antennas in the plane of transmission and θ_r is the tilt of receiving antennas. Using (4.1), considering the operating frequency to be 61.5GHz, and angular orientation θ_t, θ_r be ideally 0º at both ends of the MIMO transmission and the spacing among the receiving unit d_{Rx} as minimum as possible (the minimum achievable separation was 2.1cm during the experiments), Fig. 4.28 shows the theoretical optimal RAU spacing required for wireless transmission distance D of 5m, 6m, 7m and 8m. As only four RAU spacing values 30cm, 60cm, 90cm and 120cm were used in the experiment and it is difficult to achieve 0° angular orientation for transmitting and receiving antennas, the RAU spacing for which minimum set of EVM was obtained has been shown with error bars. The error bars show the range of RAU spacing in which the best results can be achieved. The accuracy of the results can be improved by using a small step (for example 5cm) for RAU spacings in the experiment. Fig. 4.28 shows that, for instance, minimum set of EVM was obtained at 90cm RAU spacing for 7m transmission while the error bar shows that the best results can occur between 90cm ± 30cm. For 8m wireless distance, the minimum set of EVM in the experiment were found to be at 120cm RAU spacing but the best performance could occur at any point between 90cm or above 120cm.

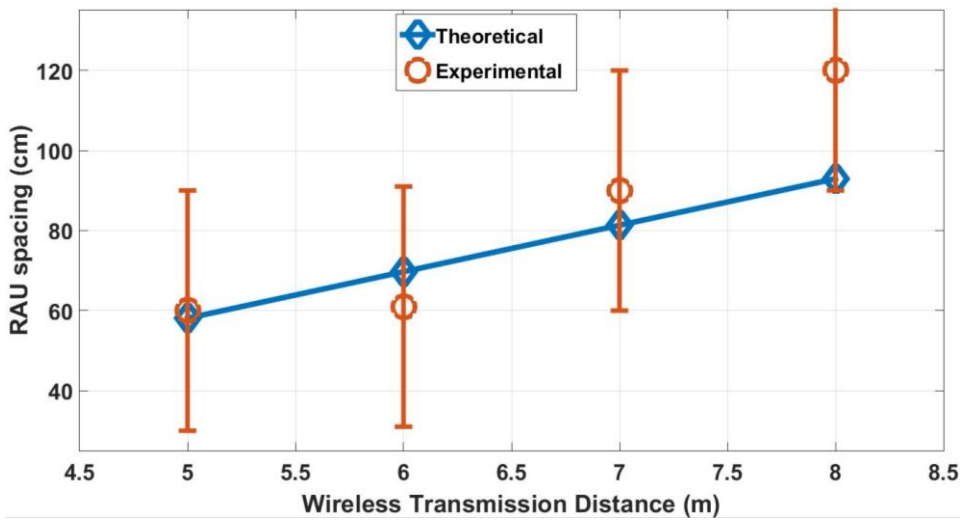

Figure. 4.28 2×2 MIMO Optimum RAU spacing results from theoretical calculations and Experimental values with error bars to represent the range between the considered RAU spacings during the experiments

4.5.4. Results from Emulation of 60 GHz MIMO and projections for longer distances

The results from the emulated MIMO approach are shown in Fig. 4.29 for a wireless transmission distance of 5m. STBC processing is performed after individual measurements of channel coefficients and the results show that improvement in EVM is achieved using the emulated MIMO processing, as compared to SISO transmission. This shows the achievement of the spatial gain through the measurement approach for 5m transmission distance.

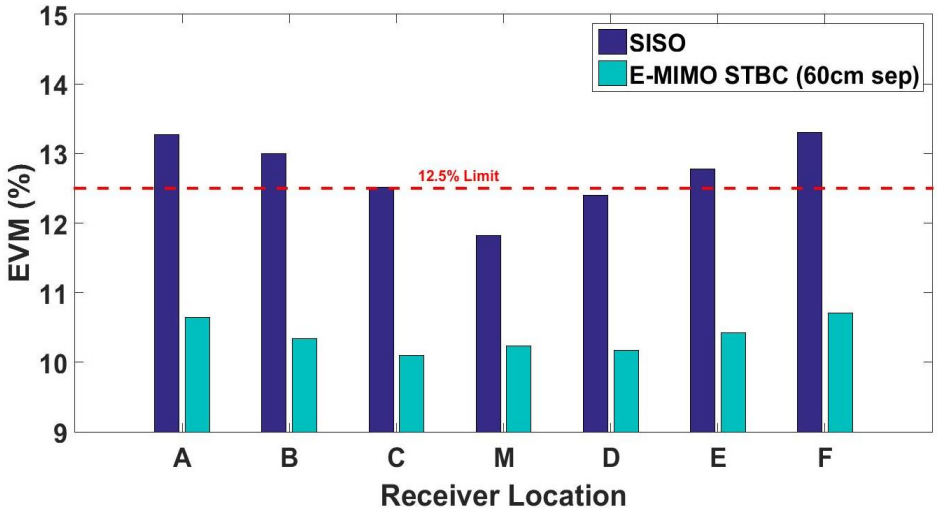

Figure. 4.29 SISO versus Emulated MIMO STBC Processing for Transmission distance of 5m

In the next step, experiments were performed using different RAU spacings and the transmission distance is increased to 6m to compare the results with real MIMO (which were shown in Fig. 4.23). As shown in Fig 4.30, the real and emulated MIMO provide the minimum set of EVM for RAU spacing of 60cm. Both results have been plotted for transmission distance of 6m with STBC processing and only RAU spacings of 60cm and 120cm have been compared for simplicity. There is a good amount of agreement in the results from both measurement approaches at 6m and Fig. 4.31 shows the results after 8m of wireless transmission which suggests that both measurements techniques provide optimum results for RAU spacing of 120cm (rather than 60cm) using the STBC approach at this wireless distance. The agreement in results at 6m and 8m wireless transmission for different RAU spacing shows that emulated MIMO technique can approximate real MIMO operation and be used to extend measurements to much longer distances which were not possible

due to hardware limitations for the two RF chains at the transmitter and receiver ends.

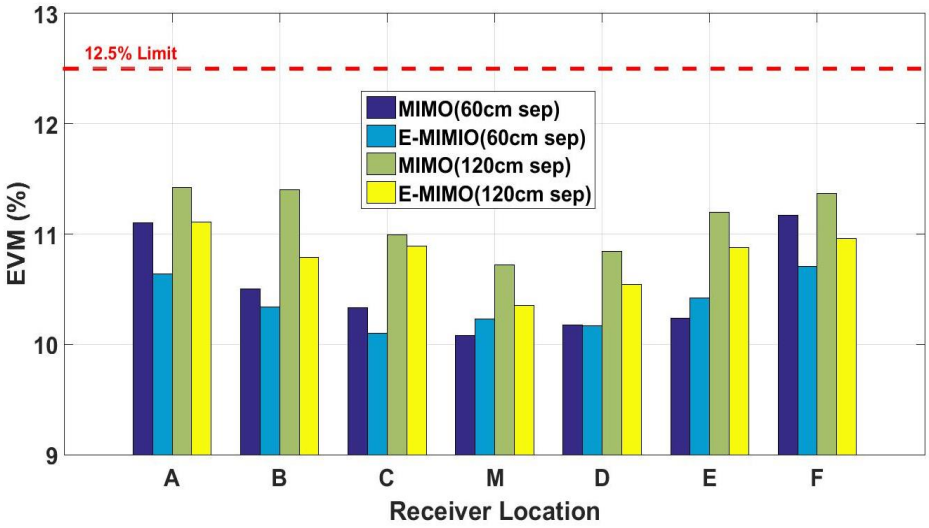

Figure. 4.30 EVM comparison of 2×2 MIMO using STBC processing at 6m transmission distance and equivalent emulated measurements

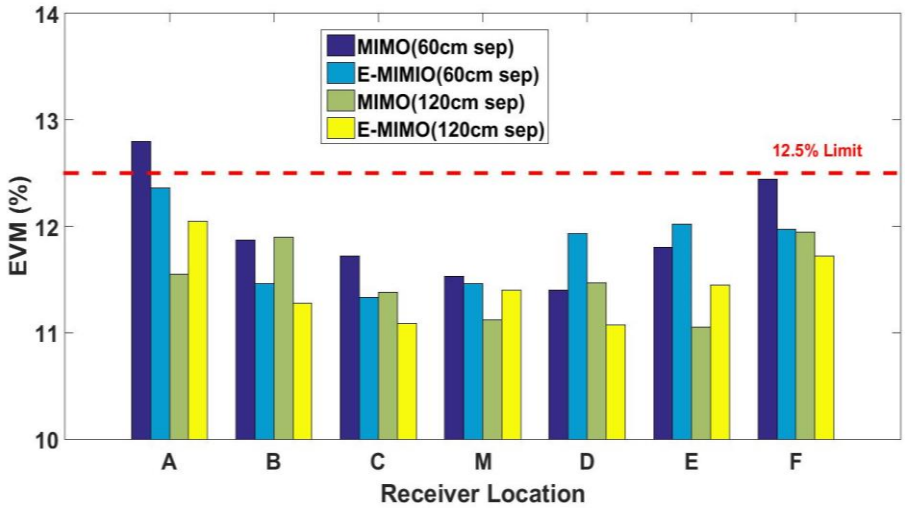

Figure. 4.31 EVM comparison of 2×2 MIMO using STBC processing 8m transmission distance and equivalent emulated measurements

In the next stage, the emulated MIMO approach is used to perform an analysis for STBC Alamouti and Zero Forcing algorithms at 9m wireless distance transmission (which was the longest possible in the seminar room). Fig. 4.32 shows the results at 9m distance for RAU spacing of 30cm, 60cm, 90cm and 120cm using emulated MIMO approach and STBC processing. The results are compared with SISO transmission at various user locations. The improvement in EVM shows that spatial gain is achieved at each user location and optimum results are obtained for the RAU spacing of 120cm. Fig. 4.33 shows the results after Zero Forcing processing

for different data sets transmitted at 0.5 Gb/s. The best set of results are obtained at the RAU spacing of 120cm with spatial multiplexing which verifies the results obtained with the real MIMO.

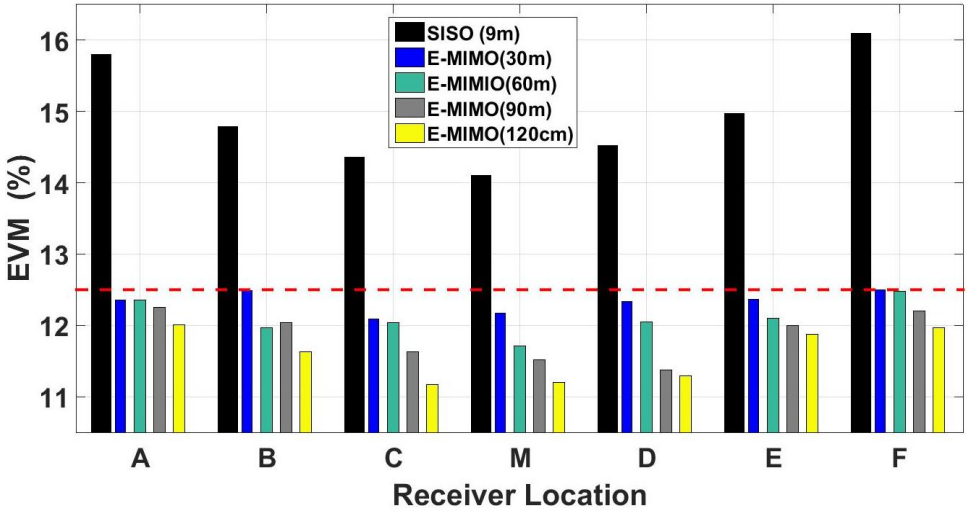

Figure. 4.32 EVM results from SISO and Emulated MIMO (STBC) at transmission distance of 9m with various transmit antenna separations for 1Gb/s data rate

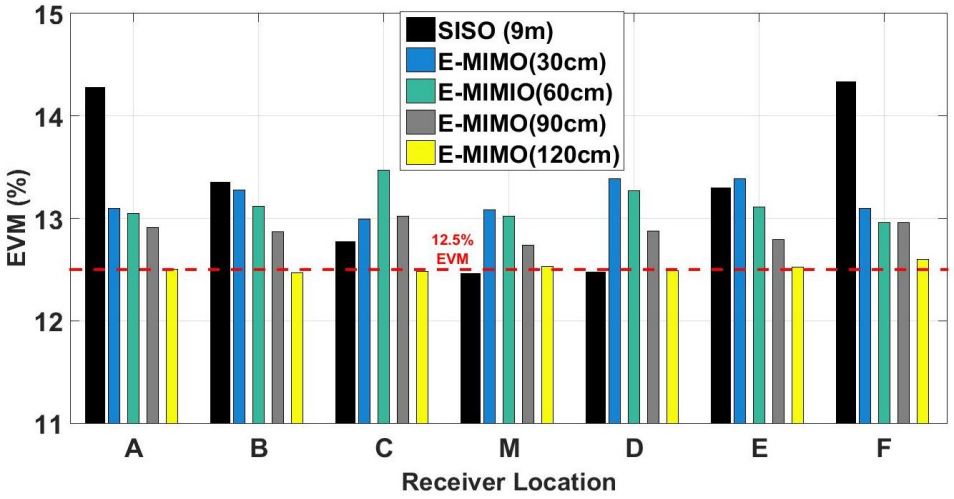

Figure. 4.33 EVM results from Emulated MIMO (ZF processing) with 1Gb/s at transmission distance of 9m with various transmit antenna separations, and SISO with 0.5Gb/s data rate

The analysis for performance improvement in terms of coverage are extended to 25m and 30m wireless transmission using the experimental setup for emulated MIMO shown in Fig. 4.15 and the measurement arrangement shown in Fig. 4.16. The results for SISO transmission for 1Gb/s using STBC processing in Table 4.1 shows the improvement in the EVM, as compared to SISO, which is below the 12.5% limit after MIMO processing. Also, Zero Forcing provides multiplexing of two 0.5 Gb/s at a slightly higher EVM which still satisfies the minimum

requirement of EVM for 16-QAM modulation with Forward Error Correction (FEC) [21].

Table. 4.1 SISO versus Emulated MIMO processing results

Distance	SISO (1Gb/s)	STBC (1Gb/s)	SISO (0.5Gb/s)	ZF (1Gb/s)
25m	14.5%	12.1%	12.3%	12.9%
30m	15.1%	12.4%	12.8%	13.3%

4.5. Summary

Experimental analysis for 2×2 MIMO at 25 GHz and 60 GHz has been presented using RoF transport. The photonic generation of 25 GHz MIMO signals is presented using overdriving of an optical phase modulator. A pair of MZM was used to modulate the OFDM encoded MIMO signals generated by AWG at 1.5 GHz IF. The modulated signals over different wavelengths and unmodulated optical lines are transported over 2.2km of fibre to the RAUs. Each RAU filters two 25 GHz apart optical lines for direct photonic upconversion using a high bandwidth photodiode. The generated 25 GHz MIMO signals are amplified and transmitted over 6m of wireless distance using a pair of horn antennas. The receiver comprises of two similar horn antennas which are placed together. The received signal is amplified, downconverted and captured using an Oscilloscope. Performance analysis of SISO and MIMO is performed at six different user locations for spatial diversity and spatial multiplexing using STBC Alamouti and Zero Forcing algorithms, respectively. The results show that performance improvement through spatial diversity is achieved using STBC at all user locations. The receiver sensitivity was found to be -50dBm after 2km of RoF transport. The effect of transmit antenna separation is analysed on the performance of 25 GHz MIMO using separation values of 40cm, 60cm, 80cm and 100cm for transmission distances of 3.5m and 4m. The EVM for each user location was found to be changed for each transmit antenna separation but optimum results were obtained at 60cm transmit antenna spacing. To achieve spatial multiplexing, a Zero Forcing receiver was used in order to combine two low data rate data streams of 0.5 Gb/s. The combined aggregate data rate of 1Gb/s was lower than 12.5% which wasn't possible with SISO transmission of 1Gb/s. The spatial multiplexing was not achieved at distances less than 4.5m and analysis was performed at 4.5m, 5m and 6m to achieve an EVM of less than 12.5%.

The experimental work on mmW MIMO was extended to 60 GHz by analyzing the performance of the 2×2 MIMO for 8m of wireless transmission. The two MIMO signals from the AWG at an IF of 1.5GHz are modulated over a set of DFB Lasers and transported over 2.2km of SMF transmission to two RAUs. At each RAU, a low bandwidth photodiode regenerates the IF signals which is amplified and

upconvereted to 61.5 GHz using an integrated transmitter module. After wireless transmission, a set of two slot array antennas is used as a receiver. Each received signal is amplified using a V-band amplifier and downconveretd to 1.5 GHz IF using an integrated receiver module to be captured by the oscilloscope. The experimental analysis was performed for various transmission distances up to 8m and transmit antenna spacings of 30, 60, 90 and 120cm. The results show that spatial diversity improves the coverage of a 60 GHz system transmitting 1Gb/s data rate for seven user locations spread over a span of 2.5m by improving the EVM performance, where EVM was higher than 12.5% limit for SISO. Results from spatial multiplexing also shows that by combining two 0.5 Gb/s data streams using Zero Forcing algorithm after 2×2 60 GHz transmission, overall data rate of 1Gb/s can be achieved at all user locations. Further investigation for effect of transmit antenna separation on MIMO performance shows that wider spacing is required for optimum results with the increase in transmission distance. Minimum set of EVM results were obtained with 60cm and 120cm RAU spacings for transmission distances of 6m and 8m, respectively, for both spatial diversity and spatial multiplexing. The experimental results for optimum RAU spacings for transmission distance of 5m, 6m, 7m and 8m were compared with theoretical predictions and found to be in agreement with them.

The 60 GHz MIMO analysis is extended to much longer distances using an emulated approach in which only one transmit antenna is used and channel coefficients are measured individually for MIMO processing. The transmit antenna is placed at two distinct positions to emulate the 2×2 MIMO and data is captured for each position to obtain the complex channel matrix *H*. The results after emulated MIMO processing showed that spatial diversity and spatial multiplexing can be achieved with similar results to that of real MIMO. The optimum spacing for 6m and 8m transmission distances for emulated MIMO was found to be 60cm and 120cm which is in accordance with the results from real MIMO which shows the validity of the approach. The agreement in results show that mmW channels are relatively static and channel measurements can be useful to extend the analysis where hardware constraints limit the experimental analysis, such as for NxN massive MIMO system as large number of RAUs have been anticipated for future systems and at very long transmission distances. The emulated MIMO was used to

extend the analysis to 9m, for which the optimum spacing was found to be 120cm. Further extension of work was performed in a corridor for 25m and 30m wireless transmission distances, in which the two RAU were placed in different corridors and MIMO processing was performed to show the feasibility of the approach.

REFRENCES

[1] N.J. Gomes, P. P. Monteiro and A. Gameiro, "Next generation wireless communications using radio over fiber", *John Wiley & Sons*, 2012.

[2] J. Kim and I. Lee, "802.11 WLAN: history and new enabling MIMO techniques for next generation standards", *IEEE Communications Magazine*, Vol. 53 (3), 2015, pp.134-140.

[3] Q. Li, G. Li, I. W. Lee, M. Lee, D. Mazzarese, B. Clerckx and Z. Li, "MIMO techniques in WiMAX and LTE: a feature overview", *IEEE Communications magazine*, Vol. 48 (5), 2010.

[4] S. P. Alex and L. M.A. Jalloul, "Performance evaluation of MIMO in IEEE802. 16e/WiMAX", *IEEE Journal of Selected Topics in Signal Processing*, Vol. 2 (2), 2008, pp.181-190.

[5] P.Y. Tsai, P. C. Lo, F.J. Shih, W.J. Jau, M. Y. Huang, Z. Y. Huang, "A 4x4 MIMO-OFDM Baseband Receiver With 160 MHz Bandwidth for Indoor Gigabit Wireless Communications", *IEEE Transactions on Circuits and Systems*, Vol. 62 (12), 2015, pp.2929-2939.

[6] P. Liu, J. Blumenstein, J, N. S. Perović, M. Di Renzo and A. Springer "Performance of Generalized Spatial Modulation MIMO Over Measured 60GHz Indoor Channels", *IEEE Transactions on Communications*, Vol. 66 (1), 2018, pp.133-148.

[7] L. Liu, W. Hong, H. Wang, G. Yang, N. Zhang, H. Zhao, J. Chang, C. Yu, X. Yu, H. Tang, H. Zhu and L. Tian, "Characterization of line-of-sight MIMO channel for fixed wireless communications." *IEEE Antennas and Wireless Propagation Letters*, Vol. 6, 2007, pp.36-39.

[8] F. Tonini, M. Fiorani, M. Furdek, C. Raffaelli, L. Wosinska and P. Monti, "Radio and Transport Planning of Centralized Radio Architectures in 5G Indoor Scenarios", *IEEE Journal on Selected Areas in Communications*, Vol. 35 (8), 2017, pp.1837-1848.

[9] J. James, P. Shen, A. Nkansah, X. Liang and N.J. Gomes, "Nonlinearity and noise effects in multi-level signal millimeter-wave over fiber transmission using

single and dual wavelength modulation", *IEEE Transactions on Microwave Theory and Techniques*, Vol. 58 (11), 2010, pp.3189-3198.

[10] "Emcore Model 1935F Datasheet," Available: http://www.emcore.com

[11] "Appointech 2.5 Gbps InGaAs PIN Photodiode Module Datasheet,". Available:
http://www.appointech.com.

[12] T. Quinlan, S. Walker. "A 16.8 dBi quasi-discoidal radiation pattern antenna array for 60GHz non-line-of-sight applications", *Loughborough Antennas and Propagation Conference (LAPC)*, 2014, pp.210- 213.

[13] Gotmic Microwave Integrated Circuits (2014): gTSC0020 Complete Transmitter 57-66 GHz (http://www.gotmic.se/txrx.html)

[14] Gotmic Microwave Integrated Circuits (2014): gRSC0016 Complete Receiver 60 GHz (http://www.gotmic.se/txrx.html)

[15] T. Quinlan and S. Walker. "A Coaxial, 60-GHz, 15.3-dBi slot antenna array", *IEEE Antennas and Wireless Propagation Letters*, Vol. 13, 2014, pp.818-821.

[16] G. Krishnamurthy,K.G. Gard, "Time division multiplexing front-ends for multiantenna integrated wireless receivers", *IEEE Transactions on Circuits and Systems*,Vol. 57 (6), 2010, pp.1231-1243.

[17] A. Honda, I. Ida, Y. Oishi, Q.T. Tran, S. Hara, JI. Takada, "Experimental evaluation of MIMO antena selection system using RF-MEMS switches", *IEEE 18th International Symposium on Personal, Indoor and Mobile Radio Communications (PIMRC)*, 2007, pp.1-5.

[18] J. Onubogu, K. Ziri-Castro, D. Jayalath, and S. Hajime, "Experimental evaluation of the performance of MIMO-OFDM for vehicle-to-infrastructure communications," *EURASIP Journal on Wireless Communications and Networking*, 2015, Vol. 183, pp.1–19.

[19] F. Bohagen, P. Orten and G.E. Oien, "Design of Optimal High-Rank Line-of-Signt MIMO Channels", *IEEE Transactions of wireless communications*, Vol. 6 (4), 2007.

[20] M. Matthaiou, D.I. Laurenson and C.X. Wang, "Capacity Study of Vehicle-to-Roadside MIMO channels with a Line-of-sight Component", *IEEE Wireless*

Communications and Networking Conference (WCNC), Las Vegas, 2008, pp.775-779.

[21] Rohde & Schwarz: "LTE System Specifications and their Impact on RF & BaseBand Circuits", 2013.

CHAPTER 5
SUBCARRIER MULTIPLEXING BASED MULTI-USER TRANSMISSION USING LEAKY WAVE ANTENNA

5.1. Introduction

Different techniques for RoF transport and mmW generation were simulated and experimentally implemented in Chapter 3. The RoF transport based on a DFB Laser link and 60 GHz generation using an integrated transmitter and receiver pair was considered as the most feasible option to perform experimental work on 60 GHz MIMO, with the available equipment in the lab, rather than photonic generation of 60 GHz using an optical two-tone signal. In Chapter 4, the coverage for 60 GHz transmission was improved using MIMO operation with STBC coding and ZF receiver for several user locations and a RoF fronthaul was proposed to achieve flexible and large transmit antenna spacing to achieve optimum MIMO performance for different transmission distances. However as a large number of users (as well as devices) are anticipated to be connected within a small vicinity in future mobile networks [1], a 60 GHz-band multi-user transmission system is presented in this chapter which includes generation of a composite SCM signal, RoF transport using the DFB laser link, upconversion to 60 GHz-band frequencies using the integrated transmitter and receiver pair, and transmission to multiple users using the beamsteering characteristics of a Leaky Wave Antenna (LWA). The LWA is a frequency selective beamsteering antenna which directs the beam to different angular locations, depending on the carrier frequency of the input signal. The LWA (designed and fabricated at the University of Duisberg, Germany) is used in the work presented in this chapter to understand and propose its possible applications for future communication systems. The LWA can be used to generate

multiple beams by feeding a Frequency Division Multiplexed (FDM) signal, consisting of multiple user-signals at different carrier frequencies, towards the spatially distributed users.

Experimental work has been performed to serve a large number of users simultaneously, resulting in a high sum data rate (aggregate data rate obtained for all users) using different QAM modulation formats. A demonstration to serve a large number of users using a single RoF link and single RF chain is shown in this chapter. An EVM analysis of individual subcarriers for large bandwidth signals is performed to understand the effect of SNR degradation due to the beamsteering behaviour of the LWA. The characterisation of the LWA transmission to theoretically calculate the sum rate is also performed using the LWA beam pattern. The work is extended to an experimental demonstration with two LWAs that shows an improvement in the coverage and spectrum efficiency of the proposed setup.

In addition, a DWDM-based system for multiuser transmission using a single LWA is presented which provides photonic generation of 60 GHz-band frequencies. Finally, the emulation of MIMO operation using STBC Alamouti coding and ZF algorithm, as presented in the previous chapter, is extended using the LWA.

5.2. Beamsteering Characteristics of Leaky Wave Antenna

A LWA consists of a rectangular slotted waveguide with a guiding structure and supports a travelling wave which propagates and radiates power continuously (as leakage) from the periodic discontinuity in the structure [2]. The designed LWA* operates in the range of 50 GHz to 70 GHz, thus comprising 20 GHz bandwidth [3]. It requires only single feed at one end using V-band end launch connector [4], which provides connection with the PCB. The PCB can be supported by a simple brass bracket as shown in Figure. 5.1. The fabricated PCB is of low cost and consists of an array of unit cells which provide passive beamsteering by producing beams in different spatial directions for different carrier frequencies. Figure. 5.2 shows the radiation characteristics of the LWA for different mmW frequencies with respect to the right-hand side and left-hand side transmission regions.

*Acknowledgment: provided by Prof. Andreas Stohr and Matthias Steeg (University of Duisberg)

Figure. 5.1 12x1 LWA PCB (dimensions 90mm×20mm) with 12 unit cells and V-band End Launch Connectors on both ends mounted on a brass bracket for support

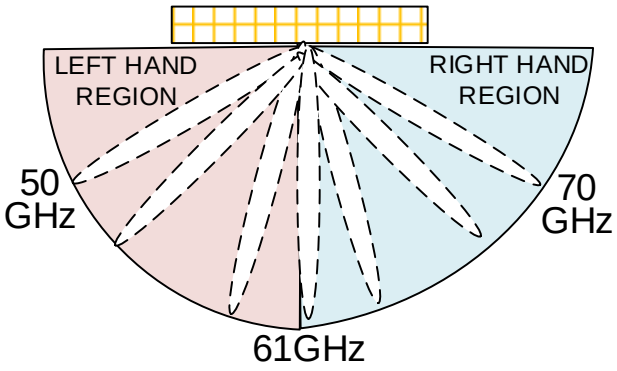

Figure. 5.2 Spatially Distributed LWA Transmission for mmW Frequencies (beam angles are not exact and are only for illustration)

The 12x1 LWA has a directional gain of 14.5dB for the main lobe (with respect to the first sidelobe). With a change of 1GHz in the carrier frequency, the LWA steers the main beam around 1.86°. Figure. 5.3 shows the HFSS® simulation results for the beam pattern for the 12x1 LWA for different carrier frequencies [5].

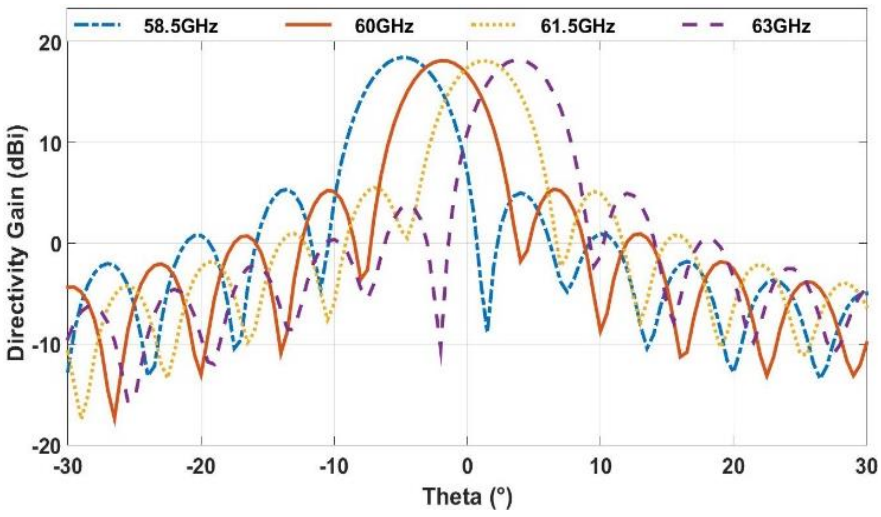

Figure. 5.3 Simulation results for 12x1 Leaky Wave Antenna for different carrier frequencies

Two versions of the LWA, 12x1 and 20x1, with array sizes of 12 unit elements and 20 unit elements, respectively, have been used in this work. As the number of cells

in the array increases, the beamwidth becomes narrower and results in an increased gain for the main lobe. Thus the 20x1 LWA has narrower beamwidth [6] and 2dB more gain than the 12x1 LWA. Figure. 5.4 shows the radiation pattern of the two LWAs for the 59 GHz and 63 GHz carrier frequencies. From the simulation results* shown in Fig. 5.4 of the beam patterns of the two LWAs, the 3dB degradation beamwidth for the 12x1 LWA and 20x1 LWA is 5.41°and 3.35° respectively. As 1GHz change in carrier frequency results in 1.86° beamsteering, the estimated 3dB bandwidth for a 12x1 LWA becomes 2.91GHz and for a 20x1 LWA is 1.8 GHz. The results can also be verified by plotting the simulation results of the antenna gain versus frequency axis as shown in Figure. 5.5. For the verification of the simulation results for 3dB bandwidth of the two LWAs, S_{21} measurements were performed using a Vector Network Analyzer (VNA, Anritsu 37369c) for the two LWAs. The 3dB measured bandwidth for the 12x1 and 20x1 LWAs was found to be 2.83 GHz and 2 GHz, respectively. This verifies that the 20x1 LWA has a sharper frequency roll-off from the centre frequency and will cause more degradation to large bandwidth signals, than the 12x1 LWA would. The possible sources of errors for the minor difference between the estimated 3dB bandwidth of the two LWAs from the simulation results and measurements from VNA are fabrication errors in the LWAs, and variations in the measurements due to V-band connectors and cables instability.

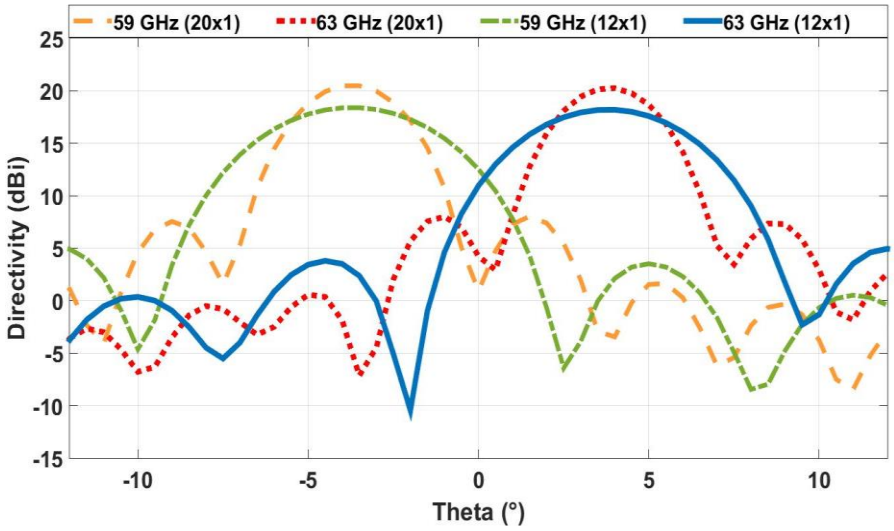

Figure. 5.4 Comparison of Radiation pattern between 12x1 and 20x1 LWA for carrier frequencies of 59 GHz and 63 GHz

*Acknowledgment: provided by Prof. Andreas Stohr and Matthias Steeg (University of Duisberg)

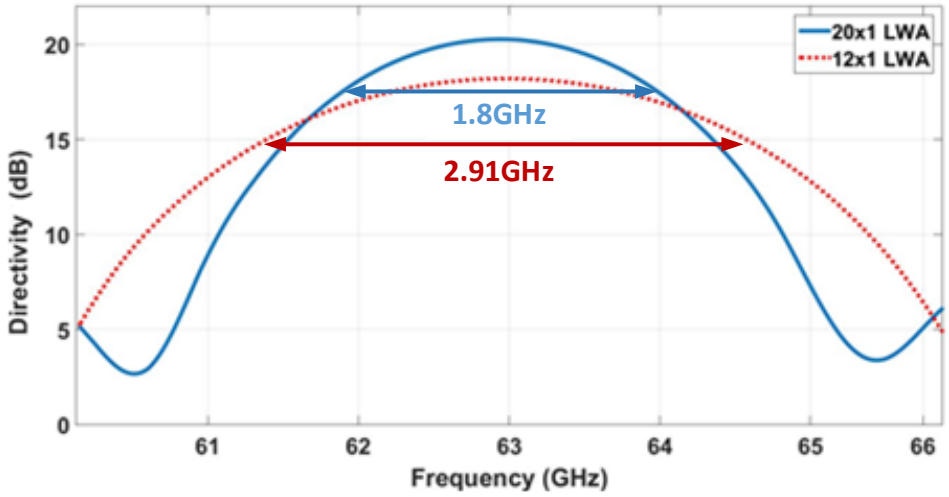

Figure. 5.5 Frequency response for12x1 and 20x1 LWA for a fixed angular location of 4°

5.3. SCM based Multi-user Transmission using LWA

The beamsteering characteristics of the V-band LWA can be used for multi-user transmission by using a composite FDM signal, comprising of different user signals at distinct mmW frequencies. The mmW frequency signal can be obtained by performing upconversion of a SCM signal, comprising of multiple intermediate frequency (IF) user-signals. The LWA produces a separate beam for each frequency signal and directs it in a specific angular direction. Multiple spatially distributed users can be served in this way, each at different carrier frequency, resulting in a high aggregate data rate. The concept diagram for the experimental setup is shown in Figure. 5.6 where the composite SCM signal at low IF frequencies is generated at the CU and is carried to the RAU using analogue RoF transport. The composite signal is upconverted to V-band frequencies using a single RF chain and the LWA is used to spatially steer each SCM subcarrier signal in a different direction. The users would be located in different spatial directions and the beams can be pointed towards them through the LWA, by use of the appropriate mmW band frequencies. Thus a number of users are served using a low cost and low complexity solution for multi-user transmission at mmW frequencies. The disadvantage of such a system is that only one frequency is transmitted to a particular angular location. A uniform distribution of the users with respect to angular locations covered by the LWA transmission is unlikely to be always the case in a practical system; multiple users may be present approximately one angular direction (perhaps at slightly different

distances), and there may be no users in other directions, which leaves some frequencies unused.

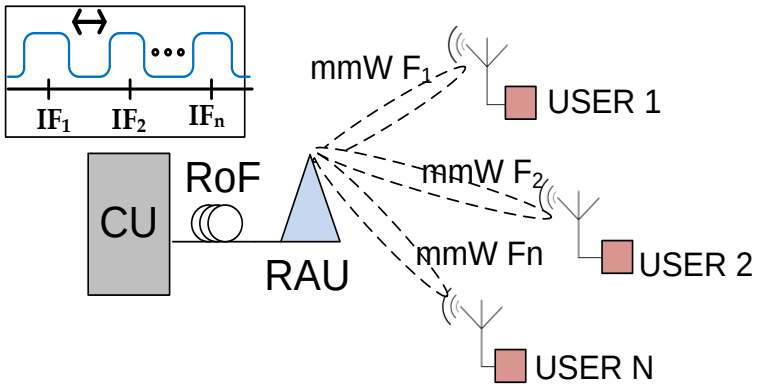

Figure. 5.6 SCM-RoF based multi-user transmission

5.3.1. Experimental Setup

Figure. 5.7 shows the experimental setup for the multi-user transmission where the SCM signal is generated at the CU for three users, each having 305 MHz bandwidth (giving a 1Gb/s data rate with OFDM 16-QAM modulation as generated in MATLAB/Simulink). The three user signals are centred at IFs of 0.5 GHz, 1.75 GHz and 3 GHz. The RoF transport from the CU to RAU using a DFB link and 60 GHz upconversion using integrated transmitter has been used here, which was explained in Chapter 3 through VPI simulations and experimental setup, and then used for the 60 GHz MIMO setup in chapter 4. The analogue waveform of the composite signal is generated using an Arbitrary Waveform Generator (AWG, Tektronix 70001A) and is modulated onto an optical carrier through the direct modulation of an Emcore 1933 DFB laser (which has a bandwidth of 4.5 GHz). After 2.2 km SMF transport to the RAU, the SCM signal is recovered by using a low bandwidth photodiode whose output is amplified by 17dB and passed through a differential balun. The integrated 60 GHz transmitter (Gotmic gTSC0020) is used to upconvert the SCM signal to 60 GHz-band frequencies which uses a LO of 10 GHz as the second input and multiplies it by 6 to produce a 60 GHz signal for upconversion. The three user signals are upconverted to 60.5 GHz, 61.75 GHz and 63 GHz, and the composite mmW signal is fed to the LWA for wireless transmission over a distance of 4m. At the user end, a 22dBi V-band horn antenna is used to receive the signal (placed in a particular location for a specific user frequency) and its output is amplified by 35dB and downconverted to IF using the

integrated receiver (Gotmic gRSC0016). The integrated receiver also uses an LO of 10 GHz with 7dBm amplitude, and amplifies the output using an internal low noise amplifier. The IF signal from the output of the integrated receiver is passed through a differential balun and is amplified by 19dB before being captured by the Tektronix Digital Oscilloscope DPO72304DX for offline processing.

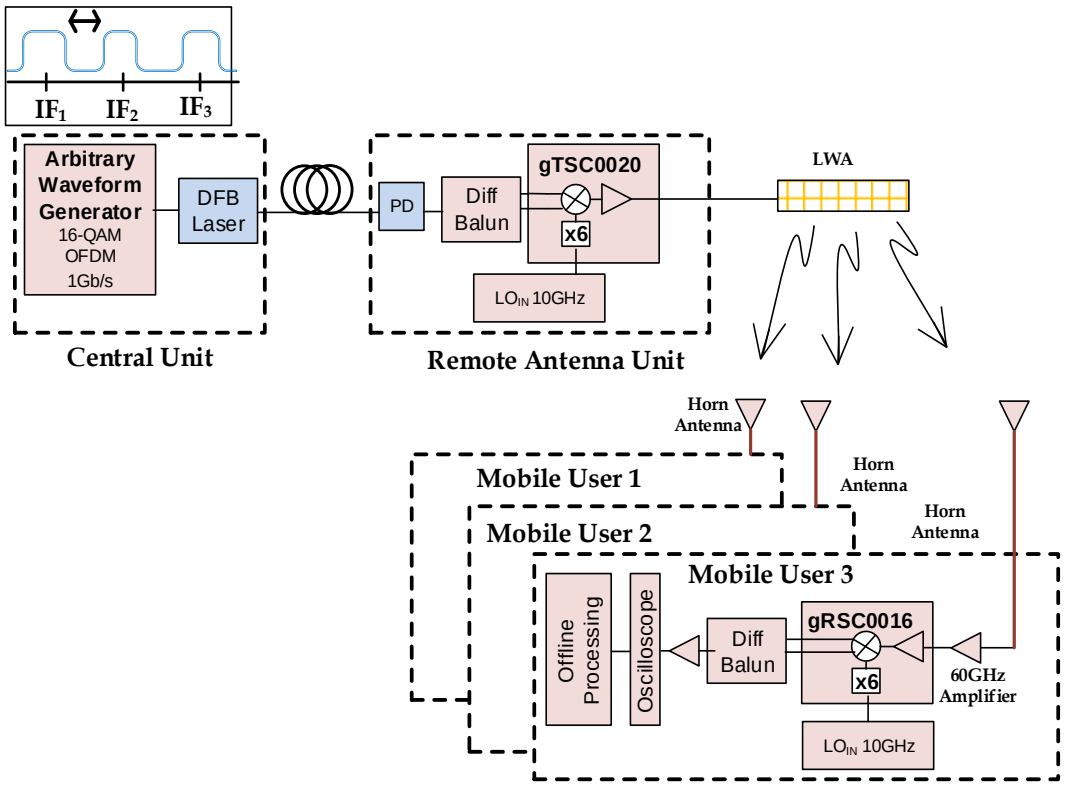

Figure. 5.7 Multi-user transmission supported by RoF setup and single RF chain

The integrated 60 GHz transmitter module can perform IQ modulation but IQ data signals cannot be generated by the AWG (Tektronix 70001A) because it has only one output port. For this reason, an IF signal is generated which results in double-sideband modulation at the RAU after performing 60 GHz upconversion through the integrated transmitter. The complete double-sideband signal is transmitted because neither a bandpass filter nor single-sideband mixer were available at the time of the experiments. Thus for a 60 GHz LO, user-signals at mmW frequencies above 60 GHz will be contained in the upper-sideband and transmitted in the right-hand region of the LWA (as shown in Figure. 5.2) and lower-sideband mmW frequencies in the left-hand region. Performance analysis for the upper-sideband user-signals only has been considered in this work for simplicity.

5.3.2. Results for Multi-user Transmission

The three user signals are captured at different user locations to evaluate the performance as the user moves from its specific LWA transmission angle as per its carrier frequency. Figure. 5.8 shows the EVM performance of user-signals from 20x1 LWA transmission which shows that the lowest EVM is obtained for each user for its particular angular location, as defined by the corresponding carrier frequency. Each user signal has a data rate of 1Gb/s and thus, the simultaneous transmission results in an aggregate data rate of 3Gb/s. By adding more users within a specific transmission bandwidth, the aggregate data rate can be increased but the number of users that can be accommodated within a specific span depends on the user-signal spacings, or guard band. The user-signal spacing is the unused part of the frequency spectrum between two adjacent user-signals which is employed to avoid interference among the channels. To serve the maximum number of users, the frequency spacing among the user-signals needs to be reduced in order to place the signals closer to each other. This reduction in guard band can introduce distortion or interference among the user-signals, which will be analyzed later in this chapter.

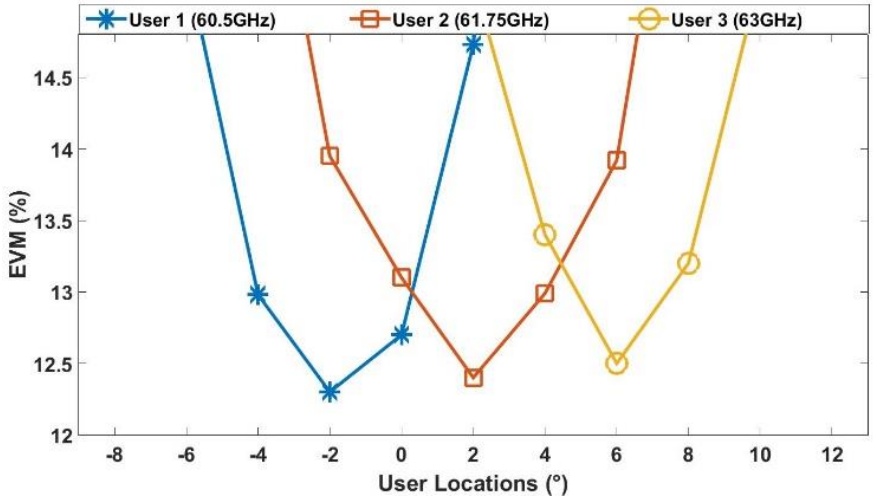

Figure. 5.8 EVM results for three users at different locations

5.3.3. Analysis on Signal-spacing for the SCM signal

As the maximum number of users that can be served depends on the user-signal spacing for the composite SCM signal, using narrower spacing will allow more users to be accommodated within a specific transmission bandwidth. But analysis needs to be performed for different signal-spacings to find the minimum spacing

that can be used without affecting the performance of the multi-user signal transmission. An experimental analysis is performed for an SCM signal with seven users, each user having bandwidth of 305MHz. The user-signal spacing of 200MHz is used in the first step, then reduced to 100MHz and finally to 50MHz, in order to analyse the performance of all seven users due to the decrease in user-signal spacing (guard band). Table. 5.1 shows the IF frequency for each user when different signal spacings are used.

Table. 5.1 IF Centre Frequencies for each user for different user-signal spacing

User	A	B	C	D	E	F	G
200MHz Guard Band	0.5GHz	2GHz	3GHz	4GHz	5GHz	6GHz	7GHz
100MHz Guard Band	1GHz	1.8GHz	2.6GHz	3.4GHz	4.2GHz	5GHz	5.8GHz
50MHz Guard Band	1GHz	1.6GHz	2.2GHz	2.8GHz	3.4GHz	4GHz	4.6GHz

The back-to-back EVM performance for each user was measured by generating the signal through the AWG, amplifying it by 10dB (using an SHF-824 broadband amplifier) and capturing the signal for each user at the oscilloscope. The measurements are performed for different user-signal spacings and results are shown in Figure. 5.9 where the lowest set of EVM are obtained by using 50MHz user-signal spacing because the overall span of the composite SCM signal is smaller for the 50MHz spacing compared to the 100MHz and 200MHz cases. The performance of the AWG degrades with the increase in generated IF frequency signals due to the bandwidth limitations of the AWG.

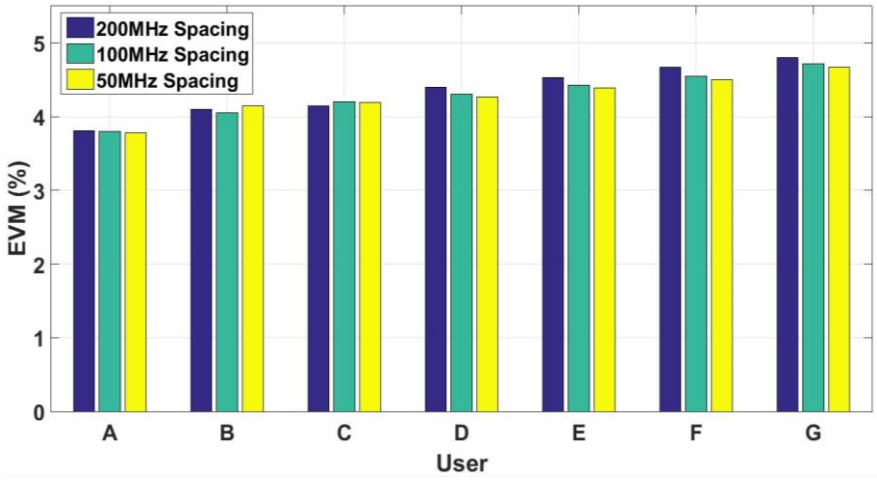

Figure. 5.9 EVM per user signal for back-to-back measurements for different user-signal spacings

The end-to-end transmission involves RoF transport of the generated IF signals, upconversion to mmW frequencies, transmission through the LWA followed by reception of the user-signal at its specific angle, downconversion and demodulation. The performance of the seven user-signals after end-to-end transmission is shown in Figure. 5.10 where it can be seen that user-signal performance degrades as the signal IF increases (similar to the results in Figure. 5.9), but this effect is more obvious after end-to-end transmission as the frequency response of the RoF link and the mmW amplifiers also degrade the performance with the increase in transmission frequency. The smaller frequency spacing provides better results as it avoids the high frequency roll-off of the AWG and RoF link. The lowest frequency spacing used in the experiments is 50 MHz, as lower frequency spacings result in a very small angular resolution for the beam directions (or user locations) which were difficult to obtain without placing the receiving horn antenna on a high precision turntable.

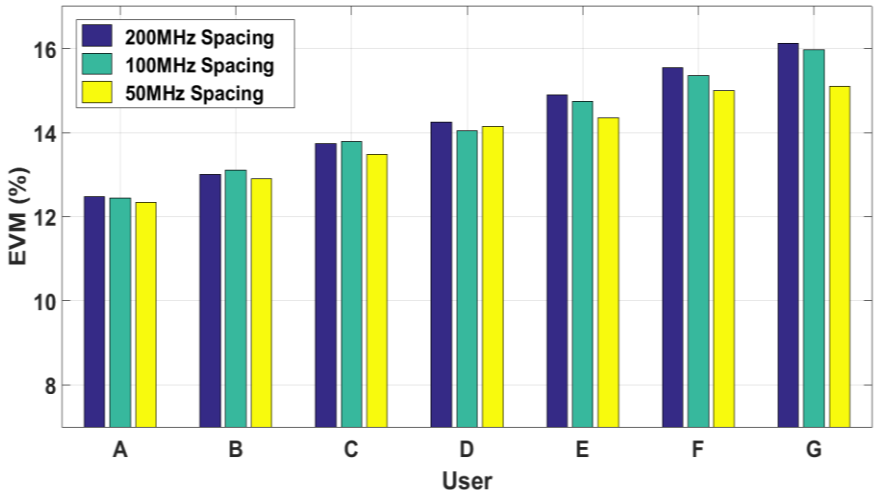

Figure. 5.10 EVM per user for end-to-end transmission for different user-signal spacings

5.3.4. Transmission to large number of users using single RF chain and a LWA

As an EVM of 15% or less is acceptable for 16-QAM with conventional Forward Error Correction [7], considering the results shown in Fig. 5.10, five users have been able to achieve EVM below than 15% for the end-to-end system due to the roll off in the performance of the AWG and RoF link. The AWG can generate a maximum 0.5V peak-to-peak output amplitude from its single channel output port and the generation of five SCM subcarriers provides enough power for each user-

signal to have sufficient SNR per signal. This is what provides the sufficient end-to-end EVM of less than 15% for 16-QAM modulation for the user with highest IF in the SCM signal. For this reason, the transmission to ten users is performed in two steps by generating data for five users in each step. Fig. 5.11 shows the experimental setup where the data for the first five users (A to E) is generated and transmitted for performance evaluation. The SCM signal consisting of the data for the other five users (F to J) is generated in the next step and transmitted through the LWA. Thus a demonstration of transmission to 10 users using single RF chain and single LWA is performed as shown in Fig. 5.11, using only the right-hand region of the LWA transmission, but real performance could be better without the limitations of the setup in which each user will have the similar EVM performance as the first user with lowest IF (12.2% as shown in Fig. 5.10). More users can be served in that case, where the minimum EVM will increase with the number of users, as the overall transmit power will be the same which will results in lower power level (hence lower SNR) for each user.

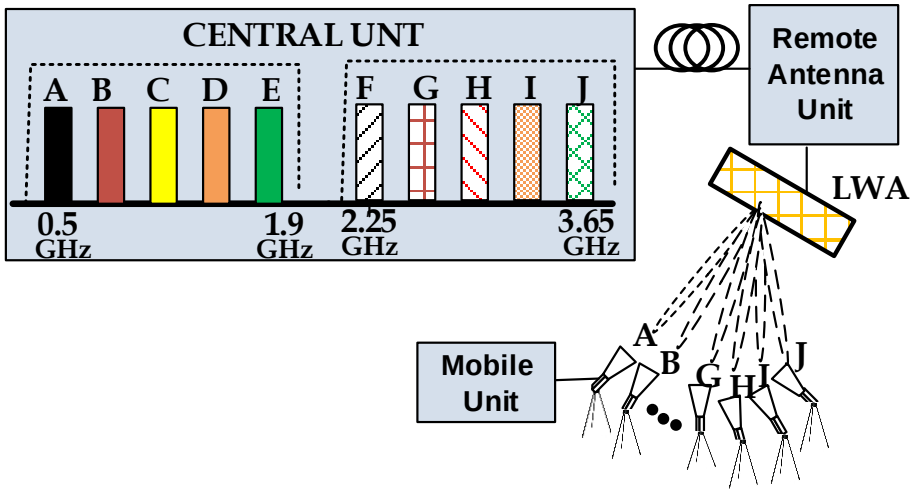

Figure. 5.11 Experimental Setup for two step transmission to 10 users using single RF chain and single LWA

The EVM performance of the ten user-signals is shown in Fig. 5.12 where the last user achieves an EVM of 15.08%. A sum rate of 10 Gb/s is achieved as each user has a data rate of 1Gb/s. Using single-sideband modulation, the left-hand transmission region of the LWA could be used to serve additional users.

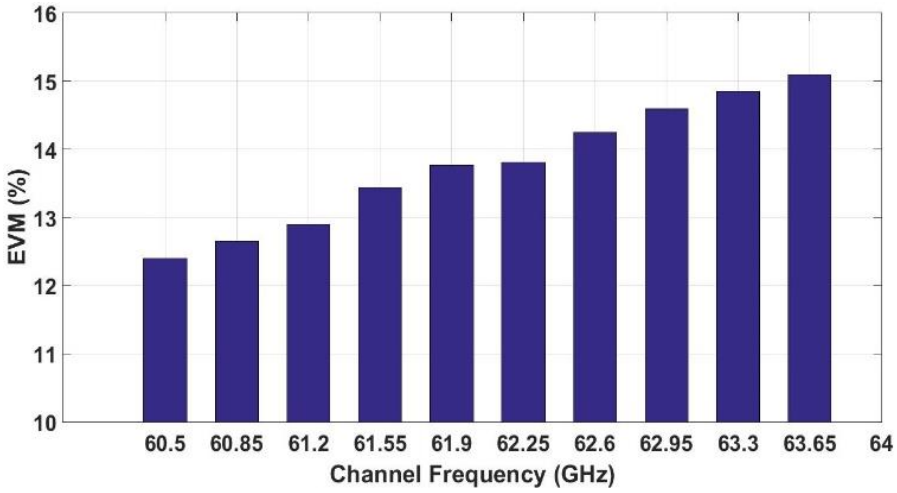

Figure. 5.12 EVM per User after LWA transmission for 10 users

With the current configuration, more users can be served within the right-hand region of the LWA by using a lower QAM level (with low SNR requirements). To show the feasibility of the system to serve more users, an experiment is performed using the two step transmission by serving ten users with 4-QAM modulation in each step. User-signals for ten users are transmitted in the first step (from A to J) and another ten in the next step (from K to T) and EVM performance is shown in Fig. 5.13 where the 20th user (IF of 7.2 GHz, upconverted to 67.2 GHz) achieved an EVM of 21.4% which is still under the limit for 4-QAM [8]. The sum rate from 20 user transmission is also 10 Gb/s as each user is being served at 0.5Gb/s with 4-QAM modulation with the same bandwidth of 305MHz per user, as in the previous case with 16-QAM data modulation.

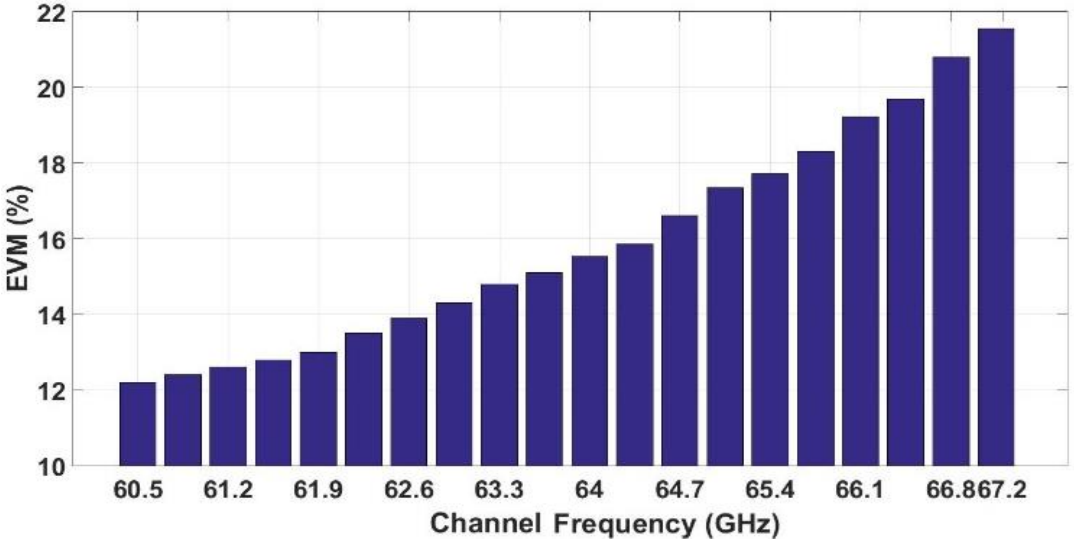

Figure. 5.13 EVM per user for twenty users (QPSK Modulation, 305MHz bandwidth, 0.5Gb/s per user)

As the performance of the users degrades with the increase in central IF, due to the limitations of the AWG and RoF link, each user could achieve a performance similar to the first user without such limitations. The 20 users occupying a total transmission bandwidth of 6.1 GHz will provide a total of 20 Gb/s sum rate in that case. The limitations of the AWG (sampling rate and maximum output power) does not support generation of high SNR subcarrier signals when present in the composite SCM signal. The SNR degrades as the signal is transported through the RoF setup and upconverted to 60 GHz at the RAU. The 60 GHz amplifier at the user end, which is used to compensate the wireless transmission loss, and integrated receiver further degrade the SNR. For this experimental work, only 16-QAM modulation was possible with the generated SNR from the AWG. Higher QAM levels (such as 64-QAM) could be used when 6dB additional SNR is available [9] from the data signal generator (AWG in this case) and much higher sum rate could be obtained.

5.4. Effect of Beamsteering on Large Bandwidth Signals and Sum Rate

Due to the beamsteering characteristics of the LWA, for a user-signal with specific central frequency, the beam gain will be maximum at the corresponding angle for that particular frequency. The gain will undergo degradation as the spectrum of the user-signal extends from the central frequency. Thus, a large bandwidth signal will experience lower beam gain (at its edges) for a user and this degradation will be greater for a 20x1 LWA than a 12x1 LWA. Due to this effect, a number of small bandwidth signals serving multiple users should achieve higher sum rate compared to few users with large bandwidth signals, as the SNR degradation will be more severe in the latter case. This section reports experimental analysis on the effect of LWA beamsteering on large bandwidth signals by evaluating the EVM performance of individual OFDM subcarriers. Following that, the LWA beamsteering patterns are used to theoretically calculate the maximum sum data rate in single and multi-user transmission (with different number of users) for a specific transmission bandwidth, and the results are compared with the experimental work carried out in the previous section.

5.4.1. Subcarrier Analysis of Large Bandwidth Signals after LWA Transmission

To analyze the effect of SNR degradation due to the frequency-selective beamsteering effect, an experiment is performed by carrying out large bandwidth signal transmission through the LWA. OFDM signals with bandwidth of 4.88 GHz are transmitted through the two LWAs. The OFDM signal has 4-QAM modulation and IFFT size of 512, with 400 data subcarriers. The EVM of individual OFDM subcarriers is evaluated to plot the EVM against the occupied frequency span of the signal. Fig. 5.14 shows the EVM after the end-to-end transmission of the 4.88 GHz signal from the two LWAs. The fluctuations in the received EVM are mainly due to the frequency dependent characteristics of the V-band connectors and cables such as insertion loss and return loss. These factors cause amplitude variations in the modulated signal [10], [11] which in turn affects the EVM results across the frequency range. As the frequency response of the V-band connectors and cables are highly sensitive to bends and kinks [12], the experiment is performed with minimum amount of bending of cables and the application of the appropriate amount of torque to the connectors. The (unavoidable) fluctuations in the EVM can be smoothed to obtain a clearer trend and to perform further analysis. The moving average filter of MATLAB is used for this purpose as shown in Fig. 5.14 with different values for the span, which is the percentage of the number of input points which are used by the smoothing algorithm in order to compute each element of the output vector. The fluctuations were smoothed using a span of 20% (0.2) and 40% (0.4) and these show similar trends with minor variations, and similar mean EVM values.

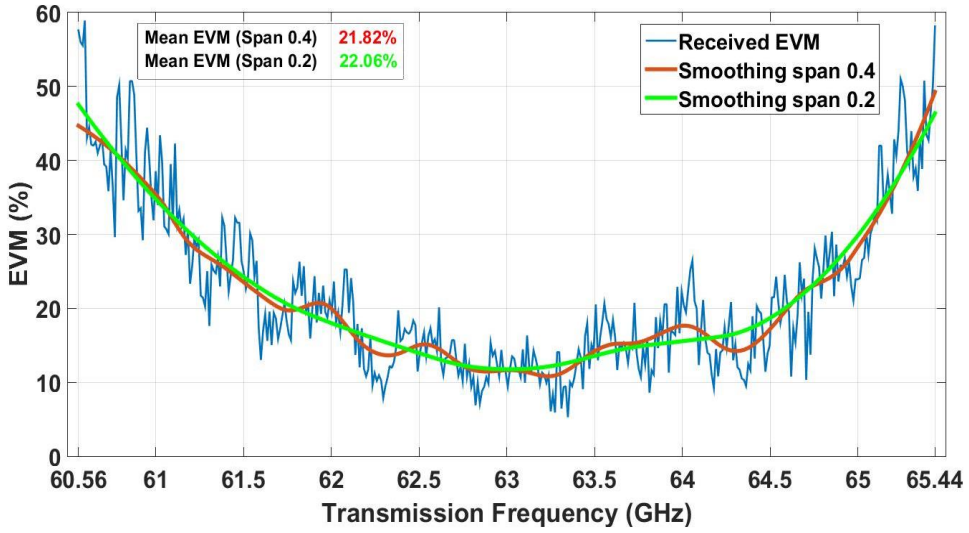

Figure. 5.14 EVM per subcarrier from transmission of 4.88 GHz OFDM signal before and after the application of smoothing function with different span values

The EVM results shown in Fig. 5.14 can be extended to estimate the 3dB bandwidth for the two LWAs, which will also verify the LWA beam patterns and VNA measurements of the S_{21} parameter. The EVM can be converted to equivalent SNR [12] to estimate the 3dB bandwidth from the experimental results. Fig. 5.15 shows the equivalent SNR obtained from the EVM results shown in Fig. 5.14 with span of 0.4, as it provides less variations. The 3dB bandwidth from the experimental results can be estimated as 1.92 GHz for 20x1 LWA and 3.05 GHz for the 12x1 LWA which is similar to the estimated bandwidth from the simulated gain pattern of the two LWAs and VNA measurements (as explained in section 5.2). For comparison, the frequency response for the 20x1 LWA and 12x1 LWA from the HFSS® simulations are also plotted, as simulation results are not prone to the variations observed experimentally. There are small inaccuracies and variations present due to the experimental equipment and the setup. For this reason, simulation results are used in the next section to theoretically analyze the effect of LWA beamsteering on sum rate for single user (large bandwidth) and multi-user cases (with different number of users).

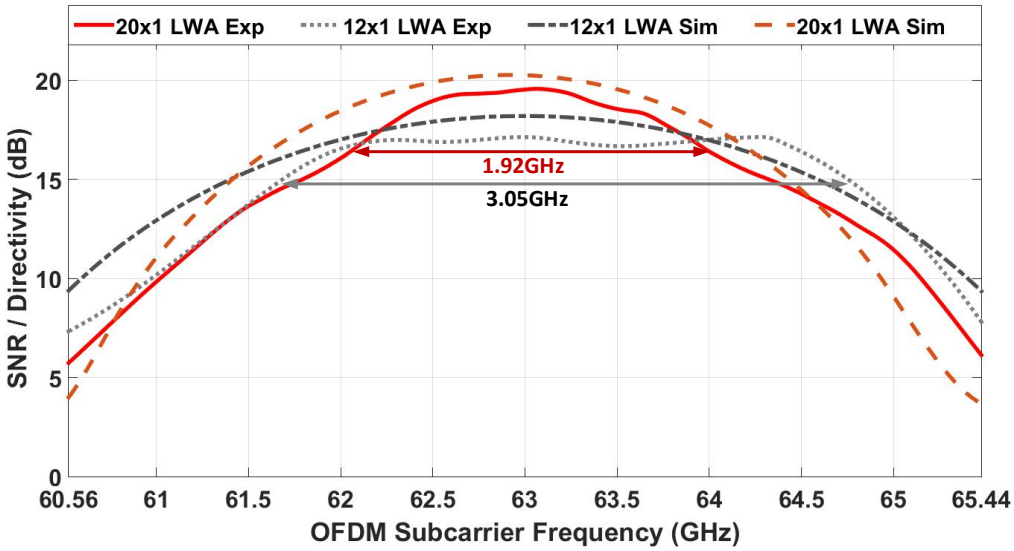

Figure. 5.15 SNR per subcarrier calculated from the EVM results for 4.88 GHz bandwidth signal transmission from the two LWAs

5.4.2. Theoretical sum rate maximization based on LWA beamsteering

With multi-user transmission using the LWA, the power for a given user-signal will decrease as the number of users are increased, if an overall fixed transmit power is assumed. At the same time, for a fixed transmission bandwidth of the system, assuming that the total bandwidth is equally divided among all the users, the bandwidth for each user-signal will decrease with increase in number of users. The decrease in bandwidth for a user will result in an increase in overall channel gain, which will mitigate the power reduction for the user. For a multi-user transmission setup with N number of total users, consider a total transmission bandwidth B_T which is divided equally among the users such that each user has the same bandwidth B_U, and has a received user SNR of SNR_U. The sum rate (aggregate data rate for all users) Rs is the sum of the data rates R_U for each of the N users, stated in terms of Shannon's equation as:

$$R_S = \sum_{U=1}^{N} R_U = \sum_{U=1}^{N} B_U \log_2(1+SNR_U) \tag{5.1}$$

To analyse the effect of LWA beamsteering on the sum rate, let us assume a system consisting of total transmission bandwidth B_T of 6.1 GHz which is divided equally for N users. For a specific maximum received user SNR whose bandwidth is narrow enough to be unaffected by the LWA beamsteering degradation, the 20x1 LWA

gain pattern, shown in Fig. 5.5, can be used to calculate the degradation in SNR for a specified user-signal bandwidth (B_U which is B_T/N) [13] - [15]. Using (5.1), the sum rate for single user transmission and different numbers of users in a multi-user transmission setup is shown in Fig. 5.16 using B_T of 6.1 GHz and reference receiver SNR of 15dB which was achieved for the first user shown in Fig. 5.13 (by converting the EVM to equivalent SNR). Fig. 5.16 shows that initially the sum rate increases with the number of users but it saturates when the user-signal bandwidth becomes small enough to not be affected by the LWA beamsteering effect. The sum rate saturates at around seven users when the user-signal bandwidth is 0.87 GHz, which shows that SNR degradation becomes insignificant for this bandwidth of user-signal. A sum rate of 30.67 Gb/s is achieved with 10 users for the B_T of 6.1 GHz. Using 3dB higher SNR for the receiver, 64-QAM modulation can be used, and sum rate of 36.6 Gb/s can be achieved as shown in Fig. 5.16. This shows that the LWA transmission is not limited to the sum rate that has been achieved in the experiments. Higher QAM modulation could have been achieved in the experiments using an AWG capable of generating high SNR for each user-signal, resulting in much higher sum rate. The data rate per user (user rate) have also been plotted which shows the trade-off between the number of users being served by the system and data rate that can be achieved for each user.

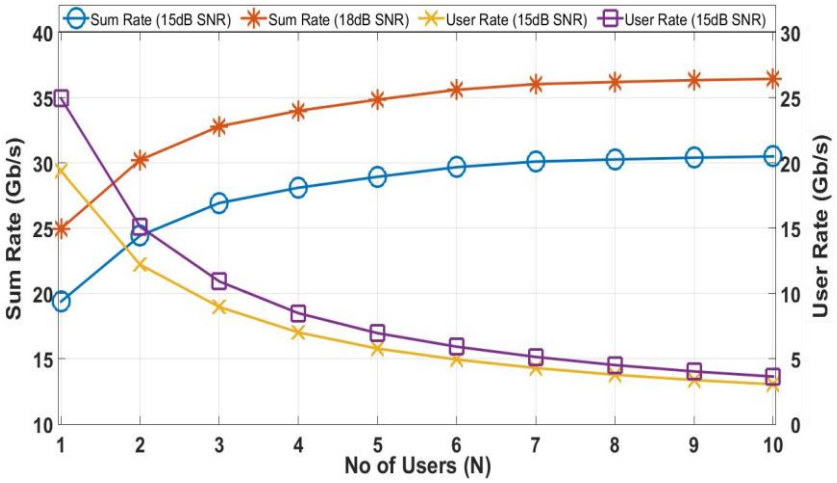

Figure. 5.16 Theoretical sum rate for different number of users for total transmission bandwidth of 6.1 GHz

5.5. Improvement in Coverage through Multiple LWAs

The demonstrated setup in the previous sections uses a single LWA to provide different user-signal beams in different directions. But, for a specific angular location, only one user-signal beam at a particular frequency is transmitted, whereas more than one user could be present at that (approximate) angle in a practical system. This causes an inefficient use of spectrum for the demonstrated setup which is mainly from having no users at some angular locations and some of the available spectrum remains unused, except for one case where all users will be located at distinct and uniformly spread angular locations. The coverage for a user is confined to one angular location only with the current setup and not available to any other angular locations when the user moves. As a solution, the transmission of multiple user-signal beams towards a particular angular location can be achieved by using multiple LWAs operated by a common RF chain. The proposed design to operate multiple LWAs simultaneously with a single RF chain can improve the spectrum efficiency as well as coverage. The increase in accessibility of the network is achieved by using an RF power divider and feeding the same upconverted composite signal to multiple LWAs, which are arranged in different geometric orientations. For a scenario with one LWA transmitting different frequencies in different spatial regions (as shown in Fig. 5.2), an additional LWA in an inverted position will transmit the same frequencies in the opposite regions. Thus different sets of frequencies will be available in the two regions (left-hand and right-hand) regions of the LWA transmission, with overlapping beams from the two LWAs. To demonstrate the feasibility and performance of the proposed design, simultaneous transmission from two LWAs is performed using the experimental setup shown in Fig. 5.17. The two LWAs are operated in series due to the lack of availability of a mmW RF power splitter in our laboratory. An SCM signal consisting of two subcarriers is generated at the CU at IFs of 0.5 GHz and 4 GHz for two users. Each user-signal has a bandwidth of 305MHz with 16-QAM modulation. After RoF transport, the two user-signals are upconverted to 59 GHz and 62.5 GHz using an LO input of 9.75 GHz to the integrated transmitter, which is multiplied by 6 and then used to upconvert the input signal. The upconverted signal is provided to the first LWA (12x1) which transmits the two signals up to a wireless distance of 4m. The other end of the 12x1 LWA is connected to the 20x1 LWA

which is placed in its inverted position and has a 50Ω terminator at its other end. The two LWAs are connected using a semi-rigid cable of 6 cm length and placed on tripods of the same height. The inverted 20x1 LWA provides for the transmission of the two user-signals in the opposite angular directions. The corresponding angles for the two user-signal beams from the first LWA for 59 GHz and 62.5 GHz become similar to the two beams from the second LWA for 62.5 GHz and 59 GHz, respectively, after minor adjustments to the tilt of the second LWA . The second LWA (20x1) provides transmission up to 0.5m only, as it receives reduced power after the transmission losses through the first LWA. This could be improved with amplification.

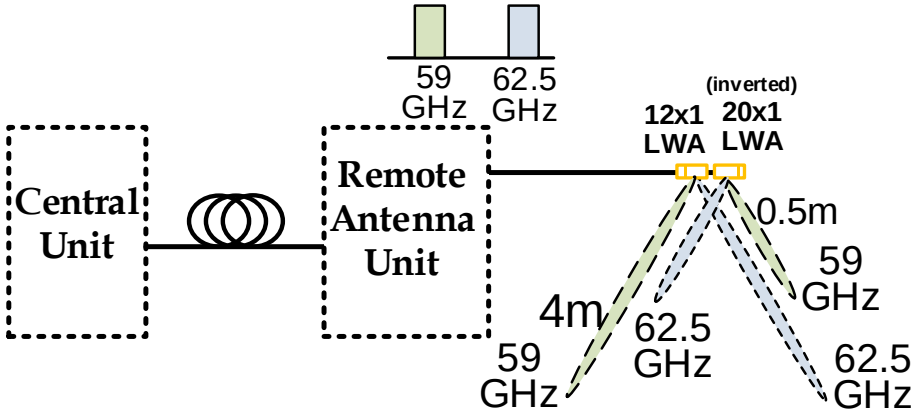

Figure. 5.17 Experimental Setup for Cascade design of LWA Transmission (the user angles and transmission distances are not up to the exact scale)

The summary of the performance of the two user-signals from the LWAs is given in Table. 5.2.

Table. 5.2 Transmission frequencies and EVM performance of the two user-signals in cascaded LWA configuration

Antenna	Transmission Distance	User-signal frequency in left-hand region	User-signal frequency in right-hand region
First LWA 12x1	4m	59 GHz EVM: 12.02%	62.5 GHz EVM: 12.5%
Second LWA 20x1	0.5m	62.5 GHz EVM: 13.5%	59 GHz EVM: 13.3%

The transmission angles for the two LWAs closely correspond to each other with different transmission frequency signals as shown in Fig. 5.18, where the layout of the measurement setup has been shown. The line drawn between the two LWAs in Fig. 5.18 represents two regions for the transmission and users were placed in these

different regions for taking measurements, as shown by A and B as user locations. The locations for the two users cannot be made precisely the same due to the placement of two LWAs side-by-side, which causes an offset for the user location, but the angle of transmission is the same. Small inaccuracies might be present due to fabrication errors and different cell size (overall width) of the two LWAs. However, the objective of this experiment is to show the practicability of the simultaneous operation of multiple LWAs using a single RF chain to improve the spectral efficiency and coverage in the 60 GHz-band.

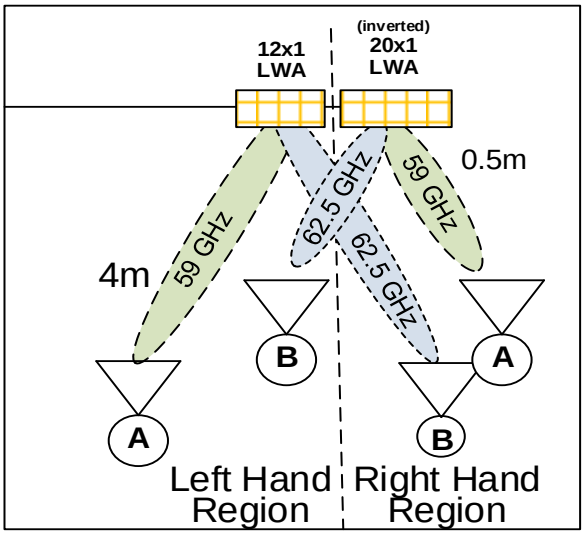

Figure. 5.18 Layout for the user locations during the experimental work on cascade operation of two LWAs

5.6. DWDM-RoF Transport and Photonic Generation of mmW for Muti-user Transmission

As discussed in Chapter 2, DWDM can also be considered for multi-user transmission to combine data signals for different users. Data from different sources are modulated onto individual laser optical carrier signals at different wavelengths and combined together to form a composite optical DWDM signal to be transported over a single fibre to the RAU. To demonstrate DWDM based multi-user transmission using the LWA, the experimental setup is shown in Fig. 5.19, where two optical wavelengths at 1554.10nm and 1555.75nm are generated using two independent CW laser sources. The 1554.10nm wavelength is modulated by a 29.25 GHz RF signal using a MZM which is biased at minimum transmission point to generate a 58.5 GHz separated optical two tone signal. In the same way, the

1555.75nm wavelength is modulated using another MZM with an RF signal of 32.25 GHz to produce 64.5 GHz separated two-tone signal. Data for two users are generated by using two amplitude-shift keying (ASK) data generators (1Gb/s data generation through Gigabit Ethernet Interface) and modulated onto each of the two-tone signals. Polarization controllers are used before each MZM to minimize the polarization dependent losses. After data modulation, the output from each MZM is passed through an optical filter to only allow the desired data modulated two-tone signal and suppress all the unwanted spectral components. The output of each filter is amplified by 30 dB using an EDFA to compensate for the insertion losses of MZMs and optical filter. The optical spectrum for the first user's channel is shown in Fig. 5.20 (top left) on an optical spectrum analyser (Yokogawa AQ6370) and for the second user's channel in Fig. 5.20 (top right); these show carrier suppression of 42dB and high optical SNR for the two-tone signals. The optical two-tone signals from both user channels are combined using an Array-Waveguide-Grating and RoF transport is performed over 500m of SMF. The optical spectrum received after the RoF transport is shown in Fig. 5.20 (bottom).

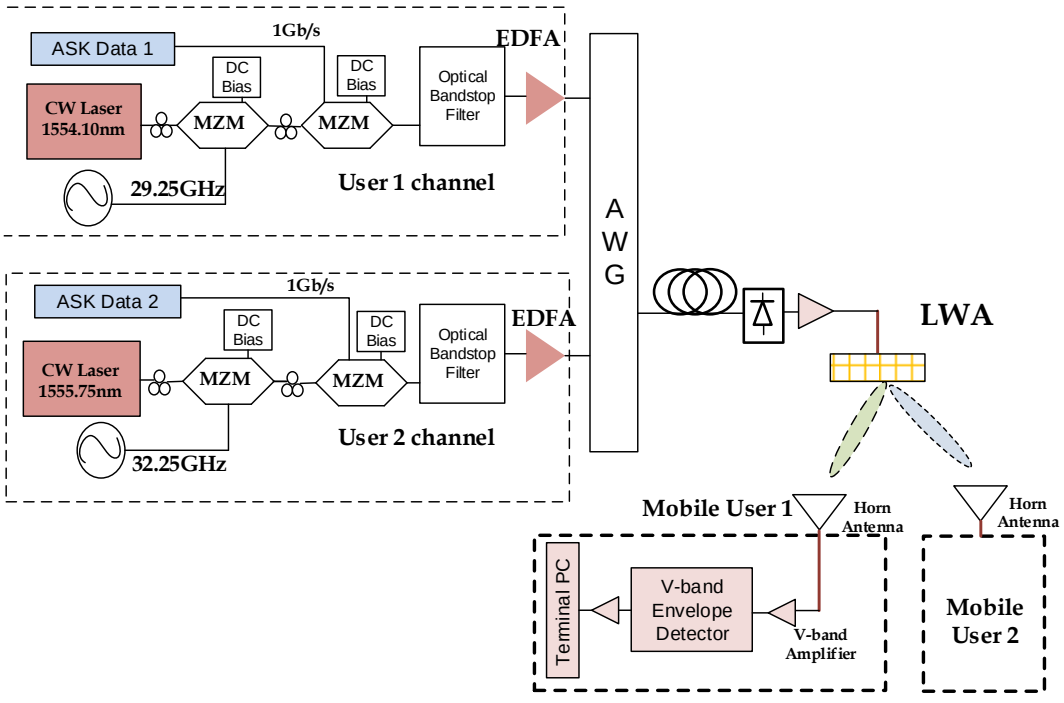

Figure. 5.19 Experimental setup for DWDM-RoF based Multi-user transmission using single LWA

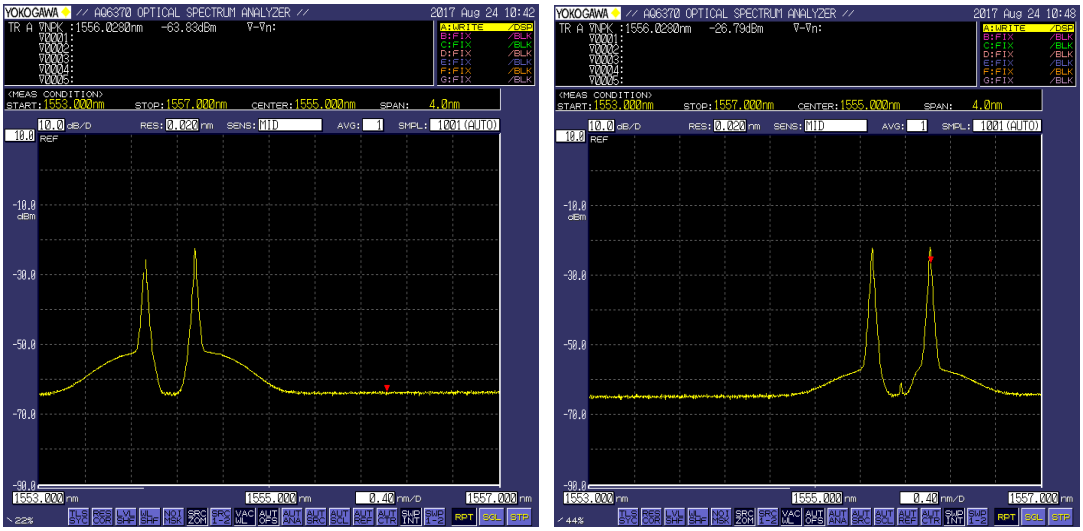

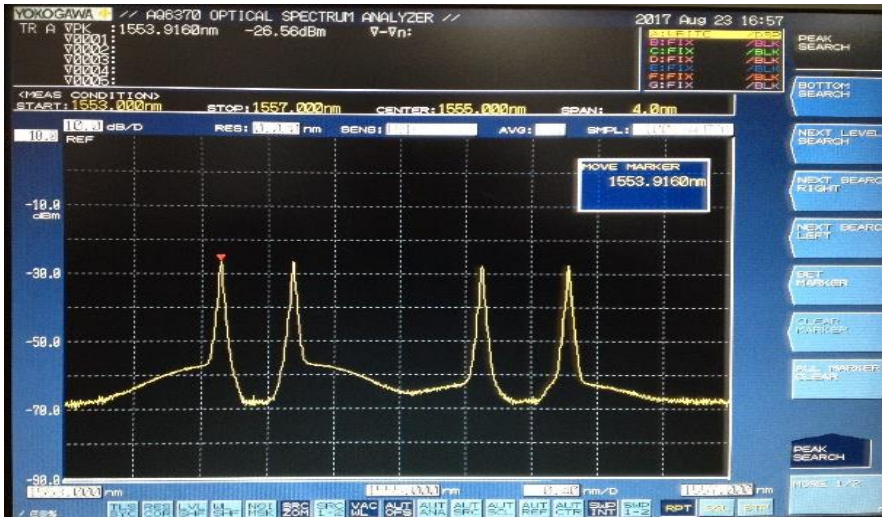

Figure. 5.20 Optical spectrum for (top left) user 1 channel (top right) user 2 channel (bottom) Spectrum after DWDM-RoF transport

At the RAU, a high bandwidth photodiode is used to perform direct photonic upconversion which generates data modulated 58.5 GHz and 64.5 GHz. Fig. 5.21 shows the RF spectrum after the photodiode which shows the two ASK modulated mmW signals. The two ASK-modulated mmW signals are amplified by a 30dB gain V-band amplifier and transmitted over the air using a LWA.

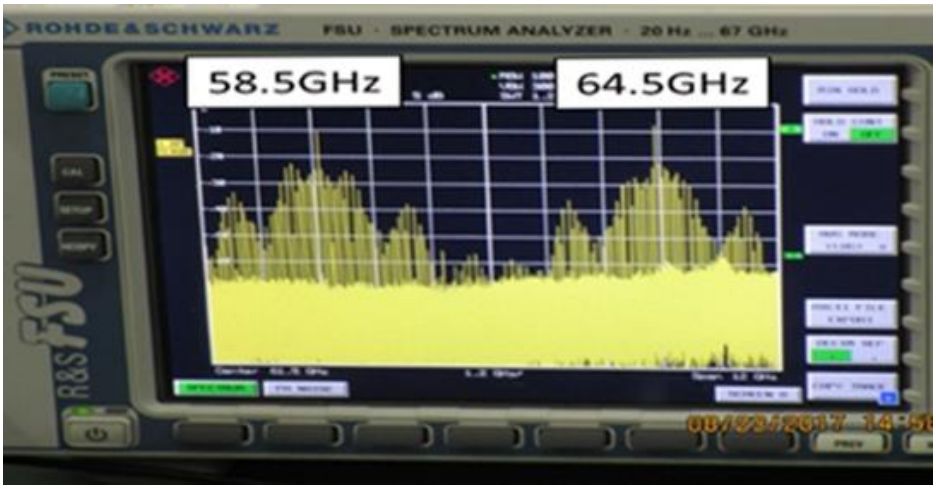

Figure. 5.21 RF spectrum after direct photonic upconversion

After wireless transmission of 1.5m, two user units are placed at the receiver end. Each unit (developed by Hitachi, Japan) consists of 25dB gain horn antenna, followed by an amplifier to boost the received signal. A mmW envelope detector is used to retrieve the ASK signal, which is amplified by a low frequency RF amplifier. The ASK signal is received by an Ethernet interface card which is attached to a PC for data transmission analysis. The results show that both users successfully achieve the 1Gb/s data rate, thus providing a sum rate of 2Gb/s. A possible application of a DWDM based multi-user transmission setup includes a Passive Optical Network (PON) [16] based optical sensor grid [17], where data from multiple sensors (in the optical domain) at the ITU specified wavelengths is multiplexed and transported remotely for future industrial automation process, where each sensor value is required to be transmitted to a specific automation and control unit [18].

The SCM based multi-user transmission setup using a single RAU can be extended using WDM (as explained earlier in section 2.4.1), in which separate wavelengths are used to serve multiple RAUs in the distribution network. The modulation of a SCM signal with large number of user-signals over a single wavelength can incorporate problems at the transmitter end, which can be avoided by modulating several small SCM signals over different WDM wavelengths.

5.7. MIMO processing for Spatial Diversity and Spatial Multiplexing using LWA

The experimental work on emulation of 60 GHz MIMO explained in the Chapter 4, carried out through individual channel coefficient measurements using single transmit-receive antenna pairs, was based on a standard gain horn antenna transmitter. To achieve maximum signal strength in the LOS transmission, the horn antenna was tilted manually towards the receiving antennas. The beamsteering characteristics of the LWA can be used to achieve simplification of operation for mmW MIMO transmission at different user locations. The objective of using an LWA-based system for mmW MIMO is to analyse the amount of flexibility that can be offered by the LWA and the performance improvement that can be achieved using such a setup. Fig. 5.22 shows the experimental setup where two MIMO data channels are generated at an IF of 0.5 GHz using the Arbitrary Waveform Generator (Tektronix 7122c). After RoF transport, the signals are upconverted to 59 GHz using an LO of 58.5 GHz (using an LO of 9.75 GHz which is multiplied by 6 by the integrated transmitter). The emulated MIMO operation is performed by using the procedure explained in the previous Chapter (Section 4.4). The channel coefficients H_{11} and H_{12} are calculated by placing the transmit antenna at position Tx1 (shown in Fig. 5.22) and capturing the data at two receiver positions (Rx1 and Rx2). In the next step, the transmit antenna at position Tx2 and data is captured at the two receiver positions to calculate channel coefficients H_{21} and H_{22}. The receiver consists of a V-band amplifier with 35dB gain and integrated receiver which downconverts the received signal to IF. The IF signal is amplified and captured by the oscilloscope.

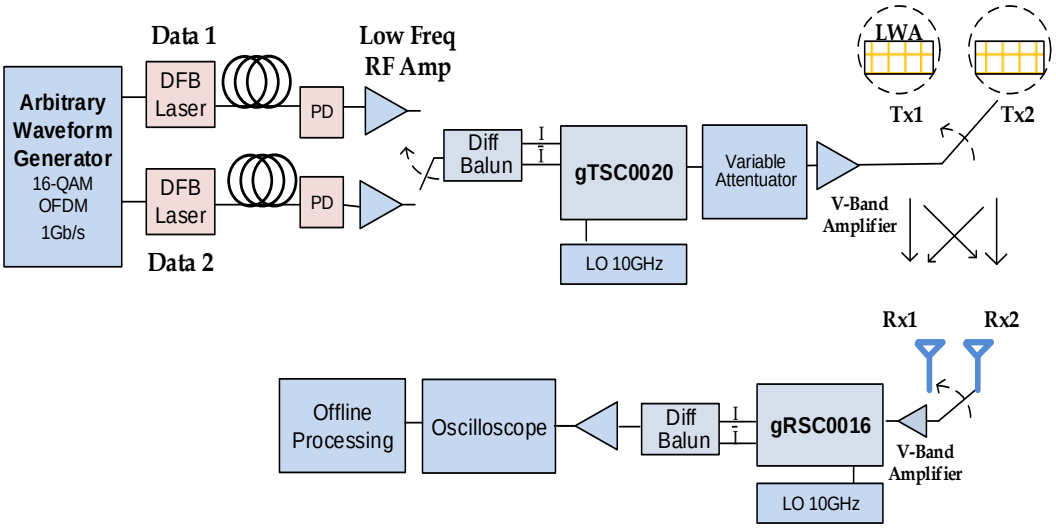

Figure. 5.22 Experimental setup for Emulated MIMO operation using LWA

The MIMO operation at 59 GHz transmission frequency is performed for the user located at position A as shown in Fig. 5.23 The transmit antenna at position Tx2 is tilted slightly to achieve the same transmission angles (for different carrier frequencies) as the transmitter at position Tx1. The IF frequency for the two MIMO signals is changed from the AWG to 2 GHz for the user at location B. The upconverted MIMO signals at 60.5 GHz are steered by the LWA towards the location B, without the need of manually tilting the transmit antenna towards the receiver. Finally, the IF from the AWG is changed to 3.5 GHz to provide MIMO operation for location C at an upconverted carrier frequency of 62 GHz.

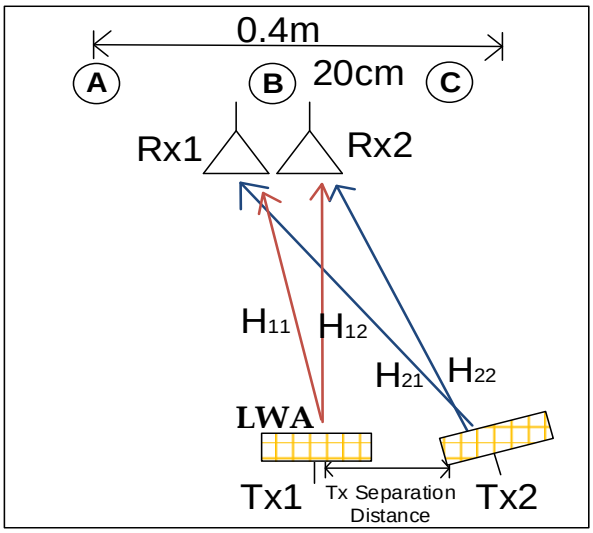

Figure. 5.23 Antenna arrangement and user locations for the experiment

Wireless transmission over 4m is performed and the transmitter separation is varied from 20cm to 40cm to observe the effect of transmit antenna spacing on the MIMO

performance. Space-time-block-coding (STBC) Alamouti is used to achieve spatial diversity and the Zero Forcing algorithm for spatial multiplexing. The results for STBC for 1Gb/s data rate transmission are shown in Fig. 5.24 which shows that for each user location, the MIMO processing improves the EVM performance through spatial diversity, as compared to the SISO results. The set of EVM for 40cm transmit antenna separation is lower than 20cm which verifies that sufficient spacings are required to achieve good performance from LoS MIMO, and that RoF fronthaul can provide flexible and wider antenna spacings for it. Moreover, LWA beamsteering through varying the carrier frequency of the MIMO signals is demonstrated here to avoid the manual tilting of the transmit antenna towards the user.

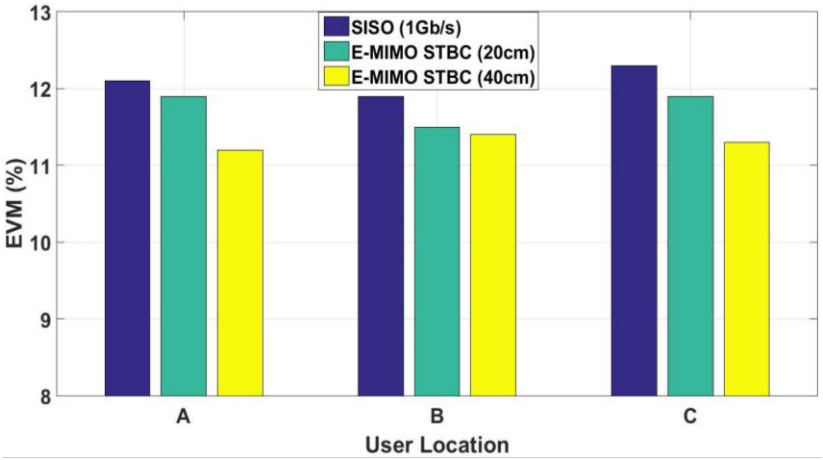

Figure. 5.24 Results for SISO and Emulated MIMO with STBC Processing

The results for ZF to multiplex two 0.5 Gb/s data streams are shown in Fig. 5.25. The results for transmit antenna spacing are higher than SISO transmission for 1Gb/s shown in previous Fig. 5.24 but the spacing of 40cm achieves lower EVM values and thus improvement in performance. The measurements were performed using only the same (12x1) LWA twice for the two transmitter locations (Tx1 and Tx2 as shown in Fig. 5.23).

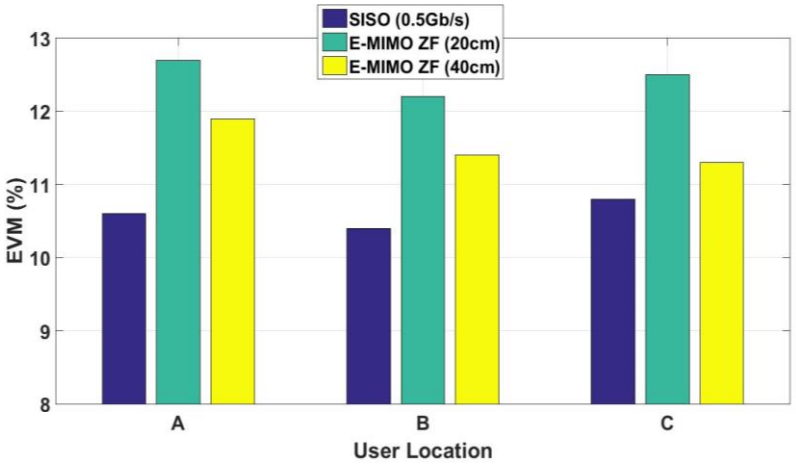

Figure. 5.25 EVM performance for SISO (0.5Gb/s) and emulated MIMO with ZF (1Gb/s)

5.7. Summary

In this Chapter, a RoF-supported multi-user transmission system has been presented which uses a single RF chain and single LWA. A demonstration of transmission to multiple users for various angular locations has been performed to show the combined use of the SCM technique and the beamsteering characteristics of the LWA for multi-user transmission. It has been shown that low user-signal spacing can be used in the SCM signal to include a large number of user-signals within a specific transmission bandwidth, without affecting the performance of the system, to maximize the number of served users. Experimental demonstration for user-signal spacing of 50 MHz is demonstrated serving ten users with 16-QAM modulation and twenty users with 4-QAM modulation using single RF chain and LWA. Sum rate of 10 Gb/s is achieved from both cases which can be increased to 20 Gb/s by excluding the bandwidth limitations of the AWG and RoF setup, and much more when higher SNR is available from the SCM signal generator to use higher order QAM levels. An investigation on SNR degradation of a wideband signal due to the beamsteering characteristics of the LWA has been performed. Transmission of a 4.88 GHz bandwidth OFDM signal and EVM analysis for each subcarrier verified that the 20x1 LWA causes faster degradation of the edges for a large bandwidth signal than the 12x1 LWA and therefore has smaller 3dB bandwidth. The gain pattern of a 20x1 LWA has been used to theoretically estimate the sum rate for different numbers of users, which shows that experimental results broadly concur with the analysis and a sum rate up to 36 Gb/s, for transmission bandwidth of 6.1 GHz, can be achieved when the sufficient SNR is available to support 64-QAM.

In addition, an experimental setup based on multiple LWAs has been presented to increase the spectrum efficiency and coverage. It has been shown that two LWAs operating in cascade with a single RF chain, can transmit different user-signals in the same angular direction. The EVM results showed that multiple-frequencies can be transmitted to a single angular location with the presented setup.

Following that, an experimental setup for DWDM-RoF-based multi-user transmission systems has been explained to show the feasibility of using different wavelengths to extend the multi-user transmission setup. Multiple SCM signal sets

can be transmitted through multiple RAUs by modulating each set on a distinct wavelength and using WDM distribution network for the RAUs. The simultaneous transmission to two users using different laser sources with 1Gb/s ASK data modulation was experimentally demonstrated, followed by direct photonic upconversion at the RAU to generate mmW signals.

Finally, MIMO transmission at 60 GHz-band using the LWA has been performed which showed that the beamsteering characteristics of the LWA can also be used to perform mmW MIMO operation for several user locations. This included serving each location at a distinct MIMO carrier frequency, which avoids the tilting of the transmit antenna towards the user locations and thus showing the flexibility in operation that can be achieved using the LWA. The feasibility of the system is shown by changing the central carrier frequency for MIMO signals with respect to each user location. The results after SISO and MIMO transmission showed that improvement in performance can be achieved using spatial diversity and spatial multiplexing. In Chapter 3, the transmitting horn antennas were tilted physically to provide the best power for the LOS transmission, which is not required for the LWA due to its beamsteering characteristics.

REFERENCES

[1] R. Keating, R. Ratasuk and A. Ghosh, "Investigation of Non-Orthogonal Multiple Access Techniques for Future Cellular Networks", *IEEE 86th Vehicular Technology Conference (VTC-Fall),* 2017, pp. 1-5.

[2] D.R. Jackson, C. Caloz and T. Itoh, "Leaky-wave antennas", *Proceedings of the IEEE*, Vol.100 (7), 2012, pp.2194-2206.

[3] K. Neophytou, S. Iezekiel, M. Steeg and A. Stöhr, "Design of PCB leaky-wave antennas for Wide angle beam steering", *IEEE 11th German Microwave Conference (GeMiC),* 2018 ,pp. 152-155.

[4] 1.85mm RF Centric End launch connectors "https://www.centricrf.com/connectors/end-launch-sma-2-92-2-4-1-85-1-0-connectors /1892-04a-5-1-85mm-end-launch-connector/"

[5] M. Steeg, N. Yonemoto, J. Tebart and A. Stohr, "Substrate-Integrated Waveguide PCB Leaky-Wave Antenna Design Providing Multiple Steerable Beams in the V-Band", *MDPI Electronics*, Vol. 6 (4), 2017.

[6] M. Steeg, M. Lange, A. Stöhr and Y. Leiba, "Low-latency GbE 60 GHz TDD transceiver using SiGe-RFICs and PCB leaky-wave antennas", *IEEE 11th German Microwave Conference (GeMiC)*, 2018, pp. 156-159.

[7] H.M. Oubei, J.R. Duran, B. Janjua, H-Y. Wang, C-T. Tsai, Y-C.Chi, T.K.Ng, H-C. Kuo, J-H. H, M.S. Alouini, G-R. Lin and B.S. Ooi, "4.8 Gbit/s 16-QAM-OFDM transmission based on compact 450-nm laser for underwater wireless optical communication" *Optics Express*, Vol. 23 (18), 2015, pp. 23302-23309.

[8] A. Nkansah, A. Das, N. J. Gomes and P. Shen, "Multilevel modulated signal transmission over serial single-mode and multimode fiber links using vertical-cavity surface-emitting lasers for millimeter-wave wireless communications", *IEEE Transactions on Microwave Theory and Techniques*, Vol. 55 (6), 2007, pp.1219-1228.

[9] Keysight Technologies, "Microwave and Millimeter Signal Measurements - Tools and Best Practices", *Application note*, 2017.

[10] Agilent Technologies, "8 Hints for Better Millimeter-Wave Spectrum Measurements", *Application note 1391*, 2002.

[11] Keysight Technologies, "Microwave and Millimeter Signal Measurements, Tools and Best Practices", *Application Note 5990-8892EN*, Dec 2017.

[12] R.A. Shafik, M.S. Rahman and A.R. Islam, "On the extended relationships among EVM, BER and SNR as performance metrics", *4th IEEE Int. Conf on Electr. and Comput. Eng. (ICECE'06)*, Bangladesh, 2006, pp.408-411.

[13] R. Hranac and B. Currivan, "Digital transmission: Carrier-to-noise ratio, signal-to-noise ratio, and modulation error ratio." *Broadcom Corporation and Cisco Systems*, white paper, 2012.

[14] C. Rauscher, v. Janssen and R. Minihold, "FREQUENT MEASUREMENTS AND ENHANCED FUNCTIONALITY", *Fundamentals of spectrum analysis*, Rohde & Schwarz Germany, 2007.

[15] IEEE 802.16 Broadband Wireless Access Working Group, "Correction to Rx SNR, Rx sensitivity, and Tx Relative Constellation Error for OFDM and OFDMA systems", *IEEE C802.16maint-05/112r8*, 2005.

[16] S. Shimizu, G. Satoshi and N. Wada, "Demonstration and performance investigation of all-optical OFDM systems based on arrayed waveguide gratings", *Optics Express*, Vol. 20 (6), 2012, pp.B525-B534.

[17] L. Yen, Z. Zhang, K. Wen, W. Pan and B. Luo, "Optical sensor networks for high-speed railway applications", *IEEE 9th International Conference on Optical Communications and Networks (ICOCN)*, 2010, China, pp. 128-129.

[18] ZVEI – German Electrical and Electronic Manufacturers' Association, "5G for Connected Industries and Automation", *White paper, 5G Alliance for connected industries and automation (5G-ACIA)*, April 2018.

CHAPTER 6
CONCLUSION AND FUTURE WORK

6.1. Conclusions

The use of mmW frequencies is a promising solution to the current RF spectrum congestion and increasing demand of high data rates. The technical challenges related to the implementation of mmW systems include limited coverage due to the Line-of-Sight (LOS) nature of mmW and high cost of mmW frequency components. Deployment of large number of RAUs is required to address the limitations of the coverage at mmW transmission and use of RoF transport from the CU to these RAUs can offer many advantages such as low loss transmission, ultra-high capacity fronthaul for high data rates and support for low cost mmW generation. RoF transport also allows flexible and large RAU spacings which is required by the mmW MIMO systems, in order to achieve improvement in the performance and reliability through spatial diversity, and data rate through spatial multiplexing. RoF technology is also useful to transport data for multiple users through different multiplexing-over-fibre techniques and can provide a low cost and low complexity RAU design for multi-user transmission.

In this thesis, various features of the mmW communication for future wireless systems have been analyzed including photonic generation of mmW for MIMO operation using a single optical phase modulator (PM), performance analysis of mmW MIMO to achieve spatial diversity using the STBC Alamouti algorithm and spatial multiplexing using the Zero Forcing algorithm, and multi-user transmission using multiplexing-over-fibre transport and frequency-selective antenna. The experimental work on RoF-supported mmW MIMO include different aspects which were not considered or performed in previous work [1]-[6]. This involved the

proposal and demonstration of single PM based generation of two mmW separated optical two-tone signals for MIMO operation. The investigation of the *amount of improvement in coverage and data rate* that can be achieved from RoF supported distributed mmW MIMO at *several user locations*, as compared to SISO performance, has been performed for the first time. Particular MIMO algorithms have been mentioned and used for mmW MIMO work, which were not specified before, to understand the performance of a defined MIMO scheme. As a first instance, the verification to achieve wider RAU spacings with the proposed analog RoF fronthaul, to achieve optimum mmW MIMO performance at longer transmission distances, has been performed. In addition, an emulation of mmW MIMO to measure channel coefficients individually for MIMO processing has been achieved to extend the analysis to much longer distances. Finally a *novel* low cost, low complexity mmW multi-user transmission system, using single RoF link and single RF chain with single transmitting antenna has been presented and characterized, whereas previous works for multi-user transmission [7]-[11] have been performed using a large number of RF chains and multiple antenna units.

The conclusions from this thesis are as follows:

- Experimental analysis on RoF supported 25 GHz and 60 GHz MIMO showed that improvement in coverage and data rate, as compared to SISO, is achieved for various user locations using STBC Alamouti and Zero Forcing algorithms, respectively. The analysis on physical spacing of RAUs for various transmission distances demonstrated the importance of optimum RAU spacing to achieve minimum set of EVM performance at multiple user locations with mmW MIMO and verified that wider spacing is required for longer wireless transmission distances, for which Analog RoF fronthaul is proposed.
    - Experimental results showed that flexible and wider RAU spacing can be achieved using RoF fronthaul for mmW MIMO, to obtain minimum set of EVM values for several user locations through spatial diversity and spatial multiplexing.

- A unique DWDM-RoF setup based on a single PM for mmW MIMO has been presented to generate two independent mmW separated optical two-tone signals, which provides stable and low cost mmW generation using direct photonic upconversion for MIMO operation, and able to provide Gb/s data rate and substantial power budget for indoor wireless transmission.

- An emulation of mmW MIMO through individual measurement of channel coefficients using single antenna pair and performing offline MIMO processing on the captured data, showed that spatial diversity and spatial multiplexing can be achieved with similar results to that of MIMO performed with two antenna pairs. It was concluded that mmW channels are relatively static during the measurements and emulated MIMO can be used to extend the analysis to longer distances or to make projections of N×N massive MIMO.

- A low cost and low complexity RoF supported 60 GHz multi-user transmission has been proposed and experimentally demonstrated using single RoF link, single RF chain and single RF transmitting antenna for the first time , to serve a large number of users.

    - The setup involved SCM signal generation, analog RoF transport using low bandwidth optical components, an integrated transmitter at the RAU for upconversion of user-signals and a LWA to serve multiple spatially located users by performing conversion of Frequency Division Multiplexing (FDM) signal to Spatial Division Multiplexing Access.

    - From the experimental results using SCM-RoF based 60GHz multi-user transmission system with single LWA, it was concluded that low user-signal spacing in SCM signal does not affect the performance of the system and can be used to maximize the number of users within a specific transmission bandwidth. Experimental demonstration for 50MHz user-signal spacing to serve 20 users (each user with 305MHz bandwidth) within the transmission bandwidth of 7.05GHz was shown, achieving a sum rate of 10 Gb/s,

and much higher sum rates can be achieved using the presented system with improved SNR level of the generated SCM signal.

- Analysis on individual OFDM subcarriers of a 4.88 GHz bandwidth signal through the LWA showed that large bandwidth signals suffer from SNR degradation at its edges as the magnitude response of LWA drops with the angular dispersion from the central frequency. The characterization of LWA based multi-user transmission showed that sum rate increases with the number of served users but it saturates when user-signal bandwidth becomes small enough to not to be affected by the LWA beamsteering effect.

- A multiple LWA based 60GHz multi-user transmission was proposed and demonstrated with a single RoF link and single RF chain which showed that improvement in coverage and spectral efficiency by transmitting different frequency beams towards the same angular location.

- Experimental demonstration of a DWDM-RoF based 60GHz multi-user transmission using single LWA was presented as a first instance which showed the feasibility to extend multi-user transmission system using multiple optical wavelengths and performing direct photonic upconversion at the RAU for mmW generation. Multiple wavelengths can modulate different SCM signals simultaneously, in a DWDM distribution network for multiple RAUs, where each RAU performs multi-user transmission using a specific (transported) SCM signal.

6.2. Future Work

Future work can explore other techniques to extend the experimental work on RoF transport for mmW MIMO and multi-user transmission

- Resource allocation in mmW MIMO systems can be used to further improve the performance through spatial diversity and spatial multiplexing. In a RoF

supported multiple RAU system, the components at each RAU (photodiode, power amplifier, etc.) may not have similar characteristics, so the power restrictions per RAU will be different. For a mobile user, the geometric position for each RAU is different and similar performance at each user location can be achieved by dynamic allocation of power. Dynamic resource allocation can also be useful for the RoF supported LWA based multi-user transmission system by using power allocation coefficients for multiple user signals, to efficiently utilize the transmit power according to the power budget of the users. As users will be randomly distributed with respect to the distance from the transmitting antenna, more power can be allocated to the far located users to achieve better balance and increased capacity. Similarly, in a multi-user multi-service system, users with high bandwidth can be served with more power allocation to maintain an adequate SNR for all the users being served.

- The low bandwidth RoF link and 60GHz transmitter/receiver based multi-antenna system can be used for an extended transmission system in which a fixed access node is used with a remote node. Fig. 6.1 shows such a system setup in which Multiple-input-single-output (MISO) technique is used to transmit the two STBC coded signals from the RAU to the single receiving antenna using 2x1 Alamouti STBC technique. The received signal is processed at the remote node and modulated over an optical carrier and is distributed to various locations or mobile base stations (MBS) through the fixed access node, where it is converted to IF signal using a photodiode and upconverted to be transmitted using a single antenna. Single-input-Multiple-output (SIMO) techniques such as Maximal Ratio Combining (MRC) and Equal Gain Combining (EGC) can be used by the two receiving antennas to achieve receiver diversity. Thus a low complexity, low cost and single fibre link based system to distribute the MIMO signals can be achieved without using WDM or high-bandwidth optical modulators.

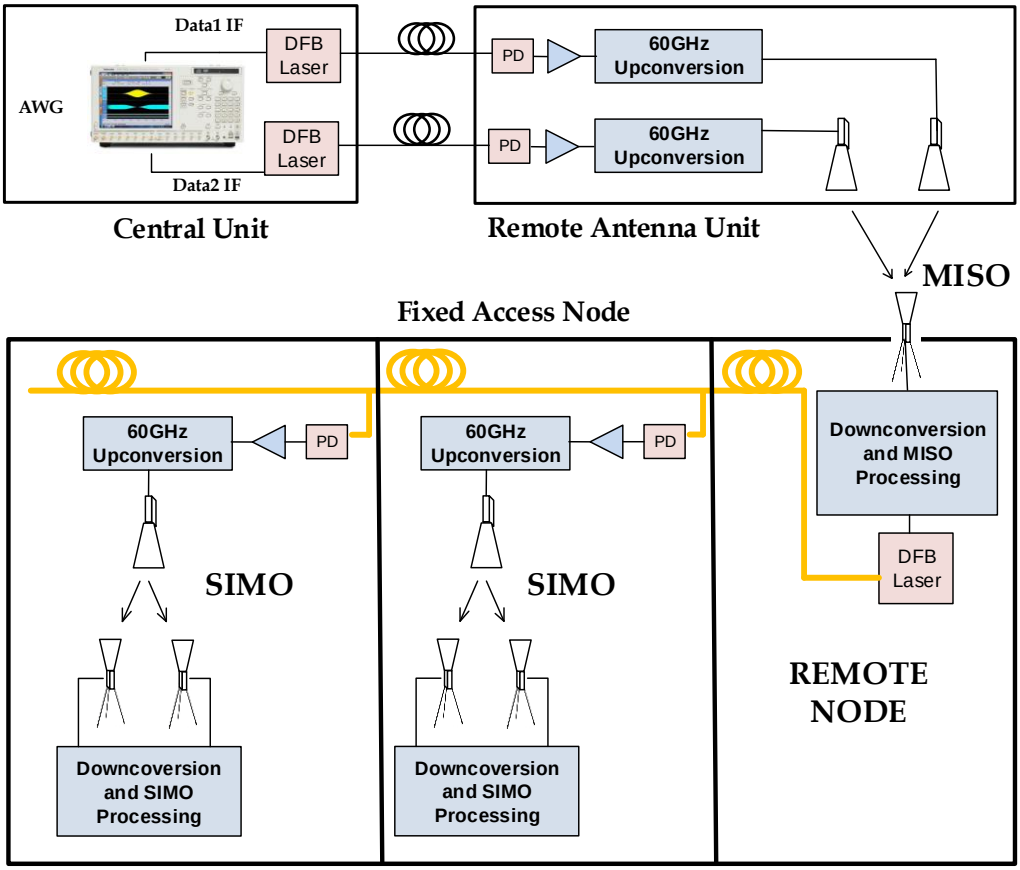

Figure 6.6.1 Remote Node based setup to extend the MIMO transmission using single fibre link

REFERENCES

[1] A. Kanno, T. Kuri, I. Hosako, T. Kawanishi, Y. Yoshida, Y. Yasumura and K.I. Kitayama, "Optical and millimeter-wave radio seamless MIMO transmission based on a radio over fiber technology", *Optics Express*, Vol. 20 (28), 2012, pp.29395-29403.

[2] M. Kong and W. Zhou, "Delivery of 12QAM single carrier signal in a MIMO radio-over-fiber system at 60GHz", *IEEE Photonics Journal*, Vol. 9 (3), 2017.

[3] C.H. Lin, C.T. Lin, H.T. Huang, W.S. Zeng, S.C. Chiang and H.Y. Chang, "60-GHz optical/wireless MIMO system integrated with optical subcarrier multiplexing and 2x2 wireless communication", *Optics Express*, Vol. 23 (9), 2015, pp.12111-12116.

[4] L. Cheng, M.M.U. Gul, F. LU, M. Zhu, J. Wang, M. Xu, X. Ma and G.K. Chang, "Coordinated Multipoint Transmissions in Millimeter-Wave Radio-Over-Fiber Systems", *Journal of Lightwave Technology*, Vol. 34 (2), 2016, pp.653 - 660.

[5] S. Inudo, Y. Yoshida, A. Kanno, P.T. Dat, T. Kawanishi and K. Kitayama, "On the MIMO Channel Rank Deficiency in W-band MIMO RoF transmissions", *Optical Fiber Communication Conference (OFC)*, 2015, pp.W4G-5.

[6] B. Liu, L. Zhang and X. Xin, "MMW Signal Transmission in Coherent MIMO RoF System With Adaptive-Coded Spreading", *IEEE Photonics Technology Letters*, Vol. 27 (12), 2015, pp. 1285-1288.

[7] Z. Xiao, L. Dai, D. Ding, J. Choi, P. Xia and X.G. Xia, "Millimeter-Wave communication with non-orthogonal multiple access for 5G", *arXiv preprint arXiv*, 2017, pp. 1709.07980.

[8] A. Alkhateeb, R.W. Heath and G. Leus, "Achievable rates of multi-user millimeter wave systems with hybrid precoding", *IEEE International Conference on Communication Workshop (ICCW)*, 2015, pp.1232-1237.

[9] M. Kim, J. Lee and J. Lee, "Hybrid beamforming for multi-user transmission in millimeter wave communications", *IEEE International Conference onInformation and Communication Technology Convergence (ICTC)*, 2017, pp. 1260-1262.

[10] I.A. Hemadeh, M. El-Hajjar, S. Won and L. Hanzo, "Multi-user steered multi-set space-time shift-keying for millimeter-wave communications", *IEEE Transactions on Vehicular Technology*, Vol. 66 (6), 2017, pp.5491-5495.

[11] M.C. Filippou, D.D. Donno, C. Priale, J. Palacios, D. Giustiniano and J. Widmer, "Throughput vs. latency: QoS-centric resource allocation for multi-user millimeter wave systems", *IEEE International Conference on Communications (ICC)*, 2017, pp. 1-6.